2020

Medical applications of synthetic gene circuits and switches

BOSTON UNIVERSITY

COLLEGE OF ENGINEERING

Dissertation

MEDICAL APPLICATIONS OF SYNTHETIC GENE CIRCUITS AND SWITCHES

by

MENG LAI NICOLE WONG

B.A., University of California, Berkeley, 2012

Submitted in partial fulfillment of the

requirements for the degree of

Doctor of Philosophy

2020

Approved by

First Reader

Wilson W. Wong, Ph.D.
Associate Professor of Biomedical Engineering

Second Reader

John T. Ngo, Ph.D.
Assistant Professor of Biomedical Engineering

Third Reader

Joyce Y. Wong, Ph.D.
Professor of Biomedical Engineering
Professor of Materials Science and Engineering

Fourth Reader

Andrew J. Henderson, Ph.D.
Assistant Dean of Student Affairs for Graduate Medical Sciences
Professor of Medicine
Professor of Microbiology
Boston University, School of Medicine

Fifth Reader

Hadi T. Nia, Ph.D.
Assistant Professor of Biomedical Engineering

ACKNOWLEDGMENTS

Embarking on this degree, I did not foresee just how much I would grow as a scientist and as a person. It has been quite an experience.

I would like to thank the entirety of the Wong lab, starting with my primary academic advisor, Dr. Wilson Wong. The obstacles that naturally come with scientific research can be trying, but his advice and guidance have helped me navigate such situations. I have learned a great deal in the past six years, and have him to thank for that. I would also like to thank all the members of the Wong lab, both past and present, who got their hands dirty at the benches with me: Dr. Huishan Li, Seunghee Lee, Justin Letendre, Chloe Ding, Menna Siddiqui, Eric Bressler, Dr. Xi Kang, Deboki Chakravarti, Janghwan Cho, Atsushi Okuma, Benjamin Weinberg, Matthew Brenner, and Katri Sofjan. Their encouragement and support have been imperative, and I am immensely thankful for them. In particular, I would like to recognise Dr. Huishan Li for her joint efforts on the NS3 CAR project. It started off as a small endeavour, but has morphed into something greater that would not have been possible without her.

Over the past two years, I have also been fortunate enough to work with Dr. Marc Hild and Elizabeth Frias at the Novartis Institutes for BioMedical Research on the recombinase-based reporter project. On top of being wonderful individuals to work with, they have been generous with their time and help on this collaboration, for which I am entirely grateful. I would also like to thank Frederic Sigoillot and Walter Carbone for their work on the CRISPR screen, as well as other members of the Chemical Biology and Therapeutics division for their day-to-day help.

A huge thanks goes to my family and friends for being my pillars of strength. I am in the debt of my parents who, for several years thought a Ph.D. in biomedical engineering was the same as a medical degree, may not know much about science but continue to encourage me throughout this journey. Words cannot describe how much I owe to my now husband, Ian Goh. From keeping me company as I work late nights, to bringing me sustenance when I'm busy, I would not have made it this far without him. Lastly, I would like to thank my dogs, Kingsley and Lyra, for their kisses of support.

MEDICAL APPLICATIONS OF

SYNTHETIC GENE CIRCUITS AND SWITCHES

MENG LAI NICOLE WONG

Boston University College of Engineering, 2020

Major Professor: Wilson W. Wong, Associate Professor of Biomedical Engineering

ABSTRACT

Synthetic biology enables us to create artificial systems using existing biological components, allowing for an exertion of control over the system so that we can further understand how these components interact or bestow them with new capabilities. A multitude of such applications have emerged in recent decades, among them the introduction of protein chimeras and genetic circuits to cells that can be used to accelerate the development of medical treatments and make them safer. T cell immunotherapy is an example of such a technology, and has shown promising results in the treatment of various cancers. However, a persisting obstacle is the inability to control the activity of these engineered cells, as they can become overactive or display off-target activities. We have developed two approaches for controlling T cell activity: a dual small molecule gated ZAP70 switch, and a collection of drug-inducible chimeric antigen receptors (CARs) encompassing the NS3 protease domain. These artificial components allow for increased regulation over T cell therapy and can potentially make T cell therapy safer in the clinic. In addition to improving the safety of clinical treatments, engineered mammalian cells can also act as pathway-sensitive reporters for use in the discovery of gene and drug targets in large-scale screens. However, in traditional compound screens,

temporally transient and weak responses may not be detected. Additionally, the decision of what constitutes a “hit” cell population in genome-wide screens can be relatively arbitrary, and thus key target genes could be missed. To address this, a recombinase-based circuit was developed that provides cells with memory, enhanced sensitivity, and an analog-to-digital readout. This reporter facilitates the screening process and enhances both drug and genome-wide screens.

CITATIONS TO PREVIOUSLY PUBLISHED WORK

Portions of this dissertation are reproduced from material that has been published or is in preparation for publication.

Sections of Chapter 1 were published as:

Wong NML and Wong WW. Engineering a Dual Small Molecule Gated ZAP70 Switch in T Cells. ACS Synth Biol. 2018;7(4):969–977. Epub 2018/03/28. doi: 10.1021/acssynbio.7b00394. PubMed PMID: 29589904; PMCID: PMC5985775.

TABLE OF CONTENTS

LIST OF TABLES

LIST OF FIGURES

CHAPTER ONE: Engineering a dual small molecule gated ZAP70 switch in T cells

1.1 Introduction

In the field of synthetic biology, tools are often created to either control of modify a cell's behaviour. This can be used to change the way a cell senses, processes and responds to signals, which can endow biological systems with new functions. As the field has developed over the years we have increasingly seen how these functions can translate to useful purposes in medicine. Just a few of these applications include the embedding of genetic circuits into paper to serve as diagnostic tests for disease, and the engineering of yeast to produce high amounts of an antimalarial drug precursor [1, 2].

Recent years have also seen the successful application of synthetic biology to cellular immunotherapy where it has shown promising results in the treatment of cancer. This form of therapy involves the removal of a patient's immune cells, genetically engineering them to make them more effective against cancer cells, then reintroducing them into the patient. Oftentimes, modified receptors are expressed on the immune cells to help target them specifically to tumour cells. These receptors most often consist of engineered T cell receptors (TCRs) or chimeric antigen receptors (CARs). TCRs are endogenous to T cells, whereas CARs are synthetic, but both receptors contain extracellular domains that can be modified to target tumour-specific antigens.

Several clinical trials have demonstrated the efficacy of this therapy in treating patients with B cell malignancies, and positive responses have been observed in the treatment of other cancers, such as metastatic melanoma, colorectal cancer, and multiple myeloma [3-12]. In a clinical trial involving anti-NY-ESO-1 TCR T cells, 70% of

patients with multiple myeloma indicated either a near complete response or complete response [10]. Furthermore, in a trial where patients with refractory or relapsed acute lymphoblastic leukemia were treated with anti-CD19 CAR T cells, complete remission was observed in 90% of the patients [7]. CAR T cell therapy was also the first gene transfer therapy approved by the Food and Drug Administration (FDA), with two anti-CD19 CAR therapies cleared in 2017.

While the clinical results of T cell immunotherapy are encouraging, there are still adverse effects of the therapy that need to be addressed, most notably cytokine release syndrome (CRS) [13-18]. When T cells recognise their target antigen, one of their responses is to release cytokines to encourage proliferation and help recruit more immune cells to the site. However, when this positive feedback loop is uncontrolled, a cytokine storm can result and this overactivity can lead to patient deaths [19-22].

To improve safety, various genetic switches have been developed for controlling T cell activity, including ON or OFF switches [23-29]. While such technologies can be effective, there are still challenges that need to be addressed. Kill switches are an example of such an OFF switch, and are effective at eliminating overactive T cells by inducing apoptosis, but they also destroy the valuable therapeutic agents. This can have drawbacks if the patient requires the use of the engineered cells later during treatment. Furthermore, cells may lose expression of the suicide gene due to silencing, or develop a resistance to the gene by upregulating anti-apoptotic genes [30]. Additionally, many switches have been designed specifically for CARs and are integrated into CAR design directly, thus making them incompatible with T cells employing endogenous or

engineered TCRs. Current switch technologies are also often regulated by a single drug that can only turn ON or OFF T cell activity. To reverse the T cell activity would require the drug inducer to be degraded, which can be time consuming. In the event of CRS, symptoms can begin 1 hour after infusion, indicating how quickly the effect can manifest and highlighting the need for rapid control [31]. As such, a dual gated switch that can be regulated by two small molecules, one for ON and one for OFF function, could be more advantageous for tighter temporal control.

Zeta-chain-associated protein kinase 70 (ZAP70) is a critical cytoplasmic protein tyrosine kinase that is involved in the signal transduction of T cell activation [32-36]. During T cell activation, the SH2 domains of ZAP70 bind to phosphorylated CD3 immunoreceptor tyrosine-based activation motifs (ITAMs), positioning the kinase to phosphorylate and activate downstream proteins, such as linker of activated T cells (LAT) and lymphocyte cytosolic protein 2 (SLP76) [37-41]. Studies have shown that ZAP70-deficient T cells display defective TCR-mediated T cell activation [42-45]. Its early involvement in the activation pathway also suggests ZAP70 has extensive control over the various signaling cascades that stem from its activation, making it a suitable target for regulating T cell activity.

Despite the essential role that ZAP70 plays in T cell activation, few technologies have been developed for controlling its activity. Previous work on ZAP70 has included regulatable expression of ZAP70 in an effort to control TCR activity, as well as the creation of an analog-sensitive version of ZAP70 that can be inhibited by a small molecule [46-48]. While these methods of control are effective, regulation on a

transcriptional or translational level requires time for these processes to occur. Furthermore, tighter control over ZAP70 activity would enable more precise regulation of T cell activity.

Here, we describe a dual-gated ZAP70 protein switch for regulating early T cell signaling. The switch is generated by fusing an ERT2 domain to the above-mentioned analog-sensitive ZAP70, and shows swift temporal control using two distinct small molecules, 4-hydroxy-tamoxifen and 3-MB-PP1, to turn on and off protein activity respectively. Dynamics results indicate that the ZAP70 switch introduces tight temporal control over early signaling in the TCR pathway, with activation in less than 2 minutes and inhibition within 1 minute. The ON-OFF switch can also be used to modulate the strength of activation by varying concentrations of activator and inhibitor. While the switch was able to regulate early T cell activation markers, we found that ON switch activity resulted in stunted cytokine release, suggesting that the fusion of ERT2 to ZAP70 is inhibiting its downstream effector function. In order for the switch to meet the need for effective control in T cell immunotherapy, further exploration is needed to understand the cause of this constraint.

1.2 Results

1.2.1 Control over TCR activity

To develop a dual-gated system for regulating T cell activity, we engineered the ZAP70 to be sensitive to small molecule regulation. We found serendipitously that by fusing an ER^{T2} domain to the N-terminus of ZAP70, we were able to render ZAP70

inactive. The switch was also linked to an mCherry fluorescent protein to detect expression in cells, and facilitate later downstream sorting of switch-expressing cells. When the ER^{T2}-ZAP70 (ZE) switch was introduced into ZAP70-deficient Jurkat T cells (P116) [45], the addition of 4-hydroxy-tamoxifen (4OHT) alleviated the inhibition and allowed ZAP70 to transduce the signal originated from the TCR and subsequently upregulate expression of CD69, a marker of T cell activation (**Figure 1.1a top and 1.1b**). It was also found that certain configurations of the ER^{T2}-ZAP70 fusion protein did not exhibit this ON-activity as strongly as others (**Figure S1.1**). The addition of 4OHT to wild-type Jurkat cells or P116 did not impact CD69 expression, suggesting its specificity for ER^{T2}-ZAP70 (**Figure 1.1b**).

Previous work has shown that when the gatekeeper methionine residue of the ZAP70 kinase domain is mutated to alanine, a non-functional analog of adenosine triphosphate (ATP), the small molecule 3-MB-PP1 can bind to the ATP pocket and inhibit kinase activity. 3-MB-PP1 therefore acts as a competitive inhibitor, thus serving as an OFF switch for T cells expressing only this analog-sensitive (AS) ZAP70 allele [46]. We tested whether our ER^{T2}-ZAP70 switch could be combined with the analog-sensitive allele of ZAP70 into a single protein to generate the first dual small molecule-gated ZAP70 switch (**Figure 1.1a bottom**). Similar to the ER^{T2}-ZAP70 switch, variants of the ER^{T2} domain and analog-sensitive ZAP70 were tested, and results showed that the effectiveness of the ON activity from the ER^{T2}-ZAP70 constructs carried over to their respective ZAP70-AS-ER^{T2} (ZASE) constructs (**Figure S1.2**). ZASE2 was chosen as the final ZASE construct due to the high CD69 levels resulted in the presence of 4OHT and

anti-TCR antibody (C305), while preserving low levels with anti-TCR antibody alone. Indeed, CD69 levels indicate that the activity of the ZAP70-AS-ER^{T2} protein was induced by 4OHT and potently inhibited by 3-MB-PP1 (**Figure 1.1c**). When cells expressing the switch fused to mCherry were treated with 4OHT, an elevation of both mCherry and ZAP70 was also noted (**Figure 1.1d**). Interestingly, when IL-2 levels were analyzed for the ZE and ZASE switches, little elevation in IL-2 was observed when the switches were turned on compared to what was observed for the activation of wild-type ZAP70, suggesting that there may be functional limitations to the ON-OFF switch (**Figure S1.3**). There is, however, a small IL-2 increase with ON switch conditions in comparison with the other combinations of small molecules, though this is more prominent in the ZE switch than ZASE. Furthermore, 3-MB-PP1 has shown slight nonspecific inhibition of wild-type ZAP70, though its effect is minimal (**Figure 1.1c**). The inhibitor showed the same non-specificity for ER^{T2}-ZAP70 as well, which was expected (**Figure S1.4**).

1.2.2 Dynamics of the ZAP70 switch

Upon activation of the TCR, a rise in intracellular calcium is known to occur [49-51]. To test the dynamics of ZASE, P116 cells expressing the switch were loaded with the Indo-1 AM dye to measure intracellular calcium flux while treated with various combinations of 4OHT, 3-MB-PP1, and anti-TCR antibody. To study the dynamics of ZASE ON activity, cells expressing the ZAP70 switch were incubated with 4OHT at different time points relative to stimulation of the TCR. When the TCR was stimulated, a transient increase in calcium was observed. Subsequent addition of 4OHT resulted in a

further increase in calcium levels. This elevation in intracellular calcium was initiated immediately after 4OHT was added, though peak calcium levels were achieved in just below 2 minutes (**Figure 1.2a top**). Treatment of cells with 4OHT alone resulted in no calcium flux, until the TCR was stimulated. At this point, the increase in calcium was greater than if 4OHT had been added post-C305 (**Figure 1.2a bottom left**). Cells pre-incubated with 4OHT overnight prior to stimulation of the TCR showed an increase in calcium when the TCR was stimulated, which was comparable to stimulation of the TCR alone. However, the peak calcium level was sustained for a longer time (**Figure 1.2a bottom right**).

ZASE-expressing cells were then tested with various combinations of 4OHT and C305 to ensure that activation required both of these molecules. When 4OHT alone was added to cells, no calcium flux was observed, and addition of C305 alone resulted in a slight increase in calcium levels. The largest increase in calcium was observed when cells were treated with both 4OHT and C305 (**Figure 1.2b top**). The same conditions tested in cells expressing wild-type ZAP70 indicated calcium elevation whenever C305 was added, with peak levels slightly higher than what is observed with ZASE. These cells did not seem to be affected by the presence of 4OHT, though a mild dip in calcium was seen when 3-MB-PP1 was introduced, likely due to nonspecific inhibition of wild-type ZAP70 (**Figure 1.2b bottom**). Additionally, the dynamics of wild-type ZAP70-expressing cells were recapitulated by wild-type Jurkat cells. P116 cells expressing no ZAP70 displayed a small increment in calcium when C305 was added, and it should be noted that a basal level of signaling is present even in the absence of ZAP70. This slight increase is likely

due to ZAP70-independent TCR activation pathways that have been tied to intracellular calcium release, but the cells were otherwise unaffected by the molecules (**Figure S1.5**) [52].

It has been previously shown both in vitro and in vivo that 3-MB-PP1 is able to fully inhibit analog-sensitive ZAP70 in less than a minute, thus providing a rapid OFF switch [46]. To verify quick temporal control using 3-MB-PP1, inhibition conditions were also assessed. Combinations of activation using 4OHT and C305, and inhibition using 3-MB-PP1 were tested. Activated ZASE-expressing cells that were subsequently inhibited with 3-MB-PP1 showed calcium levels brought down to basal within 1 minute. When these cells were activated but not inhibited, a sustained calcium level was observed. Treatment with only 3-MB-PP1 indicated no change in calcium levels (**Figure 1.2c top**). Simultaneous addition of C305 and 3-MB-PP1 resulted in a diminished calcium increase compared to cells that were not treated with inhibitor (**Figure S1.6**). Though complete shutdown was not instantaneous, this demonstrates the immediate inhibitory effect 3-MB-PP1 can have on ZASE. The inhibition conditions tested on wild-type ZAP70 cells also demonstrate more clearly that wild-type ZAP70 is marginally inhibited by 3-MB-PP1, as cells without the inhibitor contrastingly maintain their elevated calcium levels (**Figure 1.2c bottom**).

To verify that the ZAP70 switch can still be turned ON following inhibition by 3-MB-PP1, cells expressing the switch were pre-incubated with 4OHT and 3-MB-PP1, then washed with media containing only 4OHT. These cells were then rested for various intervals of time and activated. CD69 levels were measured as a marker for T cell

activation. Within 2 hours of washing out the drug and activation of cells, CD69 expression in ZASE-expressing cells increased from basal levels to that comparable to cells that had not been inhibited with 3-MB-PP1 (**Figure S1.7 top**). This indicates that the inhibitor does not irreversibly bind the switch, and ZASE is able to reactivate fairly quickly following shutdown by the inhibitor. Pre-incubation of wild-type Jurkat cells with the inhibitor did not hinder CD69 expression, and ZAP70-deficient cells were unaffected by the inhibitor or C305 (**Figure S1.7 bottom**).

1.2.3 Modulation of TCR activity

In a clinical setting, patient variability may require treatment conditions to be tailored to the individual. The desired level of T cell activity can also depend on the stage of treatment, and intended immune response. As such, we systematically characterized the dose response profile of ZASE activity with 4OHT and 3-MB-PP1 by measuring CD69 levels, and showed that 10uM of 3-MB-PP1 can inhibit activity of ZASE at all tested concentrations of 4OHT (**Figure 1.3a**). To reduce nonspecific inhibition of wild-type ZAP70, a focused dose response was performed in the range of 0 - 10uM and found that 7.5uM 3-MB-PP1 was sufficient for shutting off ZAP70 activity (**Figure 1.3b**). Induction of the switch using 4OHT also occurs as an abrupt change between 0.01uM to 0.1uM 4OHT, though the more detailed dose response reveals a gradual increase in T cell activity within this range (**Figure 1.3b**). These gradual changes indicate that the intensity of T cell activation can be controlled by altering the concentrations of activator and inhibitor used. The same dose response of small molecules was additionally tested in wild-type Jurkat and P116 cells, and displayed no effect on activation of these cells

(**Figure S1.8**).

The modulation of T cell activation using 4OHT was further verified with calcium flux assays on cells expressing the switch. Levels of calcium reached during activation increased in a direct relationship with the concentration of 4OHT up to 0.1uM. A concentration of 0.01uM 4OHT led to no further increase in calcium compared to cells treated with no 4OHT, reinforcing the dose response profile seen with CD69 expression (**Figure 1.4**). Dynamics data for analog-sensitive ZAP70 with varying concentrations of 3-MB-PP1 has previously been established to control the extent of inhibition [46].

1.2.4 ZAP70 switch and CARs

Though both TCRs and chimeric antigen receptors (CARs) contain the CD3ζ domain that ZAP70 is known to interact with, surprisingly ZASE exhibits compatibility issues with CARs. ERT2-ZAP70 and the ZASE construct were introduced into P116 cells expressing a Her2 third generation H3B1 CAR comprising of the CD28 and 4-1BB costimulatory domains, and CD69 levels analyzed as markers of T cell activation. While 3-MB-PP1 was able to turn off T cell activation initiated by CARs, the addition of 4OHT in the absence of Her2 displayed leaky elevated CD69 levels for both ERT2-ZAP70 and ZASE (**Figure S1.9**). These raised CD69 levels were observed for Her2 CARs of varying scFv affinity, and additionally a CAR targeting CD19 (**data not shown**).

1.3 Discussion and Conclusion

The ZASE switch represents the first dual small molecule gated switch in T cells, with a true ON and OFF function that is regulated by two separate drugs. We have shown

that the switch is able to control the early T cell activation pathway, as measured by CD69 and intracellular calcium. While the mechanism for the ON switch remains enigmatic, we postulate that it may be attributed to stabilization of the fusion protein when 4OHT is bound to ERT2. This is supported by an increase in mCherry and ZAP70 levels when cells were treated with 4OHT. The use of a mutant estrogen receptor as a destabilization domain has also previously been seen with the distinct mutated estrogen receptor ligand binding domain (ERLBD), whose stabilization is recovered upon the addition of 4OHT [53]. The instability from such degradation domains has previously been shown to result in the degradation of the whole fusion protein, which could explain the ability of 4OHT to control mCherry and ZAP70 protein levels [54, 55]. It is interesting to note that certain configurations of ERT2 and ZAP70 do not encompass this ON switch activity, but rather behave similarly to wild-type ZAP70 by allowing T cells to activate whenever anti-TCR antibody is present. It is possible that the structural conformations of certain ERT2-ZAP70 configurations preclude control by 4OHT.

While in theory the ZAP70 switch should be able to control any receptor including the CD3ζ chain, its curious incompatibility with CARs suggests there is more to its mechanism, and could use additional study. Upon addition of 4OHT, higher expression of the ZAP70 switch was observed in T cells, possibly raising the basal level of CD69 and resulting in the leaky switch behaviour observed in CAR-T cells. It would also be interesting to quantify the amounts of CAR and TCR on the surface of the T cells in order to determine whether an excess of CARs to TCRs may be contributing to this leakiness. Furthermore, minimal IL-2 induction is seen following ZE and ZASE

activation. As the ZAP70 protein also functions as an adaptor protein, it is conceivable that the presence of the ERT2 domain obstructs its moderation of proteins known to regulate IL-2 production, such as Lck [56]. While early T cell activation markers CD69 and intracellular calcium are regulated by the switch, constraints on downstream effector functions like cytokine release can impede its use in immunotherapy application, and should be noted when assessing the limitations on the functionality of this ZAP70 switch.

Calcium flux assays have indicated that the dual-gated switch can be turned on in just under 2 minutes, and rapidly turned off within a minute. While ON activity takes slightly longer to reach peak calcium levels, the ZAP70 switch still exhibits tight temporal control by 4OHT and 3-MB-PP1. The small molecules also show little to no effect on wild-type ZAP70, emphasizing the specificity they have to the switch. By varying concentrations of activator and inhibitor, we were also able to modulate early T cell signaling through ZASE. The switch thus enables quick regulation over steps of the T cell activation pathway, with degrees of activity swiftly controlled by small molecule.

The inclusion of ZASE in T cells is a step toward alleviating overactivity issues that are currently observed in cancer immunotherapy. Ideally, if off-target activities are detected in time, the switch could also be used to shut off T cell activity. However, in order for ZASE to have clinical use, the issue of diminished T cell downstream effector function needs to be addressed. To determine if or how ERT2 may be obstructing ZAP70 activity, the current roles of ZAP70 should be further investigated. For example, early interactions such as ZAP70 binding to ITAMs and phosphorylation of ZAP70 by Lck should be verified. The propagation of this signaling should then be explored to

determine if ERT2 affects the ability of the kinase to phosphorylate other proteins like LAT and SLP76. If ERT2 poses a steric hindrance on the function of ZAP70, variants of ZASE could be tested that include linkers of different lengths between the two proteins. Alternatively, if an unavoidable characteristic of ERT2 is impeding ZAP70 function, the ERLBD could theoretically serve as the ON switch aspect of ZASE instead, with the added benefit of control by the same drug.

We have shown that ZASE is effective in controlling the early TCR activation pathway, but there remain further steps that need to be taken before the switch can be considered for clinical use. The first of these steps is to establish its activity in primary T cells. Though a ZAP70-deficient Jurkat T cell line was used in our studies, primary T cells express endogenous ZAP70 and this protein would need to be removed to prevent occlusion of ZASE activity. This could be done via a simultaneous knock out of ZAP70 and knock in of ZASE into the endogenous site. Alternatively, ZASE could be integrated by lentivirus and ZAP70 knocked down using methods like siRNA. If ZASE functions as effectively with TCRs in primary T cells as immortalised T cells, the next step is to test its ability to control T cell activity *in vivo* with a mouse leukemia model. While 4OHT is an active metabolite of tamoxifen and should pose few issues for *in vivo* testing, the inhibitor 3-MB-PP1 is synthetic and the safety of this drug needs to be determined before *in vivo* use. As such, there remain several hurdles that need to be overcome before this technology can be considered in a clinical setting. While our work on ZASE is preliminary, we believe that with the right enhancements and further study, it has the potential to be a suitable technology for improving the safety of T cell immunotherapy.

1.4 Methods

1.4.1 Plasmids

ZAP70 switches were introduced into human T cells using pHR lentivectors [57]. The expression of ZAP70 switches is driven by an EF-1 alpha promoter followed by a kozak sequence. Switches were tagged with an mCherry fluorescent protein through a GS linker (5'-gggtctggctccggatcaagtggtggcagc-3') to verify expression of the construct in cells and facilitate downstream cell sorting. Plasmids were packaged into lentiviruses using pDelta, Vsvg and pAdv packaging and envelope plasmids.

1.4.2 Cell culture

Lentiviruses were generated using HEK293FT cells, which were cultured in Dulbecco's modified Eagle's medium (DMEM) supplemented with 10% fetal bovine serum (FBS; Thermo Fisher, 10437028), penicillin/streptomycin (Corning, 30001CI), L-glutamine (Corning, 25005CI) and 1mM sodium pyruvate (Lonza, 13115E). ZAP70-deficient Jurkat T cells, P116, were obtained from the Weiss Lab at UCSF and cultured in RPMI 1640 supplemented with 10% FBS and L-glutamine. Wild-type Jurkat cells were cultured in RPMI 1640 supplemented with 5% FBS, L-glutamine and penicillin/streptomycin. For T cell activation, 2x105 cells were added to plate-bound C305 and incubated overnight at 37°C, 5% CO2. Cells that were not treated with 4OHT (Sigma-Aldrich, H6278-50MG; reconstituted in methanol) or 3-MB-PP1 (Calbiochem, 529582-5MG; reconstituted in dimethyl sulfoxide (DMSO)) were incubated with methanol or DMSO respectively as a control.

1.4.3 Lentivirus generation and transduction

HEK293FT cells were grown in 6-well plates and co-transfected with lentivirus packaging/envelope plasmids (described above) and ZAP70 switch-encoding vector using polyethylenimine (PEI). Supernatant containing virus was collected after 72 hours and spun down to remove remnant cells. P116 cells were infected with virus-containing media for 72 hours at 37°C before washing out the virus.

1.4.4 Surface and intracellular staining

For surface staining, cells were stained for CD69 expression using APC-Cy7-conjugated mouse anti-human CD69 antibody (BD Pharmingen, 557756) at a dilution of 1:100. Myc-tagged Her2 CARs were stained using Alexa Fluor 488-conjugated mouse anti-human myc antibody (R&D Systems, IC3696G). $2x10^5$ cells were washed twice with FACS buffer (1x phosphate buffered saline (PBS), 0.1% NaN3, 1% BSA, 2mM EDTA) before incubating with antibody in the dark at room temperature for 40 minutes. Cells were then washed and resuspended with FACS buffer before analysis on flow cytometer. For intracellular staining, cells were washed with FACS buffer prior to fixation (BD Cytofix, 554655) at room temperature for 10 minutes, then washed again. The cell membrane was permeabilized by adding 90% cold methanol to cells on ice and cold incubation for 30 minutes, followed by washing and incubation with antibody. Intracellular staining of ZAP70 protein was performed using Alexa Fluor 488-conjugated mouse anti-ZAP70 antibody (Life Technologies, MHZAP7020) at a dilution of 1:50.

1.4.5 Flow cytometry

Transduced cells were sorted for mCherry-positive cells at the Boston University Imaging Core using a Sony SH800 Cell Sorter. Cells were treated with 0.1uM 4OHT prior to sorting. Myc-tagged CAR and CD69 expression levels from T cell activation experiments were measured post-staining using an Attune NxT flow cytometer.

1.4.6 IL-2 ELISA

Supernatant from cells incubated with various combinations of C305, 4OHT, and 3-MB-PP1 was saved and tested in an enzyme-linked immunosorbent assay (ELISA) to measure IL-2 levels. The BD OptEIA human IL-2 ELISA kit (BD Biosciences, 555190) was used according to manufacturer's instructions with a 0.05% Tween-20 in PBS (Thermo Scientific, 28352) wash buffer, and remaining reagents from BD OptEIA Reagent Set B (BD Biosciences, 550534). ELISAs were performed with 96-well MaxiSorp plates (Thermo Scientific, 442404).

1.4.7 Calcium dynamics

Intracellular calcium levels were measured by loading $1.5x10^6$ cells with 8uM Indo-1 acetoxymethyl dye (Invitrogen, I1203) diluted in media (RPMI 1640 supplemented with 10% FBS and L-glutamine). Loading specifications of 45 minutes at 37°C were used. Cells were then washed in media and incubated in the dark at room temperature for 10 minutes. Prior to analysis, cells were equilibrated to 37°C, then read on a SpectraMax M5 (Molecular Devices) at 37°C. The 400/500 nm emission ratio was taken as a measurement of intracellular calcium.

1.4.8 Reactivation of ZAP70 switch

Cells were incubated with 0.1uM 4OHT and 7.5uM 3-MB-PP1 for 16 hours, followed by washing out of 3-MB-PP1 and incubating cells in media containing 4OHT for various durations (2, 4, 8, 16 hours). Cells were then added to plate-bound C305 to activate for 16 hours, stained for CD69 and measured by flow cytometry. For the 0 hour time point, 3-MB-PP1 was not washed out and cells were directly stimulated with C305. Control samples were either incubated with no 3-MB-PP1 and then activated with C305 (positive control), or incubated with 3-MB-PP1 and not activated with C305 (negative control).

1.4.9 Statistics

Data between two groups were compared using an unpaired two-tailed t-test. A *P*-value < 0.05 was considered to be statistically significant.

1.5 Figures

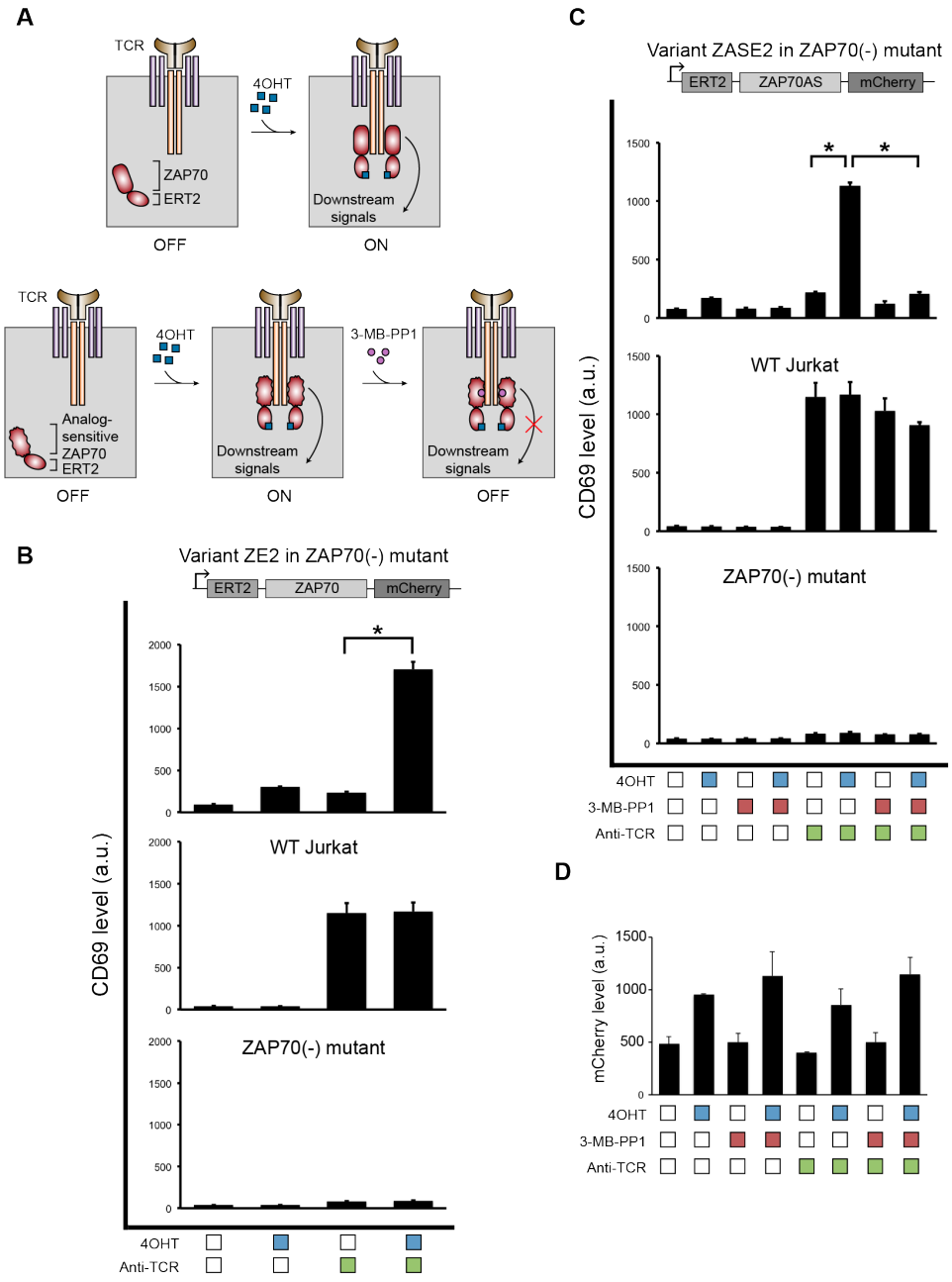

Figure 1.1: Characterisation of the ON-OFF switch with TCRs.
A) Schematic illustrating the mechanisms for the ZAP70 ON and ON-OFF switches. B) Various cell lines were treated with combinations of activator and anti-TCR antibody, and CD69 levels analyzed by flow cytometry (mean ± s.d., n = 3, *$P < 0.0001$). C) CD69 levels for cells incubated with combinations of activator, inhibitor, and anti-TCR antibody (mean ± s.d., n = 3, *$P < 0.0001$). D) mCherry and ZAP70 levels for ZASE-expressing P116 cells under various small molecule conditions.

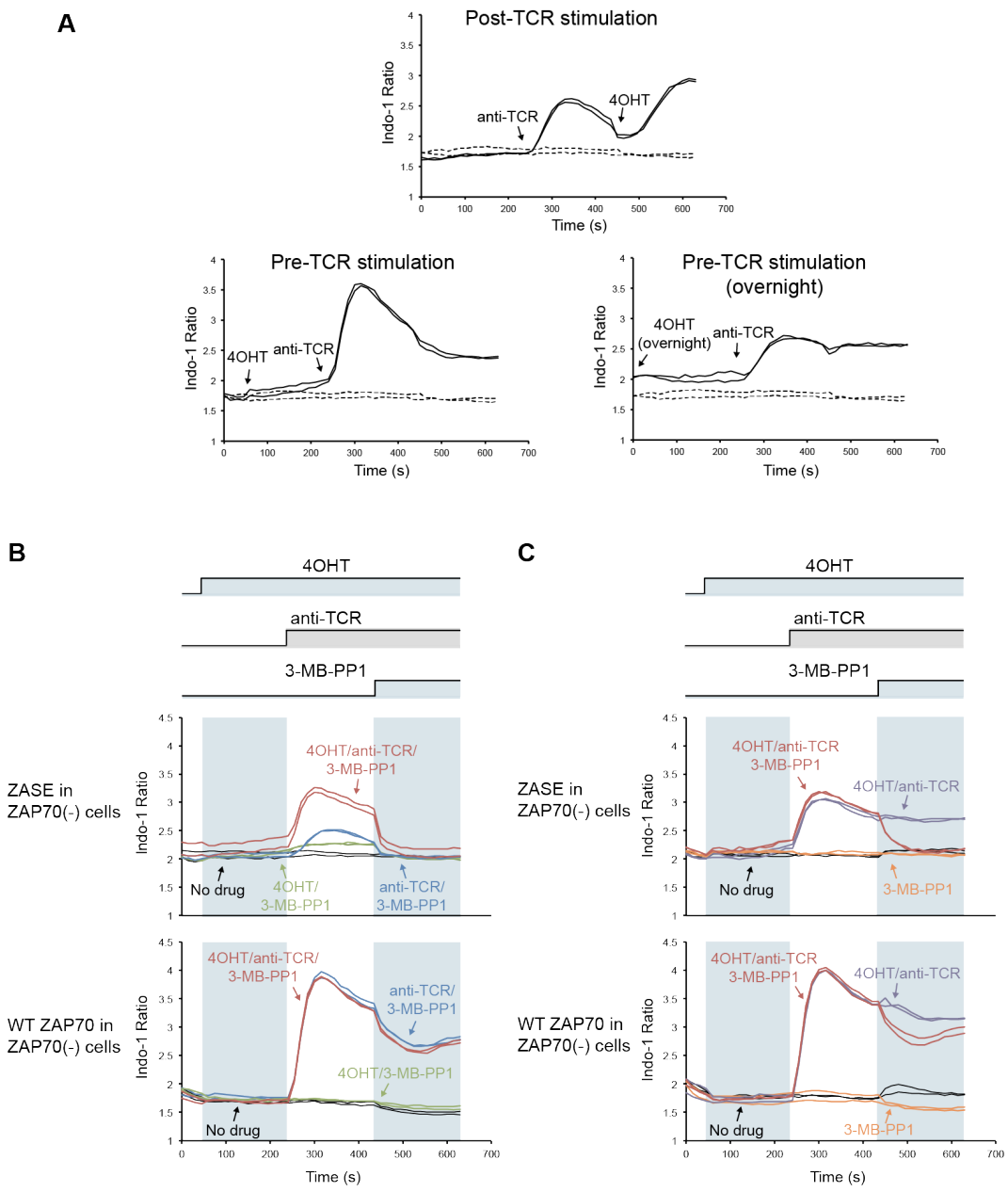

Figure 1.2: Calcium dynamics under varying small molecule conditions.
A) Intracellular calcium levels of ZASE-expressing P116 cells, with 4OHT added at different time points relative to stimulation of TCR. Control cells with no 4OHT or anti-TCR antibody are repeated in each panel for comparison with basal calcium levels. B) Activation controls for cells expressing ZASE or wild-type ZAP70. Cells were treated with or without 4OHT, and with or without anti-TCR antibody. All cells were then inhibited with 3-MB-PP1. C) Inhibition controls for cells expressing ZASE or wild-type ZAP70. Cells were treated with or without activation drugs, and with or without 3-MB-PP1.

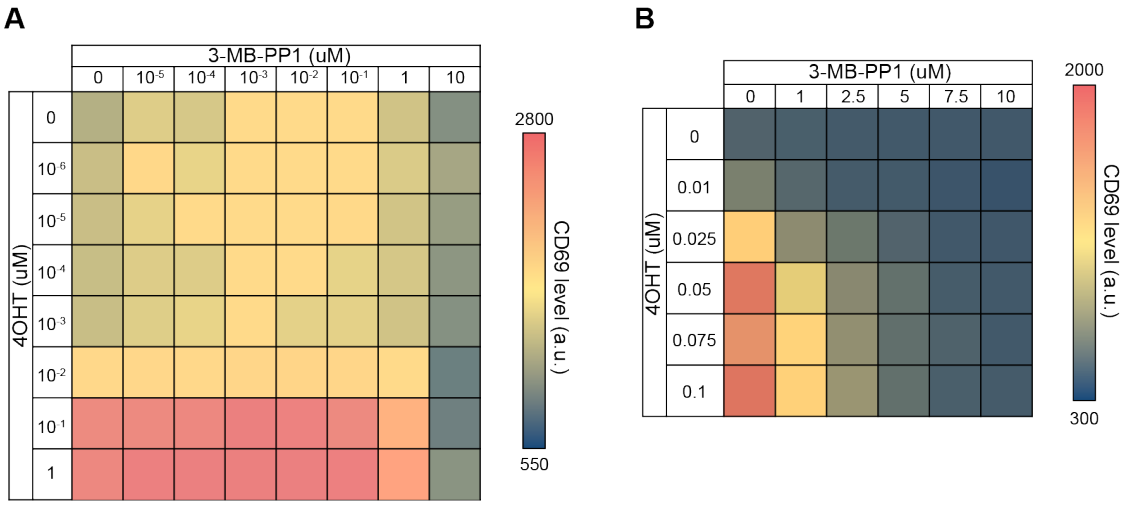

Figure 1.3: Modulation of ZASE-controlled TCR activity as measured by CD69 levels by modifying small molecule doses.
A) ZASE-expressing P116 cells were treated with various concentrations of activator and inhibitor, and CD69 levels analyzed by flow cytometry. A wide range of concentrations were tested. B) 2-D dose response for ZASE-expressing P116 cells with a narrowed range of concentrations tested.

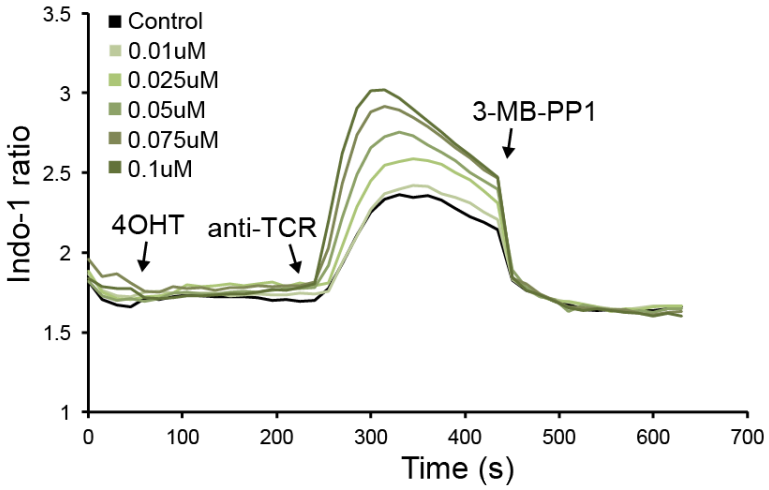

Figure 1.4: Calcium dynamics for ZASE-expressing P116 cells using a range of 4OHT concentrations.
Cells were loaded with Indo-1 AM dye and treated with various concentrations of 4OHT. Cells were then activated with anti-TCR antibody, and inhibited by 3-MB-PP1.

1.6 Supplemental Figures

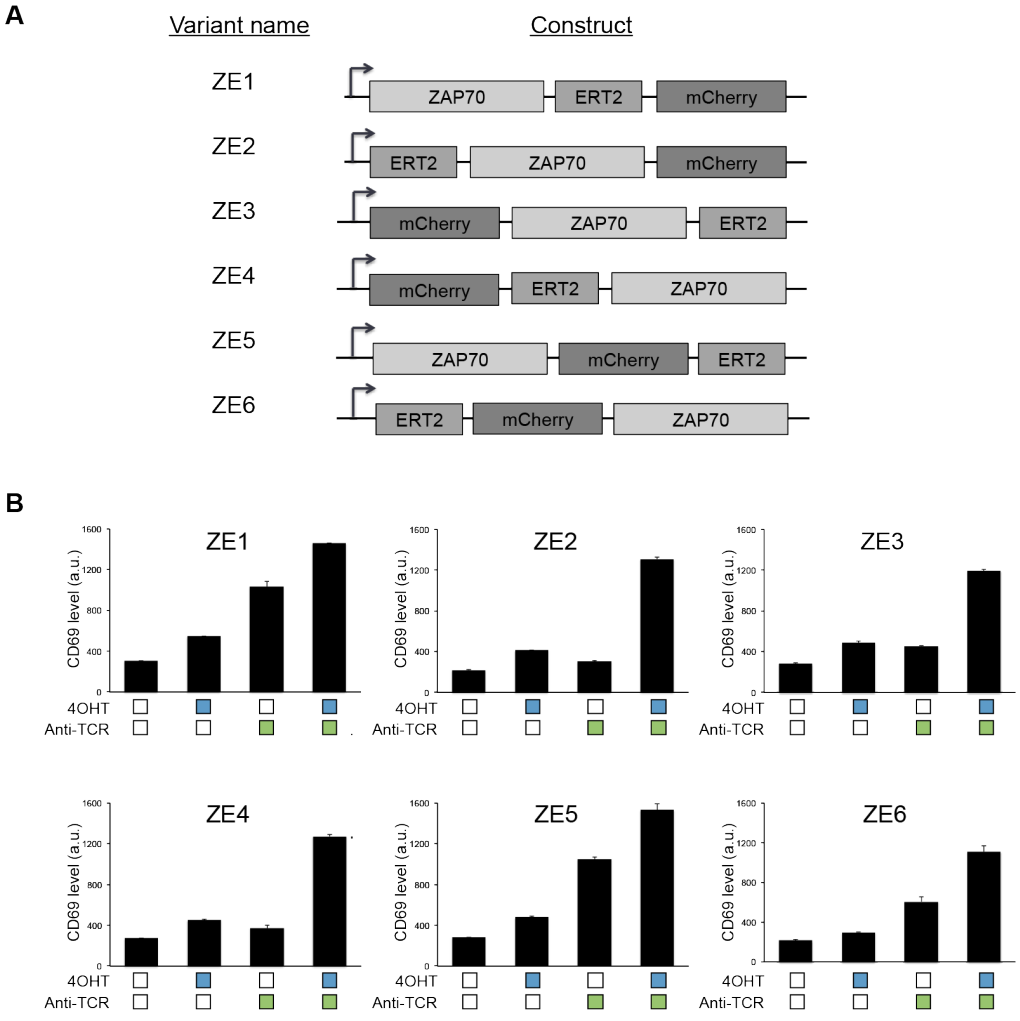

Figure S1.1: Various configurations of ZAP70 and ERT2 tested for 4OHT control. A) Diagram of constructs with different orderings of the ZAP70 gene, ERT2 domain, and mCherry fluorescent tag that were introduced into P116 cells. B) CD69 levels of cells expressing the constructs under various combinations of 4OHT and anti-TCR antibody.

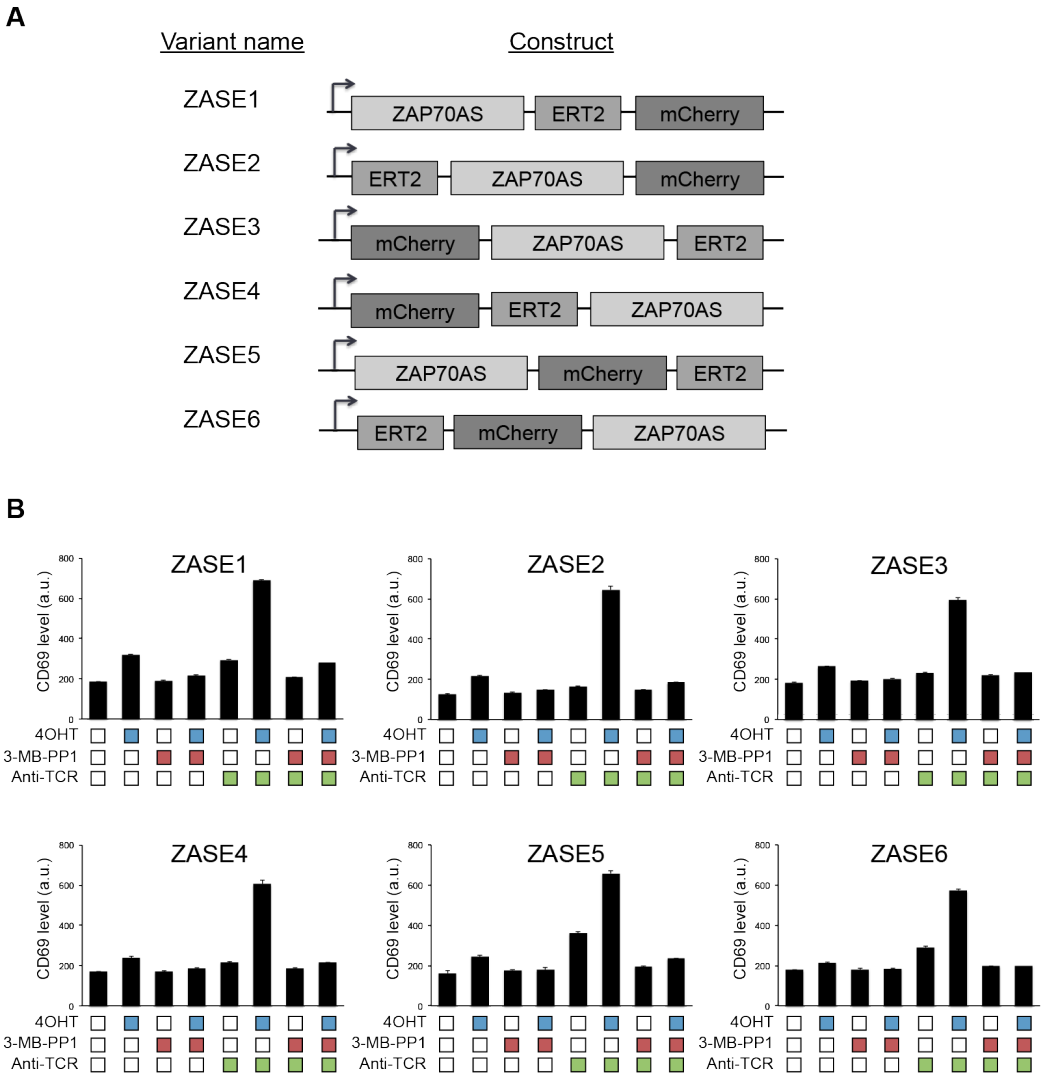

Figure S1.2: Different configurations of analog-sensitive ZAP70 and ERT2 tested for 4OHT and 3-MB-PP1 control.

A) Constructs tested, with varying arrangements of the analog-sensitive ZAP70 gene, ERT2 domain, and mCherry fluorescent tag. B) CD69 levels of cells expressing the constructs under various combinations of 4OHT, 3-MB-PP1, and anti-TCR antibody.

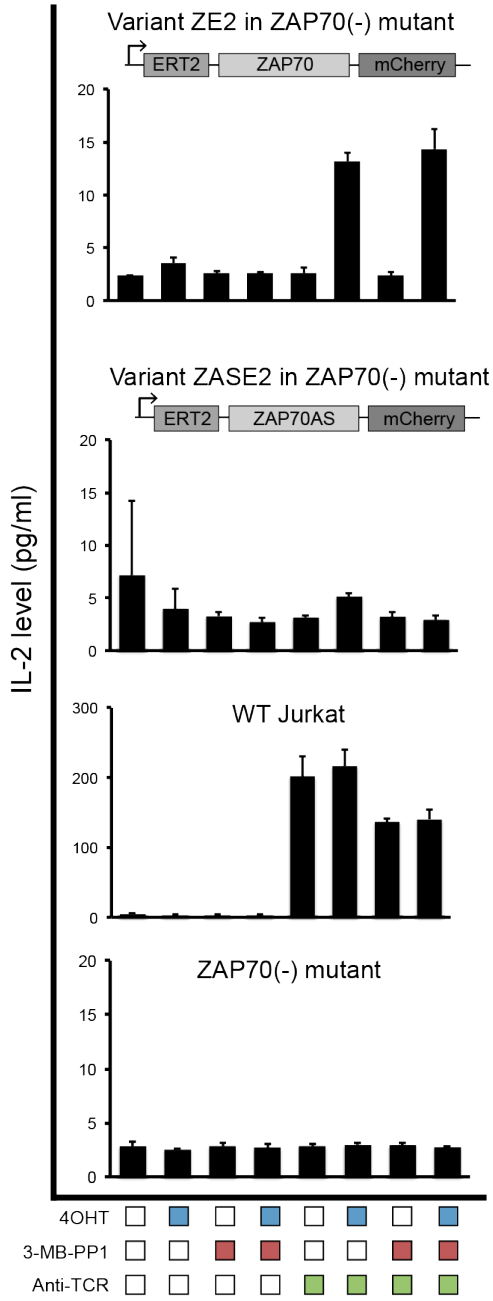

Figure S1.3: IL-2 release in cells treated with combinations of small molecules. ZE-expressing, ZASE-expressing, wild-type, and ZAP70-deficient Jurkat cells were treated with different combinations of 4OHT, 3-MB-PP1, and C305. The supernatant was tested in an ELISA to measure IL-2 levels (mean ± s.d., n = 3).

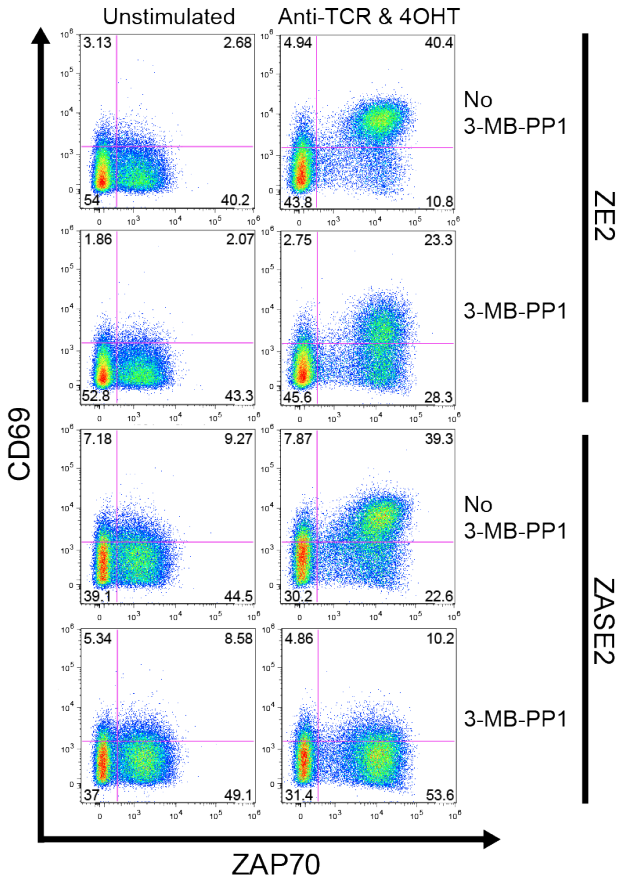

Figure S1.4: Nonspecific effects of 3-MB-PP1 on ERT2-ZAP70.
P116 cells expressing either ERT2-ZAP70 or ZASE were stained for ZAP70 and CD69 and analyzed by flow cytometry. Conditions tested were T cell activation and inhibition by 3-MB-PP1.

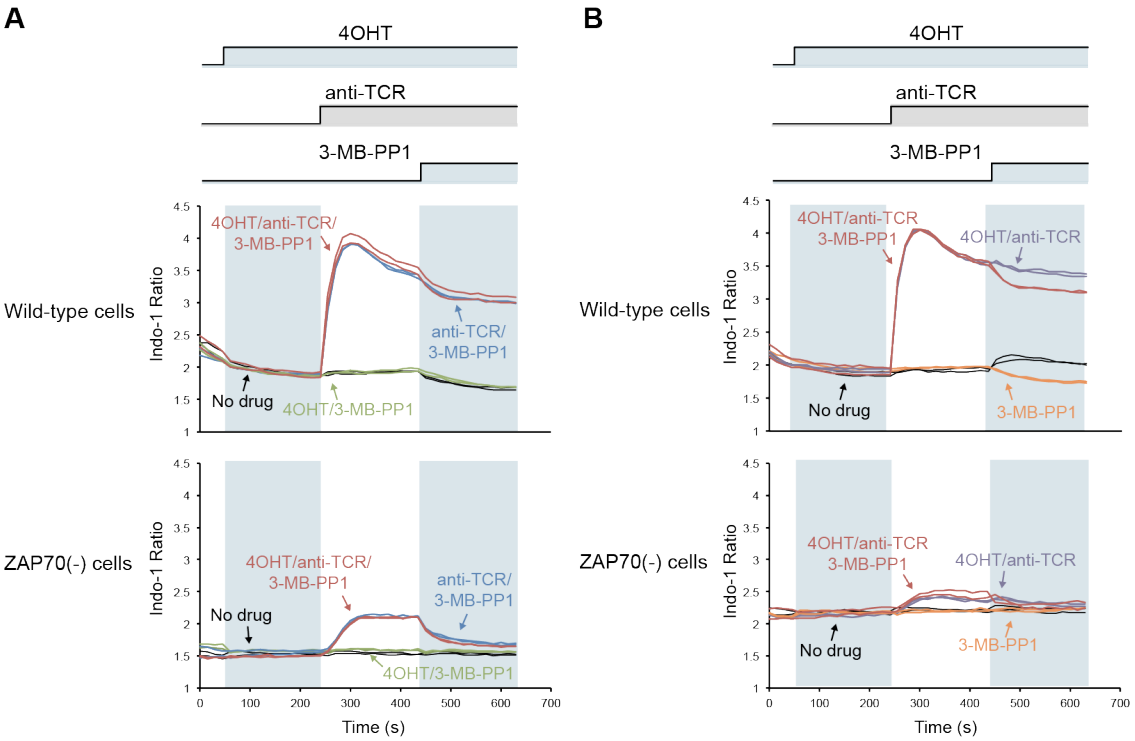

Figure S1.5: Wild-type Jurkat cells and ZAP70-deficient cells treated with various drug combinations.
A) Cells were treated with various activation conditions (4OHT or anti-TCR antibody), then inhibited with 3-MB-PP1. B) Cells were treated with or without activation conditions (4OHT and anti-TCR antibody) and with or without inhibition using 3-MB-PP1.

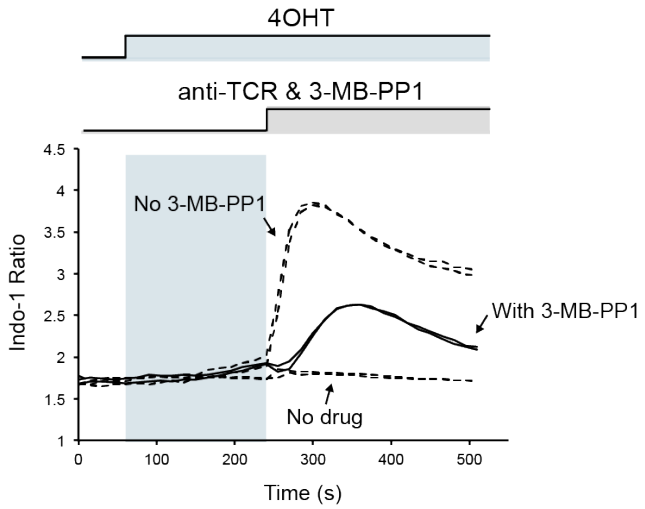

Figure S1.6: Intracellular calcium levels of ZASE-expressing cells upon simultaneous addition of anti-TCR antibody and inhibitor.
Cells were treated with 4OHT, followed by the concurrent addition of anti-TCR antibody and 3-MB-PP1, and calcium levels were monitored over time.

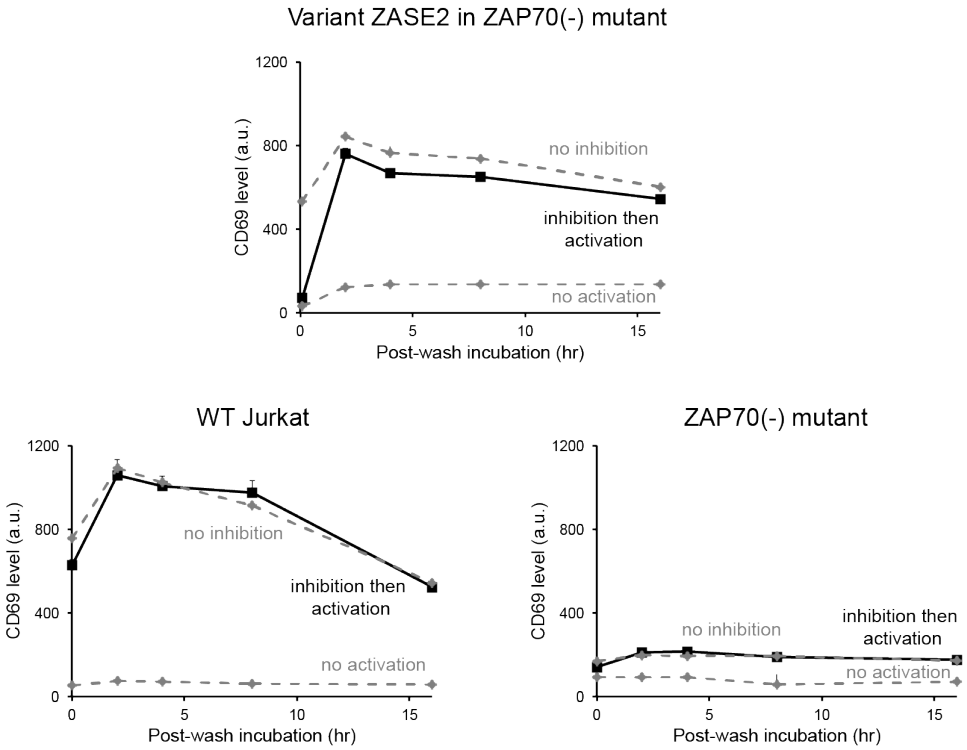

Figure S1.7: OFF-ON activity of ZAP70 switch.
Cells were incubated with 4OHT and 3-MB-PP1, followed by a washout of 3-MB-PP1. They were then left for various time points (0hr, 2hr, 4hr, 8hr, 16hr) before activation. CD69 levels were measured by flow cytometry (mean ± s.d., n = 3). Control samples include cells that were not incubated with 3-MB-PP1 but were activated (no inhibition, positive control), and cells that were inhibited with 3-MB-PP1 but were not activated (no activation, negative control).

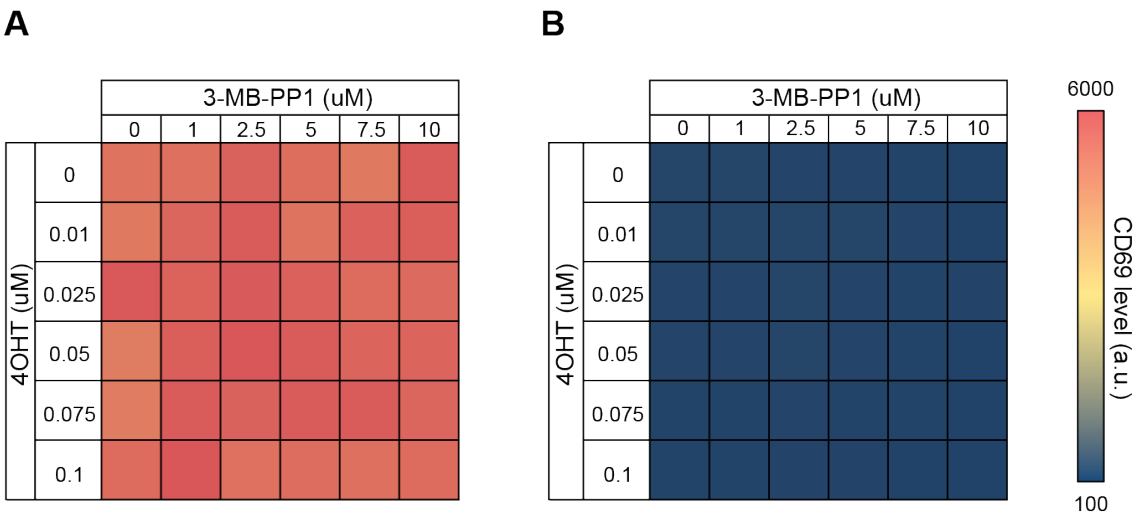

Figure S1.8: 2-D dose response under varying levels of activator and inhibitor. CD69 levels for A) wild-type Jurkat cells and B) P116 cells were quantified using flow cytometry after treatment with different concentrations of 4OHT and 3-MB-PP1.

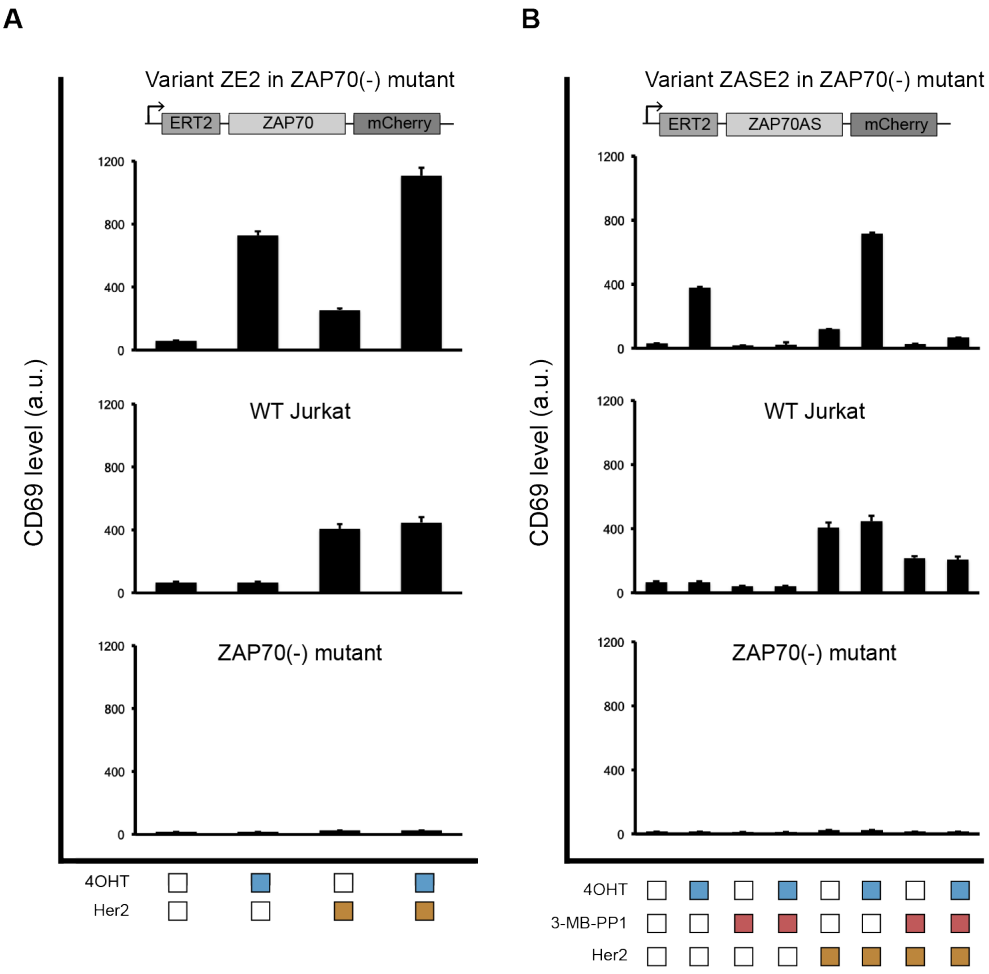

Figure S1.9: ZAP70 switch activity in Jurkat cells expressing a Her2 CAR.
A) P116 cells expressing the ERT2-ZAP70 fusion protein and a CAR were stimulated with 4OHT and Her2 antigen, and CD69 levels measured. B) ZASE and CAR-expressing P116 cells were treated with combinations of 4OHT, Her2, and 3-MB-PP1 to observe whether ZASE is compatible with CARs. CD69 levels were measured as an indicator of T cell activity.

CHAPTER TWO: NS3 CARs for drug-inducible control over T cell activity

2.1 Introduction

To address the issue of safety in T cell immunotherapy, another method of T cell control has been to engineer the receptors themselves, rather than downstream activation pathway proteins like ZAP70. One example of such a receptor is the aforementioned CAR that is gaining widespread popularity in T cell immunotherapy [58]. Several drug-inducible switches have been incorporated into the design of the CAR itself in order to address the issue of safety. While this oftentimes restricts the applicability of the technology to the CAR, these safety mechanisms have shown to be effective at controlling CAR activity. One such switch involved the engineering of the CAR hinge domain such that addition of rapamycin presented the single chain variable fragment (scFv) on the surface and allowed for signaling through the receptor [26]. Another design split the CAR into two components and brought them together in the presence of a small molecule to form a complete CAR [29]. Both of these CAR designs served as ON switches, where T cells were able to activate in the presence of a drug.

Apart from ON switches, there are several other methods of controlling CAR activity. ON switches are beneficial for implementation in potent CARs where off-target toxicity is an issue and T cells should only activate when dictated. However, in CARs deemed relatively safe, an OFF switch may be preferable. This would allow for temporary suppression of T cell activity, or an immediate response to CRS if necessary. CARs can also be designed to activate only in the presence of two antigens. This combinatorial recognition helps prevent on-target off-tumour toxicity, where low levels

of one target antigen may be present on healthy cells. Furthermore, it can aid in signal balancing of the two antigen expression levels, allowing for customisation to the patient. Dual ON-OFF switches can also be developed, similar to ZASE, which are useful for receptors that require tight temporal control. Finally, multiple CARs can also be incorporated into cells to provide the flexibility of changing T cell targets or affinity for the target. These mechanisms each have their unique advantages, while equipping the cells with a level of control.

In our design for CAR switches, we incorporated the serine protease domain of the non-structural protein 3 (NS3). NS3 derives from the hepatitis C virus (HCV) and its biological role is to proteolytically cleave the viral polyprotein at junction sites of non-structural proteins downstream of itself [59, 60]. Various technologies have been developed with respect to the NS3 domain, and though many were designed with the context of HCV treatment in mind, they can be translated for use in synthetic biology applications. For example, several FDA-approved drugs have been developed that inhibit the cleavage ability of NS3 [61-64]. Synthetic biology has exploited this feature of drug inducibility by generating drug-controllable imaging tags or degrons using the NS3 domain [65-67].

An alternate use of the NS3 domain is to bring two components together. A mutant form of the NS3 domain has been created in which one of its key residues is mutated, resulting in an elimination of its protease ability [68]. There also exist NS3-specific peptides, originally designed to serve as NS3 inhibitors for treating HCV infections [69]. However, when used in conjunction with the mutant NS3, the resulting

system no longer self-cleaves, but instead connects two parts, with each component attached to either the mutant NS3 or the peptide. Further developments regarding the NS3 domain include the engineering of "reader" proteins. These proteins were computationally designed to bind specific inhibitor-bound states of the NS3 domain, thus serving as chemically induced dimerization (CID) systems. The NS3 serves as a central receiver protein that can then be targeted to different proteins depending on which inhibitor is present [70].

Furthering the pragmatisms of the NS3 domain, we have applied it to the architecture of CARs and generated several designs in which it could be used to regulate T cell activity. The purpose of NS3 CARs is to provide increased control over the function of these synthetic receptors, and thus make CAR-T cells safer for use in cancer treatment. NS3 CARs retain the traditional components of a CAR, but have the addition of the NS3 domain that is under the regulation of inhibitors, such as grazoprevir and danoprevir. These inhibitors can block NS3 protease activity or competitively bind to the domain, making the NS3 domain quite versatile in its function. Here, we describe a number of ways the NS3 domain can be used to control CAR activity.

The first of these CARs is an ON switch, where NS3 is buried within the traditional domains of a CAR. Grazoprevir is then used to inhibit NS3 self-cleavage from the CAR, which would otherwise disassemble the receptor. The second application is an OFF switch, which involves the division of a CAR into two parts. In the absence of grazoprevir, a NS3-binding peptide links these two segments together allowing for T cell activation through the CAR, which is then disrupted if the inhibitor competes for binding

to the NS3 domain. Lastly, we explore the use of NS3 in more complex CARs designs, such as implementing the prior ON switch in a logic gate with a distinct CAR tagged with an inducible degradation domain. This AND gate is regulated by two distinct drugs, and allows for combinatorial control over CAR activity. Additionally, the aforementioned OFF switch can be applied to other CAR technologies, such as the SUPRA CAR [71]. This universal CAR allows for changing of its antigen specificity and affinity, and when used together with the OFF switch, creates an ON-OFF capability. NS3 CARs can also change T cell antigen specificity by targeting the NS3 to different "reader" proteins. This could allow us to change which receptor the T cell activates through by controlling which inhibitor is present. These advanced CAR designs exemplify the increased manipulation we can have over CAR activity using the NS3 domain, as well as the compatibility of NS3 CARs with other technologies.

2.2 Results

2.2.1 NS3 CAR as an ON switch

To explore the use of the NS3 domain as an ON switch, it was integrated into the structure of a CAR. The NS3 domain itself is flanked by NS5A/5B and NS4A/4B cut sites to allow self-excision of the protease from the CAR. In the absence of grazoprevir, NS3 excises itself, thereby resulting in a fragmented CAR that cannot signal. When grazoprevir is added, it inhibits the protease activity of NS3, thus keeping the CAR intact, and allowing for T cell activation through CAR signalling (**Figure 2.1a**). To test this, we created several versions of a CAR with NS3 positioned between different domains

(**Figure 2.1b**). The CARs were designed to target CD19 as a proof of principle.

This ON switch was introduced into primary T cells, and results showed that in the presence of CD19+ NALM6 cells and grazoprevir, CD69 and cytokine levels were elevated in the ON CAR, and furthermore in all three versions of it (**Figure S2.1a**). A traditional CAR containing no NS3 domain was tested as a comparison and indicated T cell activation whenever the target cells were present, while wild-type cells did not respond to any condition (**Figure 2.1c**). To evaluate the ability of the ON CAR to control the cytotoxicity of these T cells, the killing of CD19+ NALM6 cells was also quantified. The ON CAR showed induced cell killing in the presence of grazoprevir in all versions of the CAR (**Figures 2.1d and S2.1b**). We then varied the concentration of grazoprevir to determine if we could modulate CAR activity using drug concentration. The dose response observed in cytokine levels and cell killing indicated that we could regulate T cell activity by varying the amount of NS3 inhibitor (**Figure 2.1e**). Furthermore, the cytotoxicity of the ON CAR was tested with four different NS3 inhibitors, all of which are FDA-approved. Results showed that all four inhibitors could control ON CAR activity, with grazoprevir and glecaprevir able to induce cell killing at lower concentrations (**Figure S2.1c**).

The temporal response of the NS3 ON CAR to grazoprevir was further tested in a cell killing assay involving primary CD8+ T cells and an anti-CD19 CAR. Upon addition of grazoprevir, the killing efficiency of the cells elevated to levels comparable with cells expressing a traditional CAR. When the drug was removed, killing levels decreased to basal levels, and when grazoprevir was re-introduced the killing efficiency re-matched

previous levels (**Figure S2.1d**). This shows the ability of the ON CAR to re-activate following previous stimulation.

Testing the compatibility of the NS3 ON CAR with other scFvs, an anti-Her2 scFv was additionally explored in NS3 ON CARs expressed in primary T cells. CD69 and IL-2 levels were raised in the presence of target cells and grazoprevir for all three versions of the CAR (**Figure S2.2a**). The killing efficiencies for all three versions of the CAR were found to be comparable, and the responsiveness to grazoprevir was similar to that of the anti-CD19 NS3 CAR (**Figures S2.2b and S2.2c**). Of the three versions of the NS3 ON CAR tested, version 2 resulted in the highest cytokine release and cleanest basal levels for both the anti-CD19 and anti-Her2 CARs, and thus we proceeded with this construct in further experiments.

The NS3 ON CAR can also be applied to other immune cell types. For example, CARs can suppress immune responses when introduced into regulatory T (Treg) cells. Treg cells are responsible for maintaining immune homeostasis and tolerance, and preventing autoimmunity. Due to their unique role in the immune system, Treg cells have been under investigation as therapeutic agents for treating autoimmune diseases, such as type 1 diabetes, or preventing organ transplant rejection [72-75]. The NS3 ON CAR was introduced into Treg cells to evaluate whether it can regulate its activity. When Treg cells are inactive, CD4+ T cells are able to freely proliferate, which is then suppressed if the Treg cells become active. Thus, if the ON CAR is expressed in Treg, the cell's suppressive behaviour could be activated by the presence of grazoprevir and activation of the CAR. As a proof of principle, Treg cell lines were generated expressing version 2 of

the anti-Her2 ON CAR. To confirm the regulation of the suppressive ability of these ON CAR Treg cells by grazoprevir, we incubated these cells with anti-CD19 CAR-expressing CD4+ T cells and Her2+/CD19+ NALM6 cells in the absence and presence of the inhibitor (**Figure S2.3a**). CD4+ proliferation was evaluated by staining with a fluorescent cell tracer and tracking proliferation following 6 days of incubation. The data showed that ON CAR Tregs were able to activate in the presence of grazoprevir and suppress CD4+ proliferation. Furthermore, the efficiency of suppression was comparable with that of Tregs expressing a traditional anti-Her2 CAR (**Figure S2.3b and S2.3c**).

2.2.2 NS3 CAR as an OFF switch

To further explore how the NS3 domain could be used to advance CAR design, an NS3 OFF CAR was developed. The CAR was designed by splitting its structure into two components, similar to the design of other split drug-controllable CARs [29]. The first component contains the scFv and a NS3-specific peptide, and the second component, tethered to the membrane, contains the NS3 and the CD3ζ signalling domains. A catalytically-dead version of NS3, which carries a mutation at residue 139 of a serine to alanine, is used to avoid NS3 self-cleavage from the CAR. In the absence of grazoprevir, the peptide is expected to bind to NS3, allowing for full CAR formation and signalling. Upon grazoprevir addition, the inhibitor competes for NS3 binding, thus disrupting CAR structure and shutting off CAR activation (**Figure 2.2a**). Several designs of the CAR were tested, with the peptide placed after the hinge or various costimulatory domains, and the NS3 placed at various positions in the second component (**Figure 2.2b**).

The different permutations of these components were first tested in Jurkat T cells

and their functionality compared. These Jurkat cells were modified to express GFP upon the activation of the NFAT pathway, thus allowing us to detect T cell activation through GFP expression. Cells were transduced with lentivirus encoding both components on a single construct and the system was tested with anti-CD19 CARs. CAR-expressing Jurkat T cells were incubated with CD19+ NALM6 cells in the presence or absence of grazoprevir and the resulting GFP levels measured by flow cytometry. It was found that expression of components consisting of the scFv and peptide (component a), or the scFv, peptide and 4-1BB domain (component b), were weak and no change in GFP levels were observed here (**data not shown**). However, first components encoding CD28 and peptide (component c) or both CD28 and 4-1BB costimulatory domains and peptide (component d) resulted in CARs that could activate when mixed with target cells and shut off when grazoprevir was present. NFAT activity and CD69 expression were generally higher if both costimulatory domains were in the first component, and the combination with a second component consisting of 4-1BB followed by NS3 and CD3z (component i) allowed for even stronger T cell activation (**Figure S2.4a**). When paired with components c and d, second component i and iii resulted in the highest CD69 fold change, and thus we proceeded with component combinations c+i, c+iii, d+i and d+iii in further analysis (**Figure S2.4b**).

The NS3 OFF CAR was further tested in primary T cells, and constructs were similarly introduced. The OFF CAR consisting of components c and i was able to shut off T cell activity, as measured by CD69 and cytokine levels, whereas wild-type and traditional CAR-expressing T cells maintained their absence and persistence of T cell

activation respectively (**Figure 2.2c**). The cytotoxicity of this OFF CAR was also inhibited in the presence of grazoprevir, as was observed in a killing assay involving CD19+ NALM6 cells (**Figure 2.2d**). While activity was similarly shut off in the presence of inhibitor for other component combinations, in contrast with what was observed in Jurkat T cells, component c resulted in higher T cell activation (as measured in cytokine levels) in the absence of grazoprevir than component d (**Figure S2.4c**).

2.2.3 Advanced designs for NS3 CARs

To delve into the possible use of the NS3 CAR in more complex designs, the NS3 ON CAR was first used to create an AND gate. A dual molecule tunable logic AND gate could enhance the targeting specificity of CAR-T cells, so to do this we designed a CAR that contained a dihydrofolate reductase (DHFR) degron (DD) regulated by a second drug, to be used in conjunction with the NS3 CAR. DHFR reduces dihydrofolate to tetrahydrofolate and is essential for E. coli replication and survival, and TMP is an antibiotic that can bind to E. coli DHFR with a much higher affinity than its mammalian counterpart. Fusion of the engineered DHFR domain with a protein of interest destabilizes the protein, and when TMP binds to the DHFR domain it stabilizes the fusion protein, thus serving as an inducible protein expression system [55]. Here, we generated a combinatorial logic AND gate by distributing CAR intracellular signalling domains between two distinct scFvs with each signalling domain associated with either NS3 or the DD. Our AND gate CAR system comprised of an anti-Her2 receptor with the NS3 domain positioned between the scFv and CD3ζ domains, followed by a second anti-Axl receptor with the DD positioned after the CD28 domain, thus generating a functional

dual-molecule controllable CAR-T cell (**Figure 2.3a**).

The drug tunability of this system was tested in primary CD8+ T cells. To test the inducibility of this AND gate CAR, we co-cultured these T cells with Her2+/Axl+ NALM6 cells and varied the amount of grazoprevir and TMP. Results indicated that maximal levels of cell killing occurred when both grazoprevir and TMP were present, though background killing was observed when solely grazoprevir was added (**Figure S2.5**). Modulation of CD69 and cytokine levels was also observed by varying the amounts of the small molecules, suggesting that the level of T cell activation could be tuned using different doses of the two drugs (**Figure 2.3b**).

Furthering the applications of the NS3 OFF CAR, we also created an ON-OFF CAR by applying the design to existing SUPRA CAR technology. The structure of a SUPRA CAR includes a leucine zipper pair, half of which is attached to the intracellular CAR domains. The corresponding zipper is attached to an scFv that is externally introduced. The latter fusion protein is termed the zipFv, and when it dimerizes with the prior structure, it forms a full CAR, allowing for T cell signalling [71]. In our ON-OFF CAR, we divided the intracellular CAR domains into two components, similar to the NS3 OFF CAR, and replaced the scFv with the SUPRA CAR leucine zipper technology. In the absence of zipFv or grazoprevir, the CAR remains inactive as there is no scFv targeting it to any cell. However, when zipFv is added, the fully formed CAR allows for T cell signalling, which is then disrupted if grazoprevir outcompetes the NS3-specific peptide for binding to the catalytically-dead NS3 domain (**Figure 2.3c**).

This ON-OFF CAR was introduced into primary CD8+ T cells and IFN-gamma

levels showed that cells were able to switch on in the presence of anti-Her2 zipFv and target Her2+ NALM cells, which was then shut off when grazoprevir was present. Cytotoxicity of these T cells was additionally measured in a killing assay involving Her2+ NALM6 target cells, and results recapitulated what was observed in the cytokine data (**Figure 2.3d**).

Lastly, NS3 "reader" proteins were applied to CAR design. These "reader" proteins bind specific inhibitor-bound states of NS3, and should behave orthogonally. In our NS3 reader CARs, we adopted the danoprevir/NS3 complex reader (DNCR) and grazoprevir/NS3 complex reader (GNCR), which are regulated by danoprevir and grazoprevir respectively. Similar to the OFF CAR, the NS3 reader CARs were designed by splitting the CAR into two components. The first component consists of the scFv, CD28 costimulatory domain, and reader domain, whilst the second component encodes a catalytically-dead NS3 and the CD3z signalling domain. NS3 should bind to the GNCR in the presence of grazoprevir, and the DNCR in the presence of danoprevir, allowing us to theoretically switch its target receptor by changing the drug (**Figure 2.3e**).

Prior to seeing if the GNCR and DNCR CARs can be used in the same cell, we tested their functionality separately in anti-CD19 CARs. Previously described NFAT-GFP Jurkat cells were transduced with lentivirus encoding the NS3 reader CARs and incubated with CD19+ NALM6 target cells with or without inhibitor. GFP levels were then measured by flow cytometry to determine T cell activation. DNCR CARs showed an increase in NFAT activity when danoprevir was present, and comparably the same was seen in GNCR CARs with grazoprevir (**Figure 2.3f**).

2.3 Discussion and Conclusion

Here, we describe multiple ways in which the NS3 domain can be applied to CAR design. They include an ON switch, OFF switch, and three complex CAR designs involving each of these respective switches and NS3 "reader" proteins. Each of these CARs functions effectively, as seen with the regulation of T cell activation markers (CD69 and NFAT) and cytokine levels, as well as cytotoxicity assays. Furthermore, the activity of the ON and AND gate CARs can be tuned through the dosing of small molecules. With the ON CAR, we have additionally shown the potential of these technologies to control other scFvs and cell types.

We have shown that the NS3 ON CAR can effectively regulate the activity of T cells, but the basal killing of AND gate CAR T cells in the presence of only grazoprevir needs to be addressed. This could be arising from low activation of the NS3-containing component, which essentially forms a first generation CAR. First generation CARs activate T cells more weakly than second or third generation CARs, but it could be sufficient for triggering this basal level of cytotoxicity [76-78]. Alternatively, the basal levels could be due to inefficient degradation of the DD CAR. For the AND gate CAR to be more reliably used, this would need to be addressed.

Additionally, though grazoprevir has shown to effectively regulate NS3 CAR activity, it was noted that the level of cytokine release was lower than what is observed in traditional CARs. We postulate that receptor expression could be the reason for this, as the inclusion of NS3 in CARs results in larger constructs. This impacts lentiviral packaging capability and thus receptor expression on cells [79]. Alternatively, the

presence of NS3 in the receptor could be targeting the receptor for degradation. Further investigation into this would be required, but since cytotoxicity levels are still comparable with traditional CARs, it is possible the lower receptor expression level may not be an issue.

Though *in vitro* experiments indicate these NS3 CARs work effectively in primary T cells, it remains to be seen whether they are functional *in vivo* before they can be considered for clinical use. *In vivo* studies for the NS3 ON and OFF CARs are currently underway, and the activity of the CARs are being tested in a mouse leukemia model. While initial experiments are being performed to see if the switches can be controlled by grazoprevir, to evaluate whether the technology would address the issue of T cell overactivity, it should be studied in a CRS setting. This could be accomplished by inducing CRS in mice, using a method previously defined by others, and determining whether it can be abated by our systems by measuring correlating cytokine levels [80]. If the NS3 CARs are able to mitigate CRS, this technology could then potentially be moved forward to clinical testing. An advantage of using NS3 CARs for T cell therapy is that many inhibitors used to regulate the NS3 domain are already FDA-approved [81-83]. This suggests the system will be safe to use *in vivo* and ultimately when treating patients. Technologies incorporating existing FDA-approved drugs could potentially be cleared for use in the clinic quicker as well.

While the NS3 domain has been largely studied as a target for HCV treatment, we have expanded on its potential for use in synthetic biology applications, specifically in the design of CARs. Its use as a self-cleaving entity and CID make it advantageous in

receptor design due to its versatility in function. Furthermore, its compatibility with many FDA-approved drugs suggests it could be safely regulated *in vivo* and could potentially accelerate its clearance for clinical use. As such, we see a great promise for the use of these NS3 CARs in T cell therapy.

2.4 Methods

2.4.1 Plasmids

All CAR constructs were introduced into primary human T cells and Jurkat T cells using pHR lentivectors, and plasmids were packaged into lentiviruses using pDelta, Vsvg and pAdv packaging and envelope plasmids [57]. Expression of the CARs was driven by an EF-1 alpha promoter and kozak sequence. CARs contained either a myc or V5 tag after the scFv, or a mCherry fluorescent protein at the C-terminus in order to verify construct expression. In NS3 OFF CAR, SUPRA/NS3 OFF CAR and reader CAR experiments, both components were introduced into cells using a single construct, with the components separated by either a P2A or T2A sequence. The two components of the AND gate CAR were introduced on separate constructs.

2.4.2 Cell culture

Lentiviruses were generated using HEK293FT cells, which were cultured in Dulbecco's modified Eagle's medium (DMEM) supplemented with 10% fetal bovine serum (FBS; Thermo Fisher, 10437028), penicillin/streptomycin (Corning, 30001CI), L-glutamine (Corning, 25005CI) and 1mM sodium pyruvate (Lonza, 13115E). Primary peripheral blood mononuclear cells (PBMCs), CD4+ and CD8+ T cells were isolated

from whole peripheral blood obtained from healthy donors at the Blood Donor Center at Boston Children's Hospital (Boston, MA) as approved by the University Institutional Review Board (IRB). CD4+ and CD8+ T cells were isolated using the RosetteSep Human T cell enrichment cocktail (STEMCELL Technologies, 15022 and 15023), and PBMCs were isolated using Lymphoprep (STEMCELL Technologies, 07851). Regulatory T cells were isolated using the EasySep human CD4+CD127lowCD25+ regulatory T cell isolation kit according to manufacturer's protocol (STEMCELL Technologies, 18063). Primary T cells were cultured in X-Vivo 15 media (Lonza, 04-418Q) supplemented with 5% human AB serum (Valley Biomedical, HP1022), 10mM N-acetyl L-Cysteine (Sigma, A9165), 55µM 2-Mercaptoethanol (Thermo Fisher, 21985023), and 30-200U/ml IL-2 (NCI BRB Preclinical Repository). Jurkat T cells and NALM6 cells were cultured in RPMI 1640 supplemented with 5% FBS, L-glutamine and penicillin/streptomycin. CD19-positive NALM6 cells expressing Her2, mCherry, and GFP, or just BFP alone, were used as target cells in assays.

2.4.3 Lentivirus generation and transduction

HEK293FT cells were co-transfected with lentivirus packaging/envelope plasmids (described above) and CAR-encoding vectors using polyethylenimine (PEI). After 24 hours, media was replaced with ultraculture (Lonza, 12-725F) supplemented with penicillin/streptomycin, L-glutamine, 0.5M sodium butyrate and 1mM sodium pyruvate. Virus-containing media was collected for the following 48 hours, and spun down to remove cell debris. Viral media was then concentrated using Lenti-X Concentrator (Takara, 631232) at a 3:1 ratio and incubated at 4°C overnight prior to

centrifugation at 1500xg for 45 minutes at 4°C. To transduce primary T cells, lentiviral spinfection was performed. Cells were thawed 2 days prior to spinfection, and 1 day prior to spinfection cells were activated using Human T-activator CD3/CD28 Dynabeads (Thermo Fisher, 11131D) and cultured in 200U/ml IL-2. Concentrated virus was plated on non-TC treated 6-well plates coated with retronectin (Takara T100B), and spun for 90 minutes at 1200xg. Virus was then aspirated and activated T cells added to the virus-coated wells, followed by incubation at 37°C. To transduce Jurkat T cells, concentrated virus was diluted in RPMI 1640, mixed with cells and incubated for 72 hours at 37°C before virus was washed out.

2.4.4 Antibodies and cell dyes

To stain for CD69, an APC-Cy7-conjugated mouse anti-human CD69 antibody (BD Pharmingen, 557756) was used at a dilution of 1:100. Myc-tagged and V5-tagged CARs were stained using an Alexa Fluor 488-conjugated mouse anti-myc antibody (R&D Systems, IC3696G) and an Alexa Fluor 647-conjugated mouse anti-V5 antibody (Invitrogen, 451098) respectively. For surface staining, cells were washed twice with FACS buffer (1x phosphate buffered saline (PBS), 0.1% NaN3, 1% BSA, 2mM EDTA) before incubating with antibody in the dark at room temperature for 40 minutes. Cells were then washed and resuspended with FACS buffer before analysis on an Attune NxT flow cytometer.

2.4.5 Cytotoxicity assay

Cytotoxicity assays were carried out by incubating primary T cells and NALM6 target cells at a 1:1 effector to target (E:T) ratio overnight at 37°C. 1μM grazoprevir

(MedChemExpress, HY-15298) was added at the time of assay, and DMSO was used as a control vehicle. When testing other NS3 inhibitors, various concentrations in the range of 0-5 μM of grazoprevir, danoprevir, simeprevir, glecaprevir and boceprevir were used in dose response experiments. Following a 16 hour incubation, the supernatant was saved and cells were analysed by flow cytometry to count the number of remaining live NALM6 cells by gating for either GFP+/mCherry+ cells or BFP+ positive cells depending on the target NALM6 cell line used. Killing efficiency was calculated as the percentage of cells killed compared to control wells containing NALM6 cells and no T cells.

2.4.6 Cytokine release assay

Supernatant from cells incubated with various combinations of target cells and NS3 inhibitors was saved and tested in an enzyme-linked immunosorbent assay (ELISA) to measure IFN-gamma and IL-2 levels. The BD OptEIA human IFN- γ and IL-2 ELISA kits (BD Biosciences, 555142 and 555190) were used according to manufacturer's instructions with a 0.05% Tween-20 in PBS (Thermo Scientific, 28352) wash buffer, and remaining reagents from BD OptEIA Reagent Set B (BD Biosciences, 550534). ELISAs were performed with 96-well MaxiSorp plates (Thermo Scientific, 442404).

2.4.7 Cell proliferation assay

Cell proliferation assays were performed using the CellTrace Violet kit (Thermo Fisher, C34571) as per manufacturer's instructions.

2.4.8 Statistics

Data between two groups was compared using an unpaired two-tailed t-test. A *P*-value < 0.05 was considered to be statistically significant.

2.5 Figures

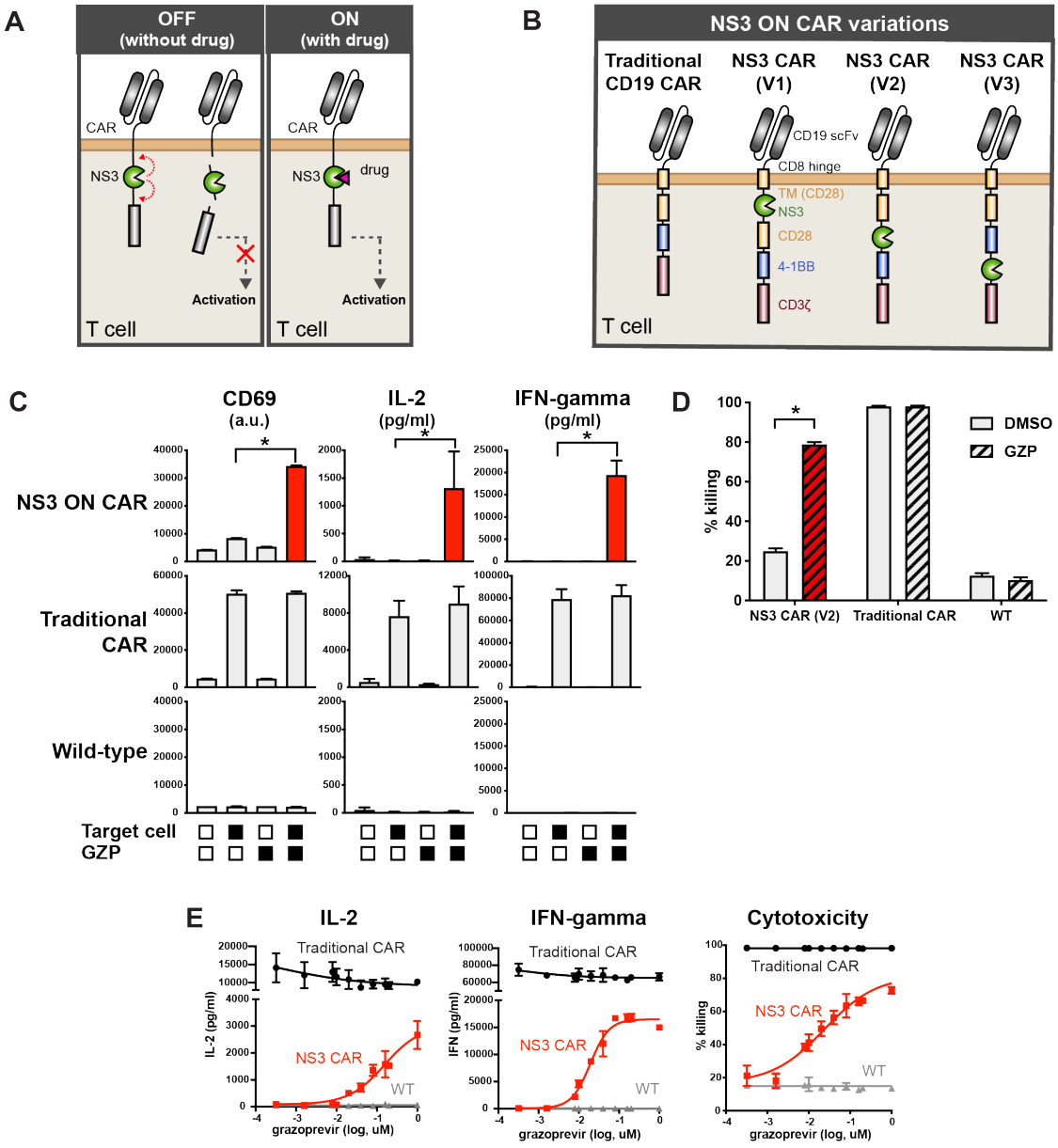

Figure 2.1: Characterisation of the NS3 ON CAR.
A) Schematic illustrating how the NS3 ON CAR functions. B) Variations of the NS3 ON CAR that were developed. C) Various primary T cell lines were treated with combinations of NS3 inhibitor and target cells, with CD69 and cytokine levels quantified (mean ± s.d., n = 3, $*P < 0.05$). D) Comparison of cytotoxicity levels of NS3 ON CAR (version 2) with traditional CAR and wild-type cells (mean ± s.d., n = 3, $*P < 0.05$). E) Dose response of various cell lines to increased levels of grazoprevir, as measured in cytokine levels and cell killing (mean ± s.d., n = 3, $*P < 0.05$).

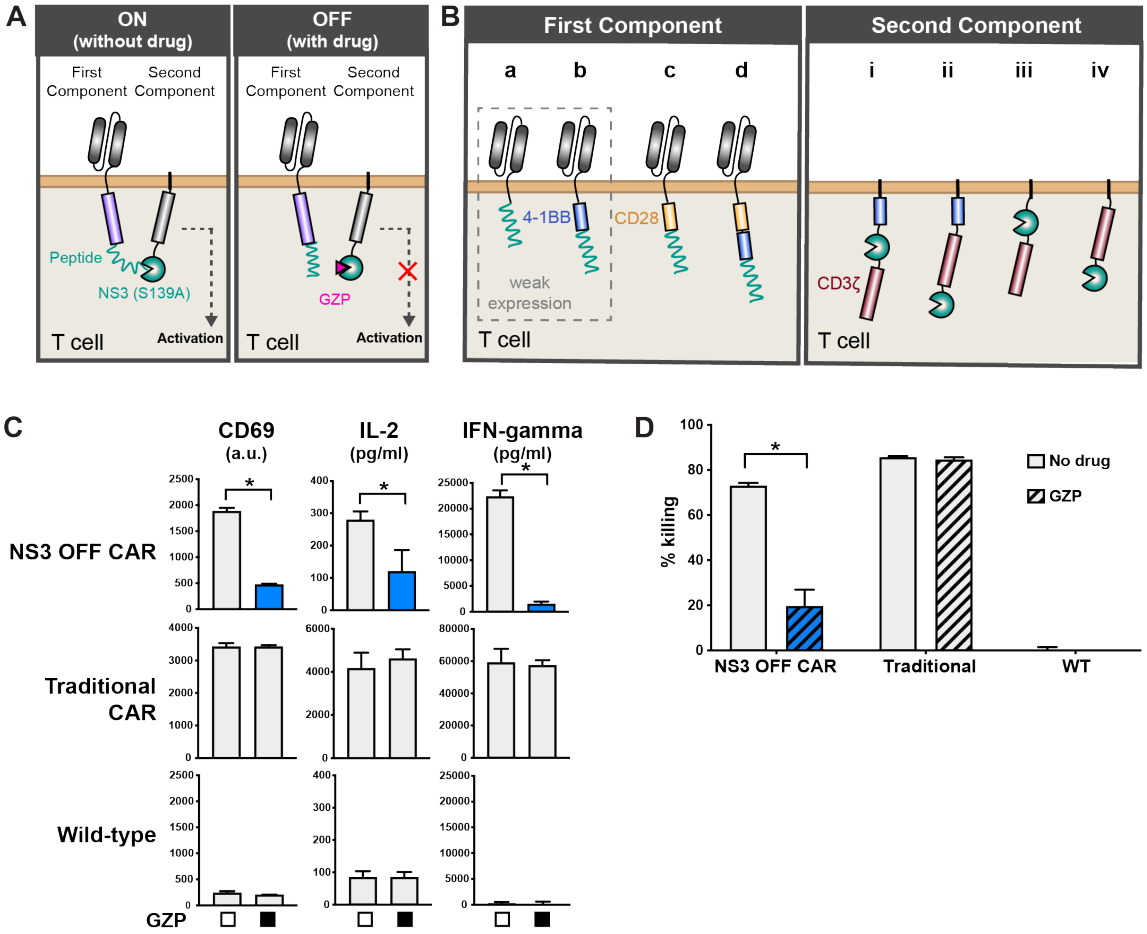

Figure 2.2: Characterisation of the NS3 OFF CAR.
A) Schematic illustrating how the NS3 OFF CAR functions. B) Variations of the two components that make up the NS3 OFF CAR. C) Various primary T cell lines were treated with or without grazoprevir (all in the presence of target cells), and CD69 and cytokine levels quantified (mean ± s.d., n = 3, *$P < 0.05$). D) Comparison of cytotoxicity levels of NS3 OFF CAR (components c and i) with traditional CAR and wild-type cells (mean ± s.d., n = 3, *$P < 0.05$).

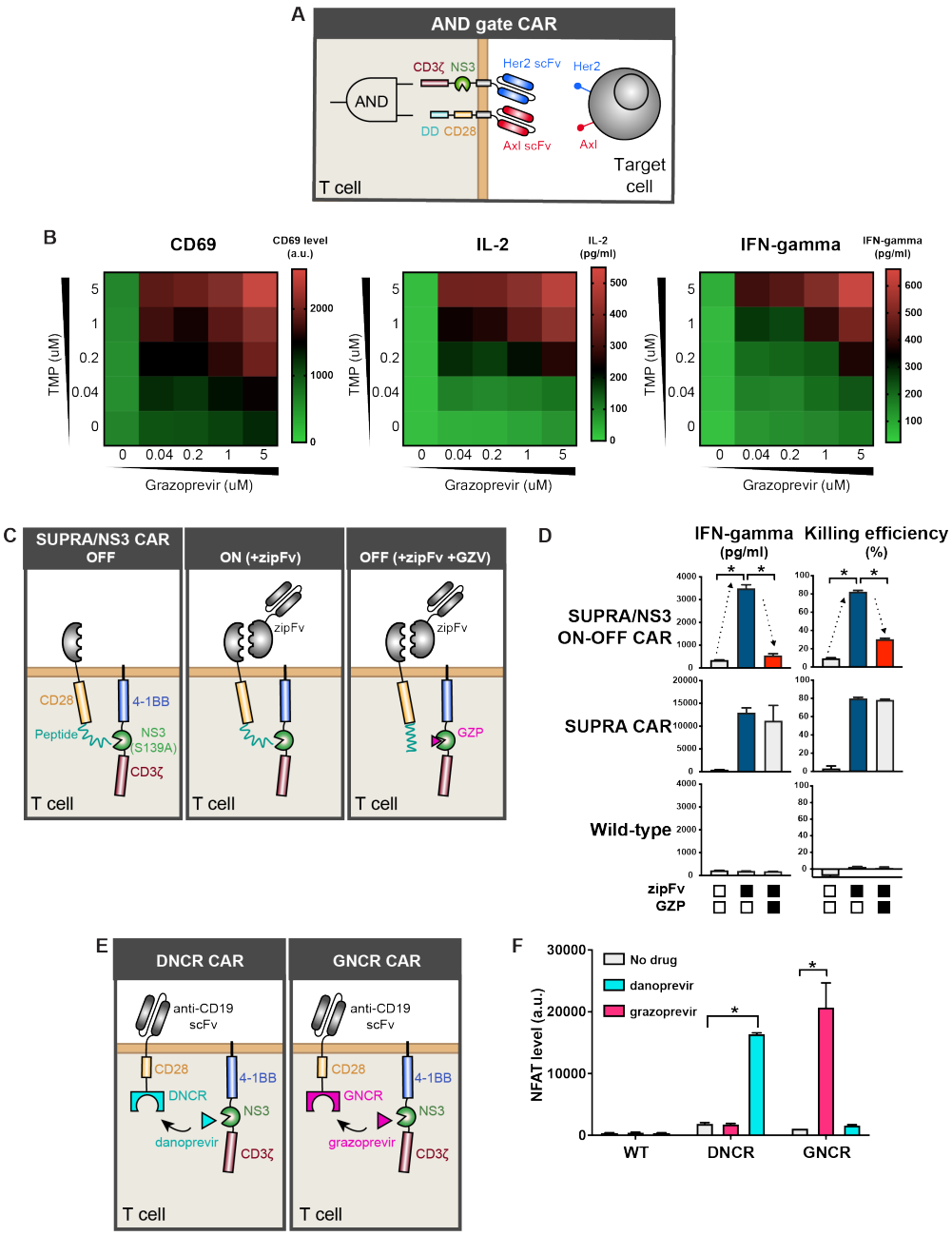

Figure 2.3: Complex designs for NS3 CARs.
A) Schematic of the AND gate CAR that incorporates an NS3 ON CAR and a distinct DD CAR. B) Dose response of the AND gate CAR in response to increased levels of grazoprevir and TMP. C) Schematic of the SUPRA/NS3 ON/OFF CAR. D) Regulation of the SUPRA/NS3 CAR using combinations of zipFv and grazoprevir, as measured by IFN-gamma and cell killing ability (mean ± s.d., n = 3, *$P < 0.05$). E) Schematic of the NS3 reader CARs. F) Ability of the NS3 reader CARs to regulate NFAT activity in Jurkat T cells (mean ± s.d., n = 3, *$P < 0.05$).

2.6 Supplementary Figures

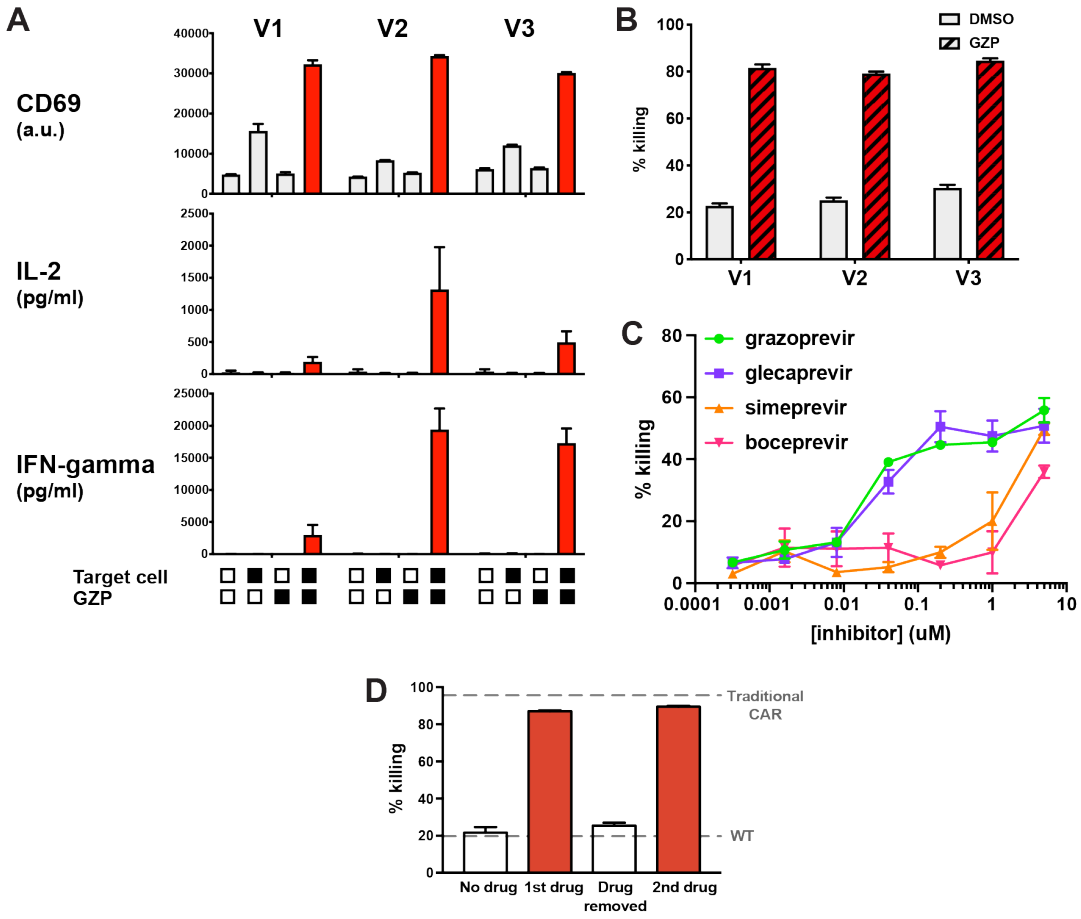

Figure S2.1: Variations of the NS3 ON CAR and further development.
A) Regulation of the activity of various NS3 ON CARs in primary T cells (measured by CD69 and cytokine levels) using combinations of target NALM6 cells and grazoprevir. B) Cell killing of target NALM6 cells using primary T cells expressing various NS3 ON CARs in the absence and presence of grazoprevir. C) Cytotoxicity of NS3 ON CAR-expressing primary T cells in response to various NS3 inhibitors (version 2 NS3 ON CAR). D) Cytotoxicity response of NS3 ON CAR-expressing CD8+ T cells to grazoprevir being added, washed out and re-introduced.

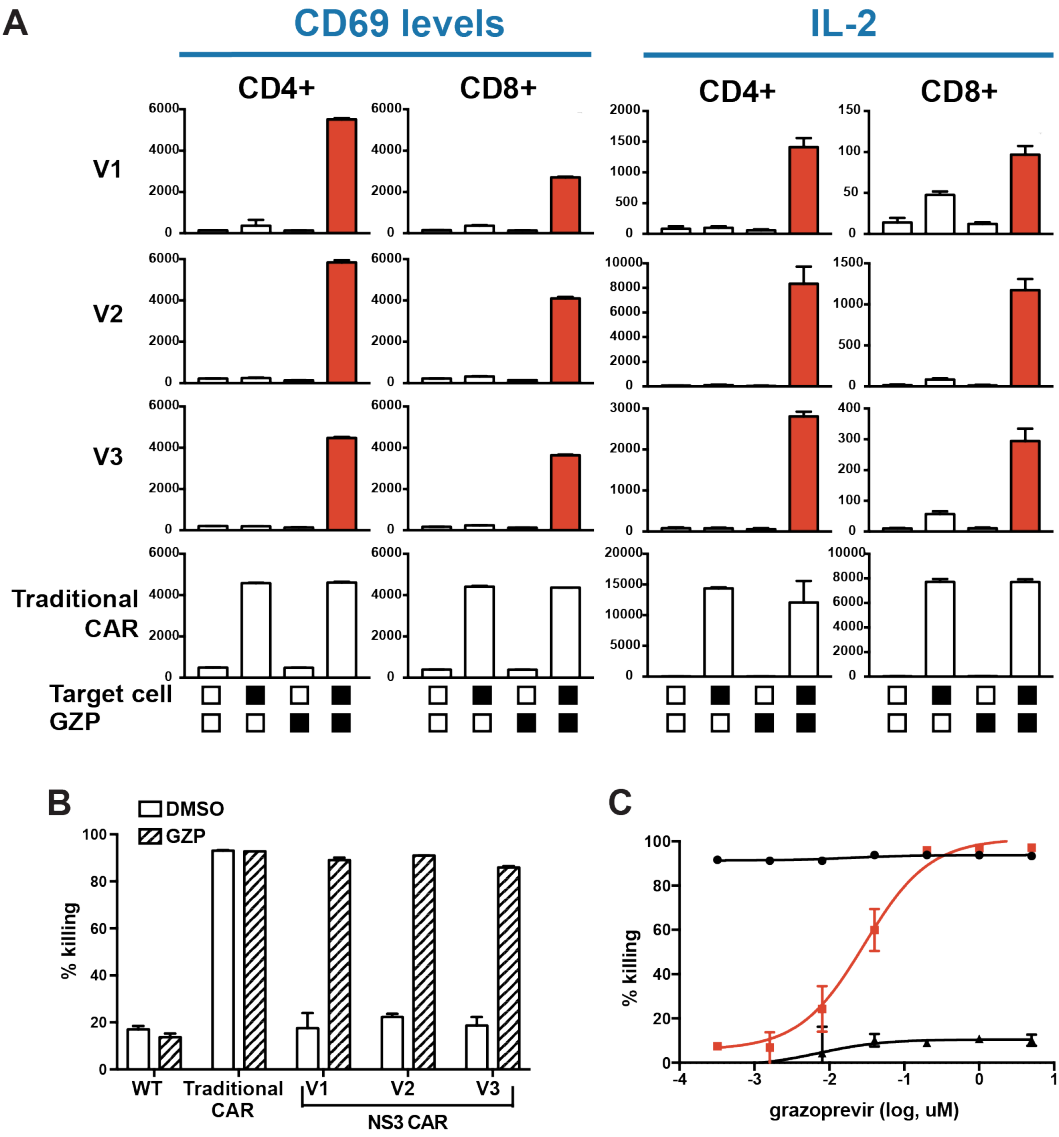

Figure S2.2: Application of NS3 ON CAR to Her2 scFv.
A) Response of variations of anti-Her2 NS3 ON CAR to combinations of target cells and grazoprevir when expressed in CD4+ and CD8+ T cell subsets. B) Cell killing ability of CD8+ T cells expressing various NS3 ON CARs targeting Her2. C) Dose response of anti-Her2 NS3 ON CAR CD8+ T cells to increased amounts of grazoprevir, as measured in cell killing efficiency.

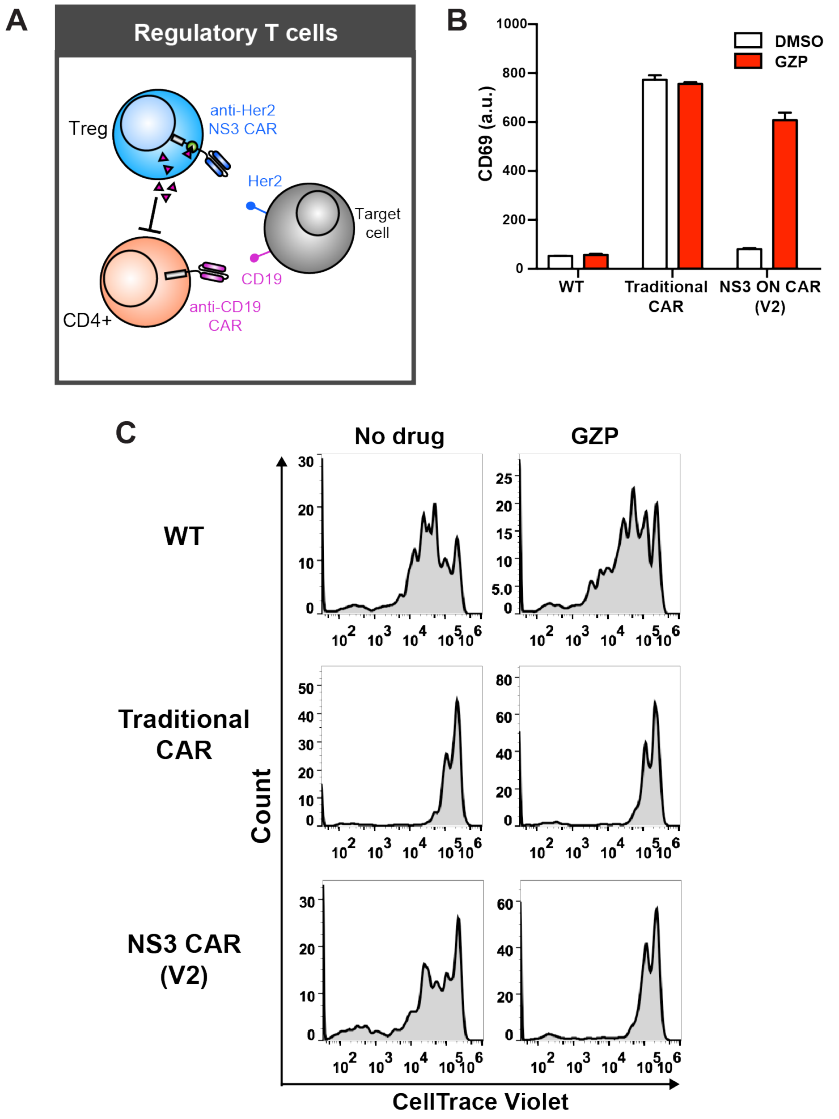

Figure S2.3: Application of NS3 ON CAR to regulatory T cells.
A) Schematic of how NS3 ON CAR-expressing T cells interact with CD4+ T cells and target NALM6 cells in proliferation assay. B) Levels of early activation marker expressed by NS3 ON CAR regulatory T cells in the presence and absence of NS3 inhibitor. C) CD4+ T cell proliferation when co-incubated with various regulatory T cell lines in the presence and absence of NS3 inhibitor.

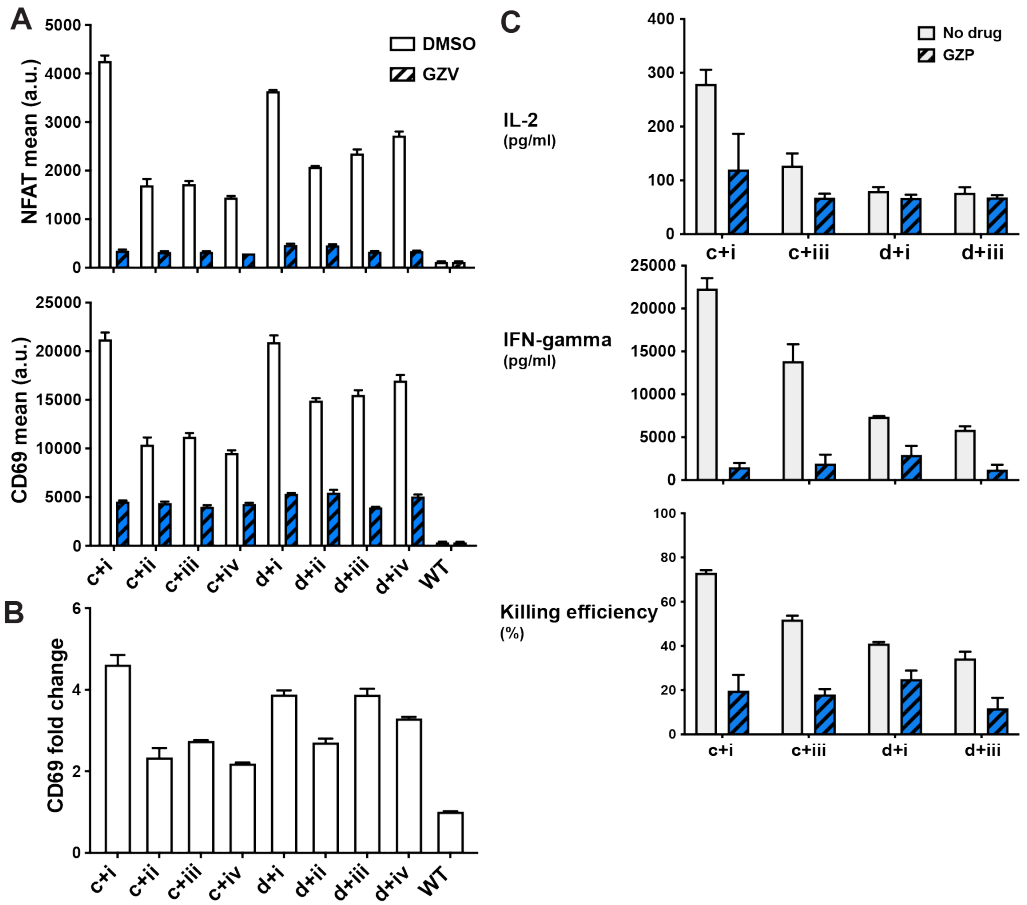

Figure S2.4: Variations on the NS3 OFF CAR.
A) Jurkat T cell activity as measured by NFAT activity and CD69 levels when variations of the NS3 OFF CAR are expressed. B) Fold change observed in CD69 levels when grazoprevir is added to Jurkat T cells expressing variations of OFF CAR. C) Cytokine release and cytotoxicity of primary T cells expressing different versions of the NS3 OFF CAR.

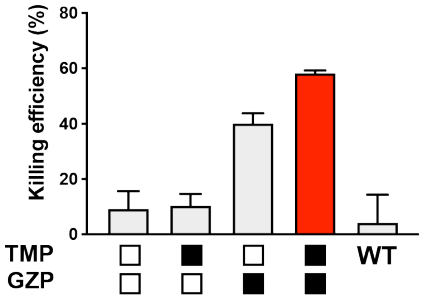

Figure S2.5: Cytotoxicity of cells expressing the NS3 AND gate CAR.
Cell killing ability of CD8+ T cells expressing the NS3 AND gate CAR in response to various combinations of TMP and grazoprevir.

CHAPTER THREE: An analog-to-digital reporter for use in high-throughput screening

3.1 Introduction

The potential use of synthetic biology in medical applications extends beyond engineering safety switches for cell therapy. In particular, synthetic circuits are widely used in the field as a means of programming cells to perform new functions, and this can be advantageous in applications such as drug discovery [84-88]. A benefit of engineering cells with these genetic circuits is the ability to control the resulting output from a given input, which can be useful when considering cell-based reporters. In current high-throughput screening methods, cells are introduced with a construct encompassing regulatory sequences driving expression of a reporter gene, such as luciferase or a fluorescent protein [89-92]. When used in drug screening, this provides a means of detecting whether a drug is able to activate or inhibit a pathway of interest [93]. Alternatively, reporters can be used in CRISPR screening to determine key genes involved in a pathway [94, 95]. However, the process of drug screening can be labour-intensive due to the large compound libraries that need to be tested at different timepoints and drug doses. In addition, determining key genes in CRISPR screens involves choosing percentages of cells with the highest and lowest reporter expression, but this cut-off can be arbitrary and lead to possibly missing key gene candidates.

To improve the design of cell-based reporters, synthetic biology components can be applied. An example of such a component is the recombinase enzyme. Recombinases derive from bacteria and fungi, and can recognise specific short nucleotide sequences to

either invert, excise, insert, or translocate the DNA between them, depending on the orientation of these sites [96, 97]. There are a variety of recombinases, each recognising different target sites, and they have been incorporated into genetic circuits for their ability to catalyse these DNA exchange reactions and create complex genetic circuits [98-102].

We have developed a cell-based reporter that utilises recombinases. The reporter consists of two components: a recombinase element, and a reporter gene element. Recombinase expression is driven by a pathway-sensitive promoter, which then allows it to permanently switch on reporter gene expression. While the basic design for this design has been previously established, we show here the intricacies of reporter optimisation needed to make it applicable to high-throughput screening [103]. Specifically, our reporter incorporates a split recombinase to reduce background activity and a distinct method of integration to enhance reporter behaviour. Furthermore, single cell analysis of our reporter indicates a digital readout, which conveys a clear distinction between “on” and “off” reporter gene expression. These characteristics result in a reporter that acts as an analog-to-digital converter, retains memory, and has high sensitivity. As a proof of principle, the reporter was designed to monitor the activator protein (AP1) pathway, specifically through induction of protein kinase C (PKC) signal transduction. The AP1 transcription factor is involved in a multitude of cell functions, such as proliferation, differentiation and apoptosis, making it important in cancer-related signalling [104].

3.2 Results

3.2.1 Development of the recombinase-based reporter

The cell-based reporter was designed to encompass two main components: a recombinase and a reporter gene. Expression of the recombinase is dependent upon a pathway-sensitive promoter, and the reporter element consists of a constitutive promoter followed by a transcription terminator flanked by recombinase sites and lastly a reporter gene. When expressed, the recombinase acts on the sites to remove the terminator, allowing for constitutive expression of the reporter gene (**Figure 3.1a**). As a proof of concept, an AP-1 pathway-sensitive promoter was used to drive expression of the FlpO recombinase, and both GFP and luciferase were included as the reporter genes to allow for flexibility in readout. Induction of the AP-1 pathway was achieved by treating cells with phorbol 12-myristate 13-acetate (PMA).

Though the design of the reporter appears simple, development was not trivial. The choice of recombinase was important, as the more potent recombinase Cre was found to lead to switching on of the reporter in the absence of any pathway agonist. Furthermore, we found that leaky expression of the recombinase during cell culture led to unwanted background activity of the reporter. To address this, a number of methods were tried including the use of shRNAs and redesigning the inducible promoter to include different minimal promoters, weaker kozak sequences, upstream open reading frames (ORFs), number of short response elements and the spacers between them. Various degrons were also fused to the recombinase in an effort to lower basal levels. However, these approaches were not able to fully resolve the issue of background activity (**Figure**

S3.1).

We found the most effective solution was to incorporate a split version of the recombinase. In this design, the two halves of FlpO were attached to a chemically induced proximity (CIP) system consisting of the domains ABI and PYL [105]. These domains are brought together by the plant hormone abscisic acid (ABA), thus forming a fully active enzyme and preventing any recombination of the reporter gene construct until the time of assay. While splitting the recombinase lowered basal activity, there remained an issue of few cells switching on. In initial efforts, the reporter was tested in HEK293 cells after Piggybac integration. Transient expression of the system showed leaky behaviour with ABA alone, likely due to the abundance of construct copies in the cell (**Figure S3.2a**). As an alternative, the system was integrated through CRISPR/Cas9 knock in at the AAVS1 safe harbour site. Integration at the AAVS1 site has been known to result in more consistent gene expression levels and a less variable cell population. As a result, we observed a dramatic shift in the number of cells that were switching on (**Figure S3.2b**). We further generated a monoclonal cell line for further testing of the switch to ensure genome uniformity.

The resulting reporter was integrated into HEK293 cells by means of two cassettes on a single construct, each containing one of the main components (**Figure 3.1b**). Various orderings and orientations of the cassettes were tested, with the most effective combination being the recombinase preceding the reporter. Whenever the first cassette was inverted, leaky reporter activity was observed in the presence of ABA alone, likely due to bleed over from the strong CAG promoter to the AP-1 promoter (**Figure**

S3.2c). To ensure that expression of the recombinase was due to activation of the AP-1 promoter, the promoter was removed and the system found to be unable to activate in the presence of ABA and PMA (**Figure S3.2d**).

Reporters that are traditionally used in compound and CRISPR screens consist of a pathway-inducible promoter followed by a reporter gene. To compare how our system compares to the classical reporter, a classical reporter was integrated into HEK293 cells in the same manner. Results showed that our system achieved a fold change of 70.5 in GFP levels, whereas the classical system had fold changes of 8.1. Moreover, the shift in GFP median between "on" and "off" states observed by flow cytometry was more pronounced in our recombinase-based system, and showed digital-like behaviour (**Figure 3.1c**). Quantification of luciferase activity showed similarly high levels in the "on" condition for the recombinase-based reporter, though fold change observed was not as high (**Figure S3.2e**).

By permanently removing the transcription terminator using the recombinase, our system also allows for maintenance of "on" activity, thus providing memory unlike the classic reporter. Both reporters were monitored for reporter gene expression over the course of 8 days and it was confirmed that while the recombinase-based reporter maintained GFP expression over time, the classical reporter experienced a drop in GFP levels after the first day (**Figures 3.1d and S3.3**). While "on" activity is maintained over time, the maximal percentage of cells that expressed GFP was achieved around 2 days after addition of the agonist. The recombinase-based reporter further showed a dose response to PMA, with "on" activity starting to drop at high concentrations due to the

toxicity of the drug (**Figure 3.1e**).

Longer incubation of the recombinase-based reporter with agonist also improved the sensitivity of the reporter. A low dose of 0.4ng/ml PMA was tested in cells over time, and the percentage of cells switching "on" increased from 12.9% to 32.2% after 4 days (**Figure 3.1f**). This suggests that our system may be able to detect weaker activating drugs in compound screens by increasing the amount of time the cells are incubated with them.

To show that this reporter can be applied to other pathways, our recombinase-based design was further tested with WNT, NFkB, and CAGA12-related promoters. In all three pathways, our system resulted in a digital readout when both the pathway agonist and ABA were present. Background levels in all three systems remained low if either ABA or the agonist was absent (**Figure 3.1g**).

3.2.2 Application to compound screening

To examine how our cell-based reporter performed in a compound screen, a library of 3492 kinase-targeting drugs was used, with 8 different concentrations corresponding to each drug. This library is used to study compound mechanism of action (MOA) and can help identify the pathway in question. We thus used this compound library to test whether the drug hits corroborated with our PKC-specific AP-1 pathway in both agonist and antagonist screens. In the agonist screen, HEK293 cells expressing our system were treated with the compound library, incubated for 5 hours, then stimulated with ABA to allow for the dimerization of recombinase domains. Cells were then incubated for 2 days and a luciferase assay was performed. The antagonist screen was

performed similarly, though stimulation was done using ABA and PMA to detect which drugs were inhibiting AP-1 promoter activation (**Figure 3.2a**).

Results from the MOA agonist screen indicated 5 compounds (C2600, C902, C3388, C2563, C3024) that showed a dose response curve, while 23 other compounds indicated an increase in reporter gene expression at the highest doses, possibly due to nonspecific activation (**Table 3.1 and Figure S3.4**). Of the 5 compounds that showed a dose response, 3 were PKC-related and the remaining 2 were involved in MAPK (C3024) and angiotensin (C2600) pathways, which have both been known to be linked to AP-1. The antagonist MOA screen yielded 383 hits, which was many more than the agonist. However, it must be kept in mind that any dose response seen with the antagonist hits could be due to the increase in compound concentration causing toxicity and cell death, thus leading to a false positive for drug-induced inhibition of the AP-1 pathway. Of these hits, several of them were found to be inhibitors of the PKC and MAPK pathways as well (**Table 3.2**).

Reconfirmation screens were then performed to validate what was observed. Due to the low number of agonist hits from the MOA library, the compounds that were included in the follow up screen consisted of these hits, with the addition of drugs known to target the same pathways associated with them. Furthermore, known active and inactive analog pairs of the drug hits were included where possible to exclude the possibility of nonspecific activation. Drugs with similar properties to the initial hits, but different potencies (i.e. range compounds), were also included in the agonist reconfirmation screen. As the antagonist MOA library screen yielded several hundreds of

hits, these hits were re-tested in the reconfirmation screen. Some hits from the agonist screen and compounds known to be inactive were added to the antagonist reconfirmation screen as negative controls. A total of 159 and 460 compounds were tested in the agonist and antagonist reconfirmation screens respectively. In addition to the luciferase assay, cell viability assays were also performed in all reconfirmation screens to verify that changes in the bulk luciferase signal were not due to cell toxicity. This was particularly meaningful for the antagonist screen, to help screen out false positives due to drug toxicity. To compare how our recombinase-based reporter compared to the classical reporter, reconfirmation screens were performed with both reporters.

The agonist reconfirmation screen indicated that the recombinase-based reporter had a higher luciferase readout than the classical reporter, observed in both hits and the positive control (ABA and PMA) (**Figure 3.2b**). Background RLU was low and comparable to that of the classical reporter. Of the 5 compounds from the MOA screen that resulted in dose responses, three were reconfirmed as hits, one was not able to be included in the reconfirmation library due to unavailability of the compound, and one (C2600) did not re-emerge as a hit. Several of the analog hits were both active and inactive analogs targeting PCSK9, and upon inspection of the dose response curve, several supposedly inactive analogs were showing a clear stimulatory response to the compound (**Figure S3.5**). Given that the original PCSK9-targeting compound (C2518) did not exhibit a clear dose response in the MOA screen, this suggests that it was possibly a nonspecific interaction to begin with. Furthermore, when maximum RLU values attained for each compound with the recombinase-based reporter were plotted, 2 groups

emerged, with one containing higher RLU values than the second. The compounds that stimulated our reporter to a higher degree were enriched in the hits from the MOA screen, range compounds for CMA1 and MAPK13 and an active analog for an EDNR-related drug (**Table 3.3**).

Antagonist reconfirmation results showed less of a distinction between hits and non-hits, with a range of RLU levels between the positive and negative controls (**Figure 3.2b**). The dose response curves for each compound in the agonist and antagonist screens were compared to cell viability assays, and inhibition due to drug toxicity and cell death eliminated several compounds that initially appeared to antagonist hits. Compared with the 383 hits from the MOA screen, 128 were reconfirmed. Of the remaining 255 hits, all showed an inhibition in signal but were filtered out during cell viability comparisons, indicating the importance of factoring in possible drug toxicity. The hits that showed no effect on cell viability were enriched in PKC and MAPK-targeting compounds, as would be expected **(Table 3.4**). Unlike the agonist reconfirmation screen, distinct populations of stronger and weaker inhibitors did not emerge (**Figure S3.6**).

There were several compound hits shared between the recombinase and classical reporters in both reconfirmation screens. A large overlap was observed between the hits for both reporters in the antagonist screen, but the recombinase-based reporter was able to pull out more hits in the agonist screen (**Figure 3.2c**). Furthermore, hits from the recombinase-based reporter were easier to detect due to the larger changes in RLU levels (**Figure 3.2d**). Additionally, there were a few compounds detected with the recombinase-

based reporter that could not be found with the classical reporter due to the minimal change in RLU levels (**Figure 3.2e**).

To verify that the hits observed in the reconfirmation screens were due to activity of our recombinase reporter, the agonist library was tested in a screen without any ABA. Results showed that no compound hits were found, indicating that the hits we were observing were due to expression of our AP-1-induced recombinase (**Figure S3.7**).

In the agonist reconfirmation screen, we were curious to see whether longer incubation of the cell-based reporter in the drug would result in a compounding of reporter readout, as was observed with the low dose of PMA tested previously. This could increase the sensitivity of the assay, so the duration between stimulation with ABA and luciferase assay readout was varied to 2, 4, and 7 days and cell densities of 20,000, 40,000, 80,000 and 160,000 cells/ml were tested to factor in possible cell overgrowth. We found that the longer cells were incubated following stimulation, the more hits emerged from the screen. Increasing the cell density also generally correlated with a larger number of compound hits. However, at the highest cell density after 7 days of incubation, the number of hits began to decrease, likely due to overgrowth of cells in the wells, limiting exposure of cells to the compounds (**Figure 3.2f**). To examine how the length of incubation impacted the compounds that were showing up as hits, a lower cell density of 40,000 cells/ml was focused on. Here, we found that the hits from 2 days of incubation were retrieved after 4 and 7 days of incubation, and the hits after 4 days carried through to 7 days as well (**Figure 3.2g**). A number of new hits emerged at the 4 and 7 day timepoints, and analysis of some of these dose response curves showed a clear response

to the drug after a longer incubation time, which could otherwise be missed (**Figure 3.2h**).

3.2.3 Application to genome-wide CRISPR screening

Due to the digital nature of our reporter's readout, we postulated that it could be useful in pooled CRISPR screens. To test this, a HEK293 cell line stably expressing Cas9 and our reporter was transduced with an sgRNA lentiviral pool. The sgRNA pool was divided into two libraries, CP1 and CP3, to accommodate the number of distinct sgRNAs being tested. The cells were then treated with either DMSO, ABA, or ABA and PMA, followed by sorting of GFP high and low populations. An unsorted population was also kept as a control to verify that all sgRNAs were well represented following transduction. All cell populations were then run through next generation sequencing (NGS) to determine which gRNAs were enriched (**Figure 3.3a**). Following compound treatment, we found that a small population of cells treated with only ABA were expressing GFP. This is exemplified in cells treated with the CP1 library, where the DMSO control showed 0.053% of cells in the "GFP high" population while the percentage was 0.45% in the ABA condition (**Figure 3.3b**). While still a small population, this suggests that the genes targeted by these gRNAs inhibit AP-1 activity and when knocked out result in constitutive AP-1 activation. When cells transduced with the gRNA library were compared to a non-transduced control, a larger population of cells fell into the "GFP low" population, suggesting these are genes that are needed to activate AP-1 (**Figure 3.3c**).

To analyse the sequencing data, a redundant siRNA activity (RSA) metric was used to assess the significance of a gene falling into the "high" (RSA up) or "low" (RSA

down) population [106]. The more negative the RSA score, the more significant the gene hit. Comparing RSA down results from the 3 treatment conditions, gene hits found to be significant in the ABA+PMA condition were not significant in the DMSO or ABA conditions, strongly suggesting that these genes are required for PKC-induced activation of the AP-1 pathway. Reinforcing this, some of the gene hits in this population were FOS, PRKCD, SHOC2, RASGRP1, ELK1 and MAPK1. As the AP-1 transcription factor is made up of heterodimers of the Jun, Fos, and activating transcription factor (ATF) families, it is unsurprising to find that knocking out FOS results in an inability to activate the AP-1 pathway. Additionally, the subsequent 5 genes are either directly linked to one of the AP-1 heterodimer families or linked through MAPK1.

Delving into the RSA up values, we were interested in which genes scored prominently in the ABA condition, but not in the DMSO condition. This would inform us on which genes would result in constitutive AP-1 activity when knocked out. While there were a number of genes in this condition, most of them were not recapitulated in the ABA+PMA condition, suggesting that they may not be real hits. SH3RF1, however, was found to be linked to JUN and has been found to be involved in JNK-mediated apoptosis [107]. Interestingly, SATB2 did come up as a gene hit in both ABA+PMA and ABA conditions, while not in the DMSO control condition, though no link to the AP-1 transcription factors is yet known (**Figures 3.3d and 3.3e**).

3.3 Discussion and Conclusion

Here, we have developed a recombinase-based reporter that provides memory, increased sensitivity, and a digital readout. This unique reporter was able to pull out weak candidates in a compound screen, as well as provide a clear distinction between "on" and "off" populations in a pooled CRISPR screen. This could enable researchers to identify disease relevant drug "hits" or uncover key genes responsible for specific cell functions or phenotypes that were previously unknown.

The digital nature of this reporter is likely attributed to its design and method of integration. As the reporter is introduced by CRISPR/Cas9 knock in at the AAVS1 locus, this limits the number of copies integrated into the genome. Compared to lentiviral or transient introduction, where several copies are introduced, site-specific knock in lowers the copy number, even when factoring in possible off-target integration. This could be the reason for the low background activity that is observed with the reporter, as it is also observed with the classical reporter when integrated in the same manner. When several copies are expressed in the cell, as was observed when the system was introduced by transient transfection, background levels start to increase when cells were treated with ABA alone. This low background activity compounded with the strength of the CAG promoter could cause the digital readout. When cells are not activated, basal levels remain low, but once the recombinase is expressed and removes the transcription terminator, the reporter gene is strongly expressed, resulting in a large fold change in expression.

In compound screens, the larger fold change results in a clearer dose response that

can be pulled out. Interestingly, our compound screen also showed that the longer cells were incubated in drug and recombinase dimerizer, the more sensitive the reporter could be. A possible reason for this could be that the cells are given more opportunity to be activated by the compound, and the retention of memory allows for an increase in signal over time. Additionally, cells that had switched "on" would continue to divide, and since the removal of the transcription terminator is ingrained in the genome of these cells, the newly divided cells would also express the reporter gene. Both of these occurrences would lead to an increase at the bulk readout level.

The increase in fold change with the recombinase-based reporter also makes it easier for pulling out candidates in CRISPR screens. Traditionally in CRISPR screening, a percentage of the highest and lowest reporter-expressing cells are selected for sequencing. However, this percentage is up to the discretion of the researcher, resulting in gates that can be too lenient or stringent. Furthermore, by selecting this somewhat arbitrary population of cells, there is an increased chance of false positive or missed candidates. The digital nature of our reporter helps to identify which cells fall in the reporter "high" and "low" populations and thus circumvent this issue. The CRISPR screen performed pulled out many AP-1 related genes using the RSA down metric, which was reproducible between all 3 compound treatment conditions. However, it was surprising that Jun and ATF-related genes were not candidates. A possible explanation is that, the AP-1 heterodimer can be composed of various combinations of these subunits, possibly substituting other subunits when one cannot be expressed. An interesting candidate to emerge from the RSA up analysis was the gene SATB2, which scored

significantly in both ABA and ABA+PMA conditions. The associated protein is known to be involved in transcriptional regulation and chromatin remodelling, and mutations in this gene have been linked to brain development and the causation of oral clefts, though no link to AP-1 is yet clear [108-110]. Further study could elucidate a novel link to the AP-1 pathway.

An important caveat to using the CAG promoter for driving reporter gene expression is the potential effect that compounds or gene knockouts can have on it. It is possible that the addition of compounds could inhibit CAG promoter activity, which would appear as though AP-1 promoter activity were being inhibited. Similarly, if a gene knockout results in the inability of the CAG promoter to activate due to missing transcription factors, this could be misinterpreted as a gene necessary for AP-1 activation instead. Thus, if this reporter is being used to screen for antagonists or pathway activators, an additional screen would need to be performed using a reporter consisting of the CAG promoter driving reporter gene expression. While this is a major drawback to the system, it must be taken into consideration whether the benefit of memory is worth performing the additional screen. Nevertheless, the recombinase-based reporter we have built remains useful for screening agonists and pathway inhibitors.

While we have shown that our AP-1 reporter can effectively function in screens, we have thus far also shown our design's compatibility with other promoters, such as WNT, NFkB and CAGA12. In its current design, our reporter provides feedback on a single pathway, which can be beneficial as its simplicity can make results easier to deconvolute. However, the recombinase circuit could theoretically be made more

complex to factor in more than one pathway-sensitive promoter, allowing for the screening of multiple pathways at the same time. This can be used to avoid counter-screening, which can save time, labour, and other resources.

Our recombinase-based reporter has the potential to improve the compound screening process. The monetary and time cost of running several compound screens can be mitigated by running a single screen using our memory-retaining reporter. Furthermore, we have shown the sensitivity of our reporter can be increased with longer incubation periods of the reporter cells in compound, suggesting weak agonist candidates can be identified. This could be beneficial if a milder drug is needed for a lower level of response, and also provides possible alternatives to drugs that patients may be unresponsive or averse to. This technology is also ready for implementation in the drug discovery process. Our system was tested in cell lines that are already used in high-throughput screening, and we have shown that our signal window is favourable for bulk luciferase readout even when scaling down to 1536-well plates. To screen other pathways of interest, the inducible promoter in our design would simply need to be swapped out, and the compound library possibly tested against a control CAG promoter.

Similarly, our reporter can also improve the pooled CRISPR screening process. Once a control CAG reporter has been tested against a full genome library, our recombinase-based reporter will be ready for use. The ability of our technology to report in a digital manner removes the arbitrary factor of gating cells in CRISPR screens, and can potentially identify novel genes related to target pathways. This could be greatly beneficial for expanding our understanding of biological pathways and also for finding

new genes for drug targets.

In chapters 1 through 3, we have seen various ways in which synthetic biology can be used to improve upon traditional medical applications. The ZASE and NS3 CAR switches are able to provide a level of safety over T cell therapy, and the recombinase-based reporter can make the screening process more effective and efficient. These engineered systems are able to enhance current methods because of the level of control we can exert over these biological systems, and are just a few examples of how synthetic biology can contribute to cell therapy and drug discovery. As the field develops, it will be interesting to see the potential impact synthetic biology can make in the realm of medicine.

3.4 Methods

3.4.1 Plasmids and transfection

Reporter constructs were introduced into the AAVS1 site using vectors flanked on both sides by homology arms to the AAVS1 locus. The recombinase-based reporter vector encoded both recombinase and reporter gene cassettes, separated by a P2A sequence. Both recombinase-based and classical reporters were followed by a selection cassette consisting of a PGK promoter driving expression of a zeocin resistance gene and blue fluorescent protein (BFP). These vectors were transfected into cells along with a plasmid encoding Cas9 and a distinct plasmid encoding a AAVS1-targeting gRNA. When the reporter was integrated through the piggyBac method, a distinct vector was used with core insulators flanking the reporter. Cells were transfected concurrently with a

separate vector encoding the piggyBac transposase. For transient transfection, AAVS1 knock in, and piggyBac integration, plasmids were transfected into cells using PEI.

3.4.2 Cell culture

The reporter cell line used in both compound and CRISPR screens consisted of HEK293T cells stably expressing Cas9 that were integrated with the reporter. Cells were passaged in DMEM supplemented with 10% FBS, L-glutamine, penicillin/streptomycin, and 1mM sodium pyruvate. Media also contained 5µg/ml blasticidin to select for Cas9-expressing cells and 400µg/ml zeocin to select for reporter-expressing cells.

3.4.3 Reporter stimulation assays

To test the activity of the AP-1 recombinase-based reporter, cells were plated at a concentration of 300,000 cells/ml in 96-well plates and concurrently treated with combinations of 100µM ABA (Gold Biotechnology, A-050-500) and 50ng/ml PMA. Cells were then incubated for 2 days and either run on flow cytometry to measure GFP levels, or lysed in a luciferase assay and measured at . Classical reporter assays were run similarly, but only incubated for 1 day due to the following loss of reporter gene expression. For WNT, NFkB and CAGA12 reporter cells, PMA was replaced with the following agonists and concentrations respectively: 50% WNT-conditioned media, 7.5ng/ml TNFα (ProSci, 91-006), 2ng/ml TGFß (R&D Systems, 240-B).

3.4.4 Compound screen

HEK293T Cas9 cells expressing the reporters were plated in white 1536-well plates and incubated overnight at 37°C. The compound library was then added to cells with each well receiving one compound, and each compound tested at 8 doses. Each

compound and dose condition was tested in replicate. Cells were then incubated in compound for 5 hours at 37°C following stimulation by ABA for agonist screens, and ABA/PMA for antagonist screens. Each plate tested contained positive and negative controls. Positive control wells in agonist screens were treated with ABA/PMA, while antagonist screens with ABA. Negative control wells in agonist screens were treated with ABA, while antagonist screens with ABA/PMA. Recombinase-based reporter cells were then incubated for 2 days at 37°C (or longer if indicated), and classical reporter cells for 1 day at 37°C. Cells were then lysed in a luciferase assay (Promega, E2650) or cell viability assay (Promega, G7570) and luminescence read on a ViewLux imager. All RLU measurements were normalised to negative controls prior to analysis.

3.4.5 CRISPR screen

HEK293T Cas9 cells expressing the recombinase-based reporter were transduced with either pooled sgRNA library CP1 or CP3, then selected for at least 2 weeks with 2µg/ml puromycin to ensure sgRNA integration. Duplicate transductions were performed for each library. Consolidation of the two libraries contains 5 distinct sgRNAs per gene, and cells were transduced to obtain 1000-fold representation of each sgRNA. Cells were then treated with DMSO, ABA, or ABA/PMA and incubated at 37°C for 2 days prior to sorting. Cell populations were gated by “off” and “on” GFP levels, with an unsorted population as a control. Genomic DNA was then extracted from the sorted cell populations using a QIAamp DNA Blood Maxi Kit (Qiagen, 51194) and sent to the Novartis campus at Basel, Switzerland for NGS. CRISPR screen data was analysed using the RSA algorithm, which calculates the probability of a gene hit incorporating the results

from multiple sgRNAs per gene [106]. RSA down and RSA up hits were searched on the STRING database v11.0 to map known and predicted protein-protein interactions [111].

3.5 Figures

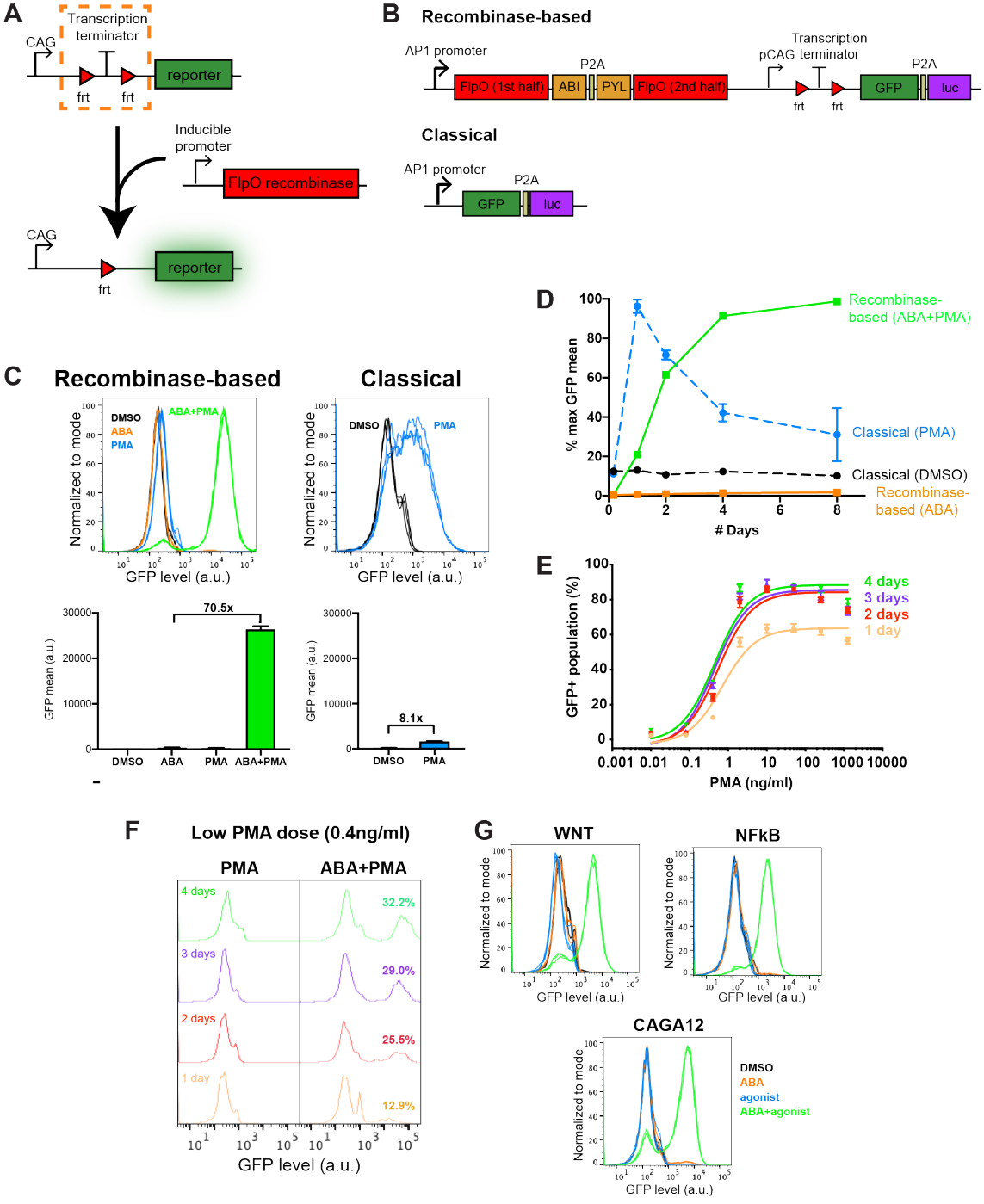

Figure 3.1: Development of the recombinase-based reporter.
A) Schematic for how the recombinase-based reporter functions. B) Construct comparison between the recombinase-based reporter and classical reporter. C) Regulation of reporter-driven GFP expression using combinations of ABA, PMA, or DMSO (vehicle

control). D) Retainment of GFP expression over time with comparison between recombinase-based and classical reporters. E) Dose response of recombinase-based reporter measured after 1, 2, 3, and 4 days' of incubation in ABA and PMA. F) Sensitivity of the recombinase-based reporter to a low dose of PMA (0.4ng/ml) over time with an increasing percentage of cells switching "on". G) Application of the recombinase-based reporter to other pathway-sensitive promoters.

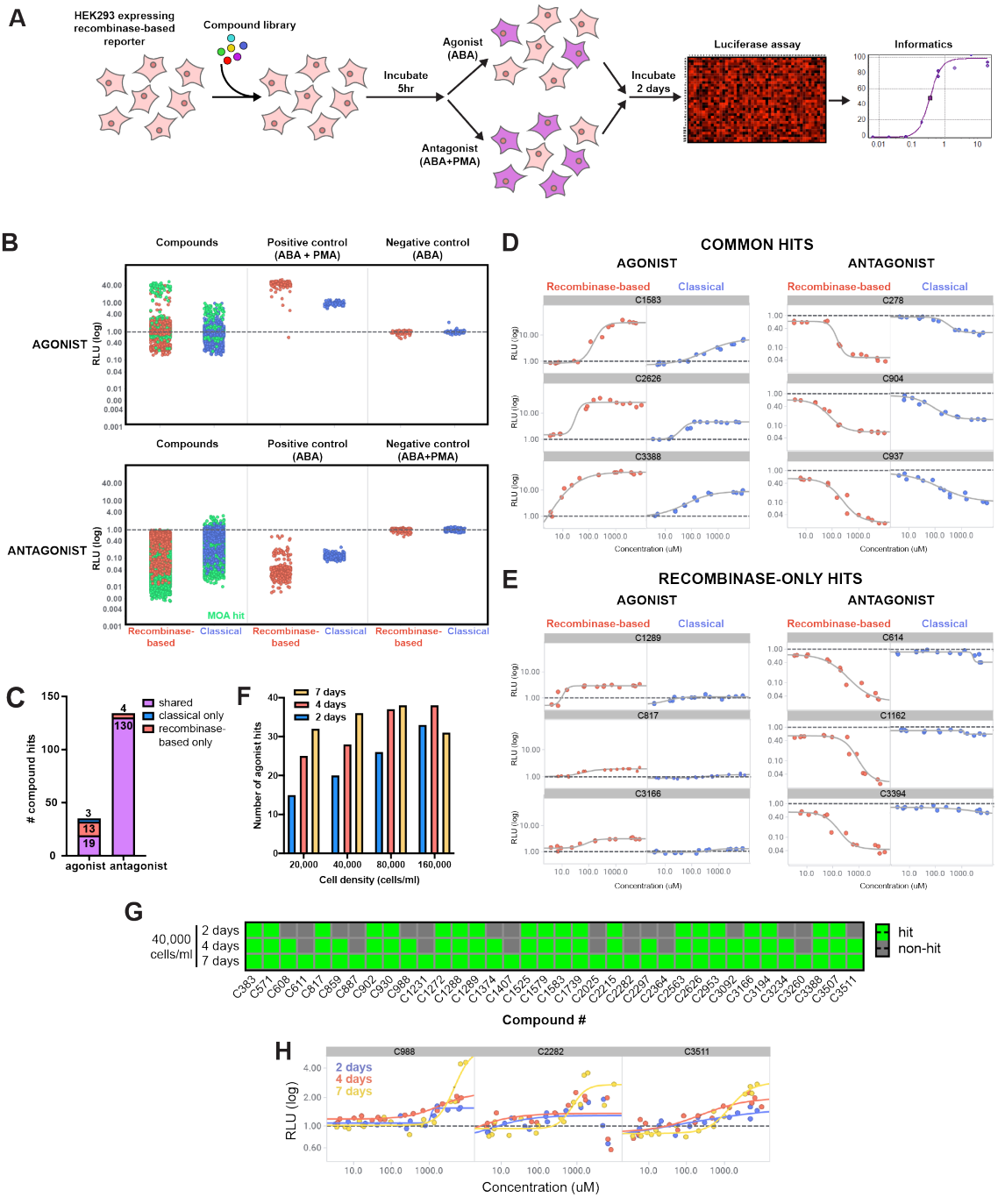

Figure 3.2: Application of the recombinase-based reporter to compound screening. A) Visualisation of the compound screening process. B) Luminescence activity of recombinase-based reporter in agonist and antagonist reconfirmation screens with each point corresponding to normalised RLU from one dose of one compound. C) Number of hits pulled from reconfirmation screens by the two reporters. D) Examples of compound hits shared between recombinase-based and classical reporters. E) Examples of

compound hits only found by recombinase-based reporter. F) Number of compound hits from agonist reconfirmation screen when cell density and incubation time (with ABA and compound) were varied. G) Accumulation of specific compound hits in the agonist reconfirmation screen with 40,000 cells/ml cell density over time. H) Examples of compound hits for the 40,000 cells/ml cell density agonist reconfirmation screen only found at the 4 day and 7 day incubation time points.

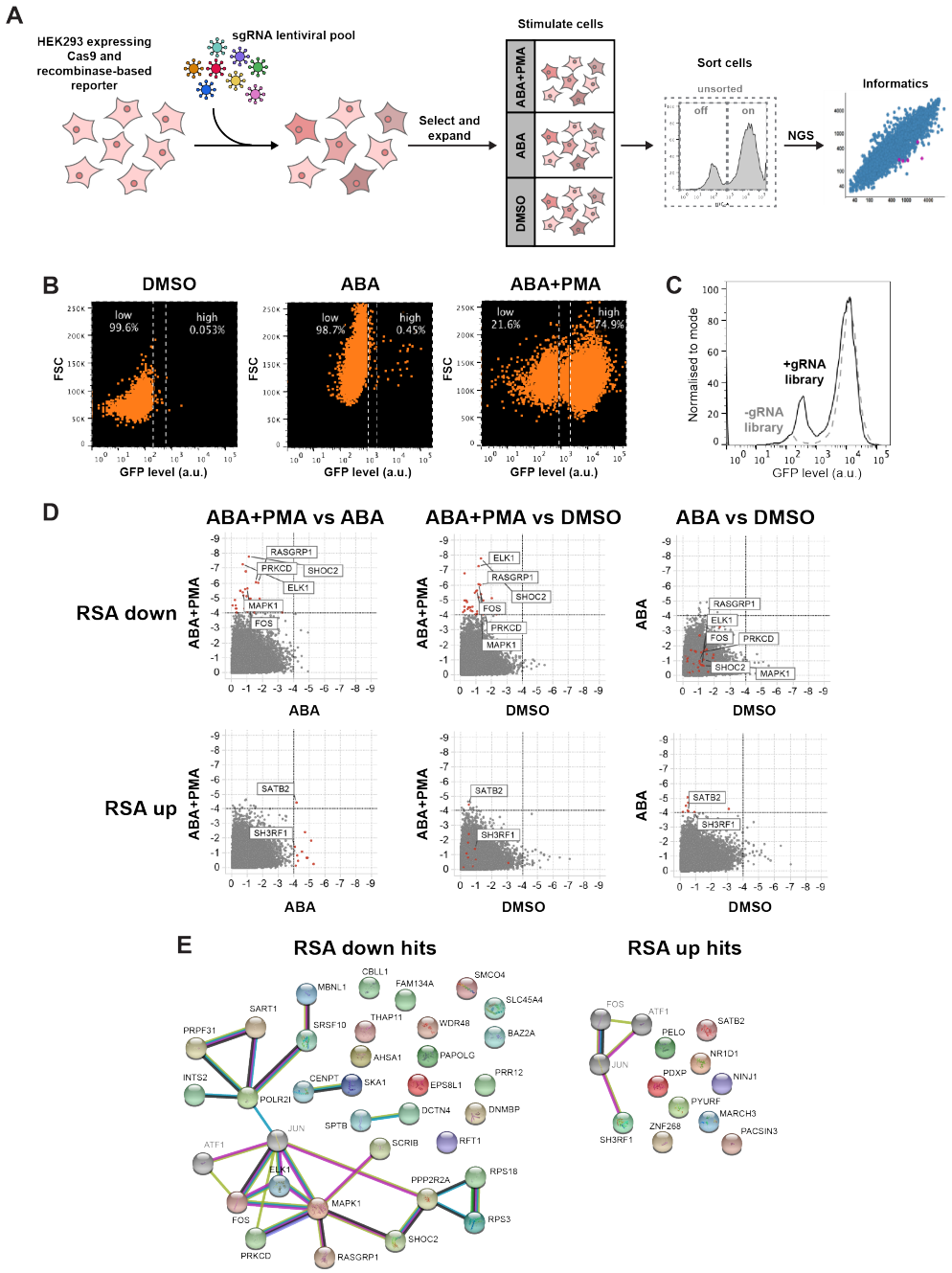

Figure 3.3: Application of the recombinase-based reporter to CRISPR screening. A) Schematic of how the pooled CRISPR screen was performed. B) GFP levels and cell sorting gates for each treatment condition for cells integrated with the CP1 gRNA library. C) Comparison of recombinase-based reporter-expressing cell activity (as measured in GFP levels) when treated with or without CP1 gRNA library. D) RSA down and up values for genes in CP1 and CP3 gRNA libraries. Gene hits scoring -4 and below are highlighted in red, with names displayed for genes of interest. E) STRINGdb analysis of RSA down and RSA up hits.

3.6 Supplemental Figures

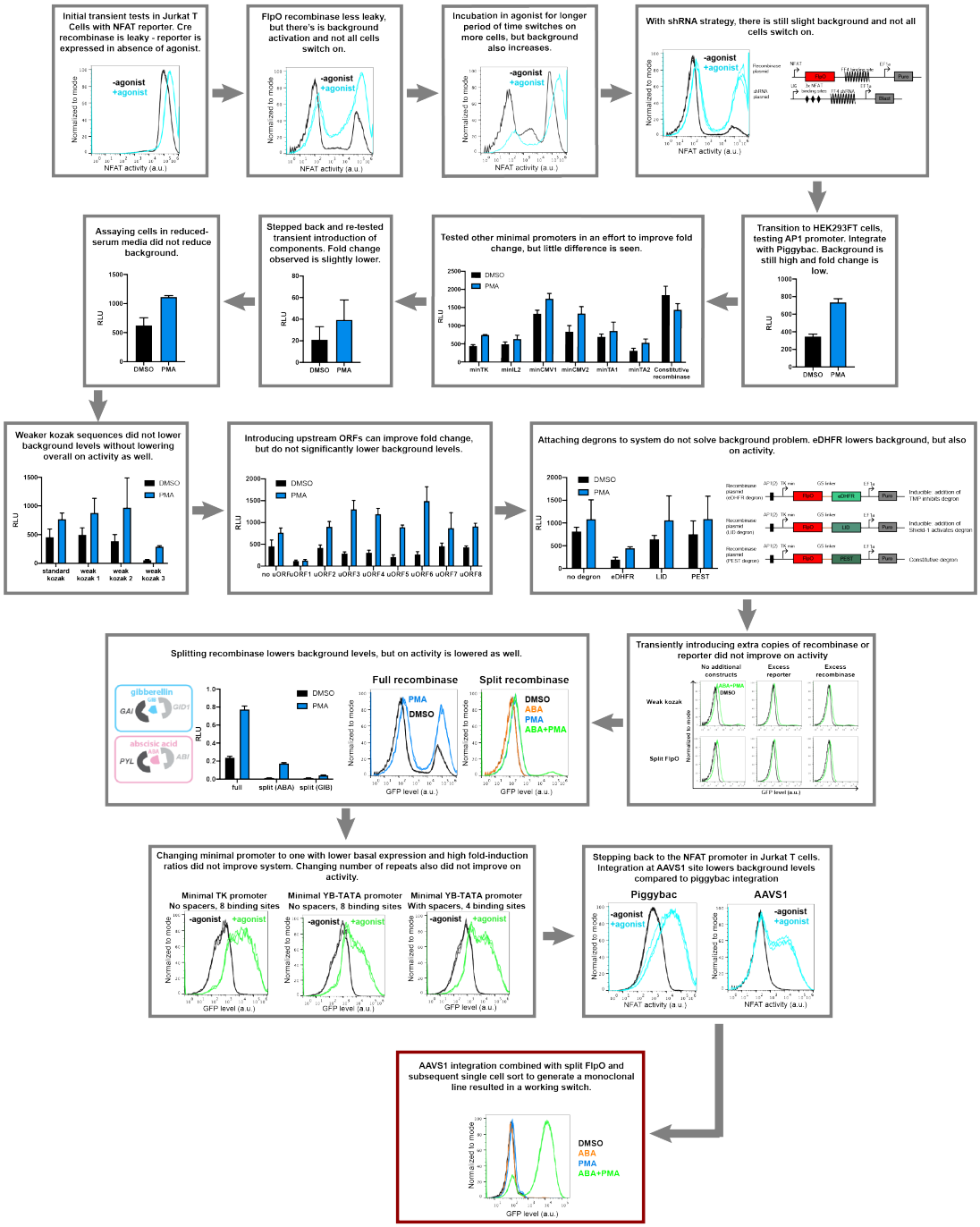

Figure S3.1: Evolution of the recombinase-based reporter.
Various stages and changes made to the recombinase-based genetic circuit in order to obtain a functional reporter. Multiple approaches were explored to reduce background activity and boost "on" signal.

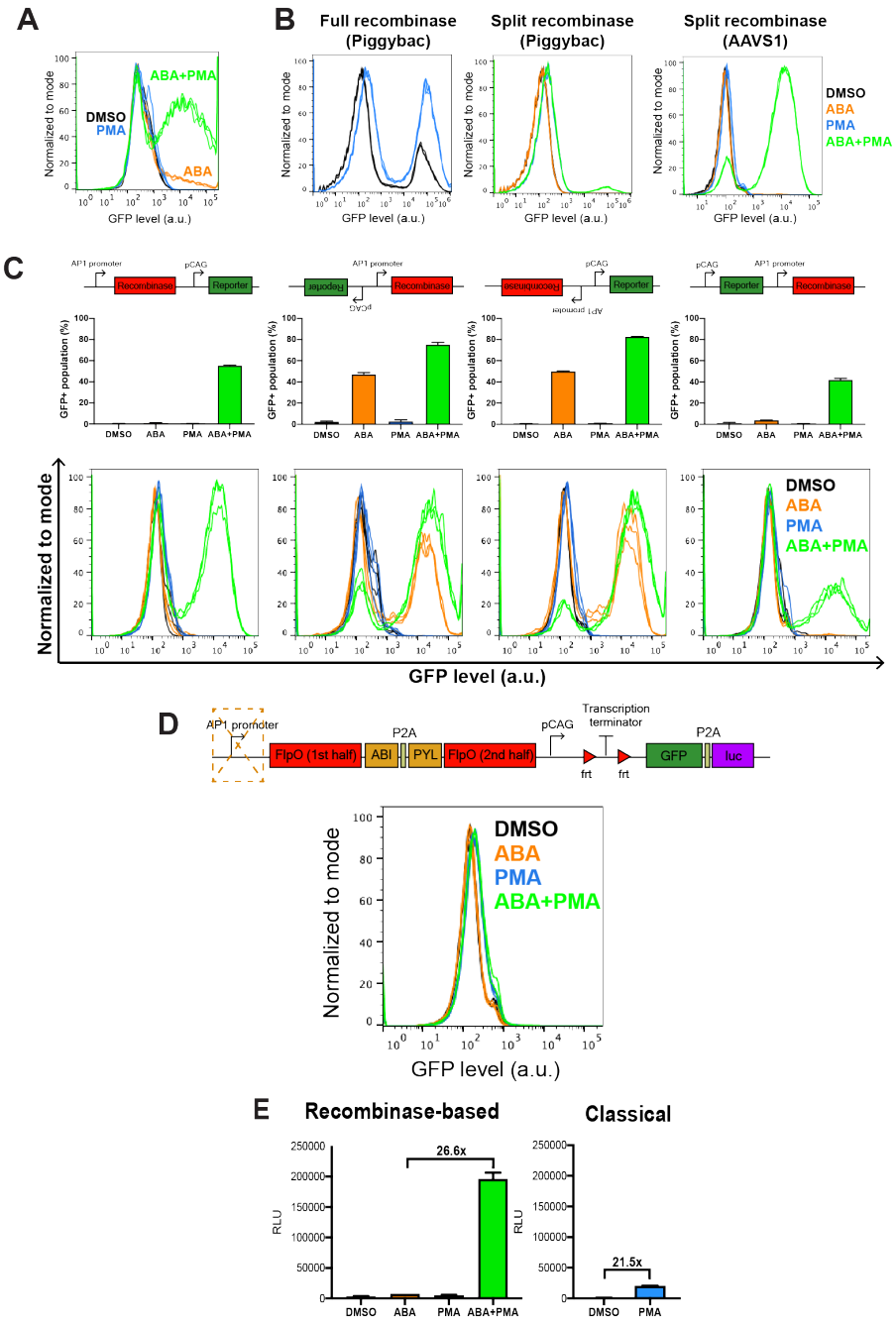

Figure S3.2: Further development of the recombinase-based reporter.
A) HEK293 cells transient transfected with the recombinase-based reporter and activity measured in GFP levels. B) Major changes made to the recombinase-based reporter to generate a functional reporter. C) Various orientations of recombinase and reporter gene cassettes tested. D) Control reporter missing the AP1 promoter was tested and GFP activity measured by flow cytometry. E) Comparison of luciferase levels obtained by recombinase-based and classical reporters.

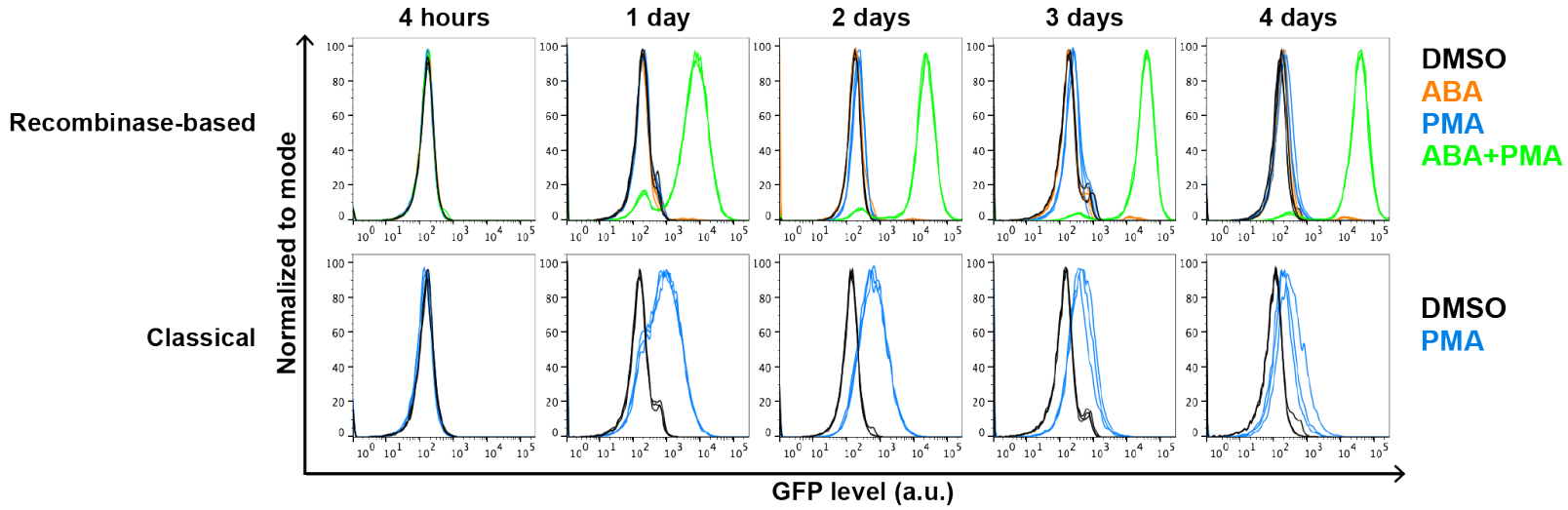

Figure S3.3: Retainment of memory in recombinase-based reporter.
Single cell data showing the retainment of GFP levels over time in the recombinase-based reporter as compared to the classical reporter.

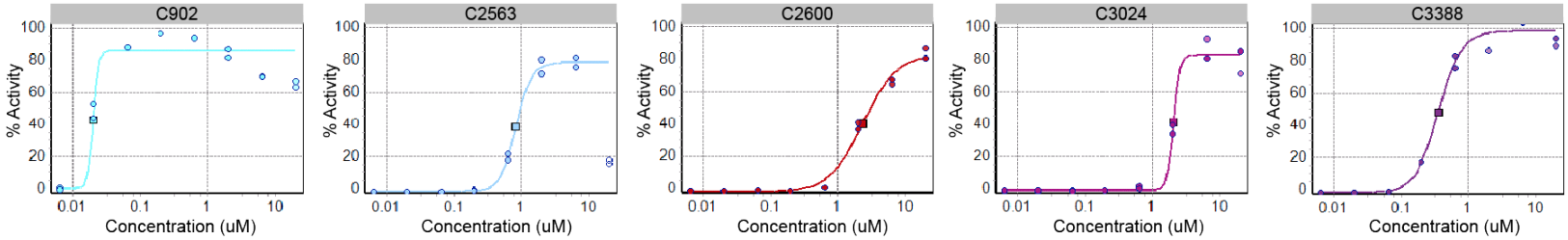

Figure S3.4: Compounds hits from agonist MOA screen.
Five compounds from agonist screen of MOA box that show a dose response to increasing concentration of drug.

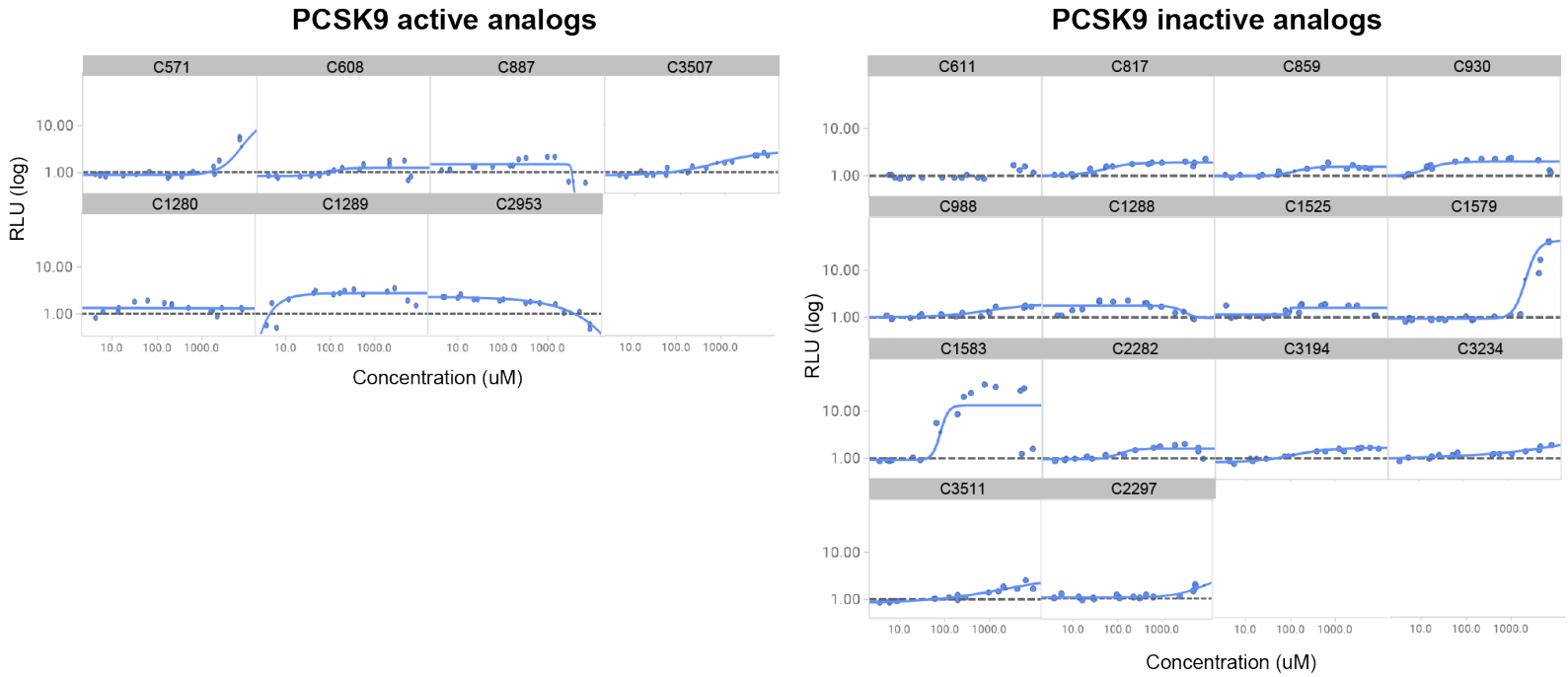

Figure S3.5: PCSK9-specific hits from agonist reconfirmation screen.
Active and inactive analog hits for PCSK9-specific compound hit from the agonist MOA screen. Displayed are the analogs that came up as hits in the agonist reconfirmation screen.

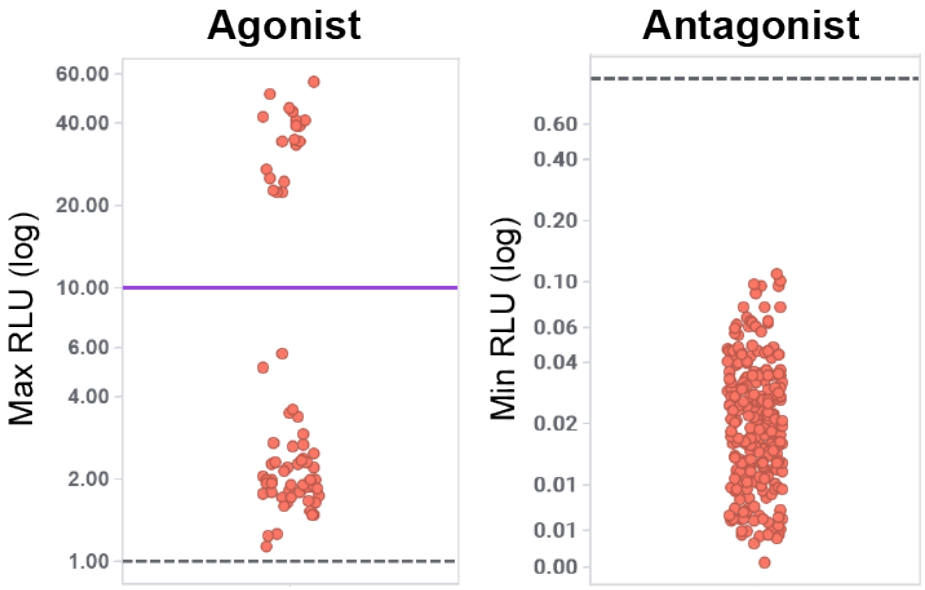

Figure S3.6: Maximum and minimum RLU measurements from reconfirmation hits.
Maximum RLU obtained by each compound hit in the agonist reconfirmation screen, and minimum RLU obtained by each compound hit in the antagonist reconfirmation screen.

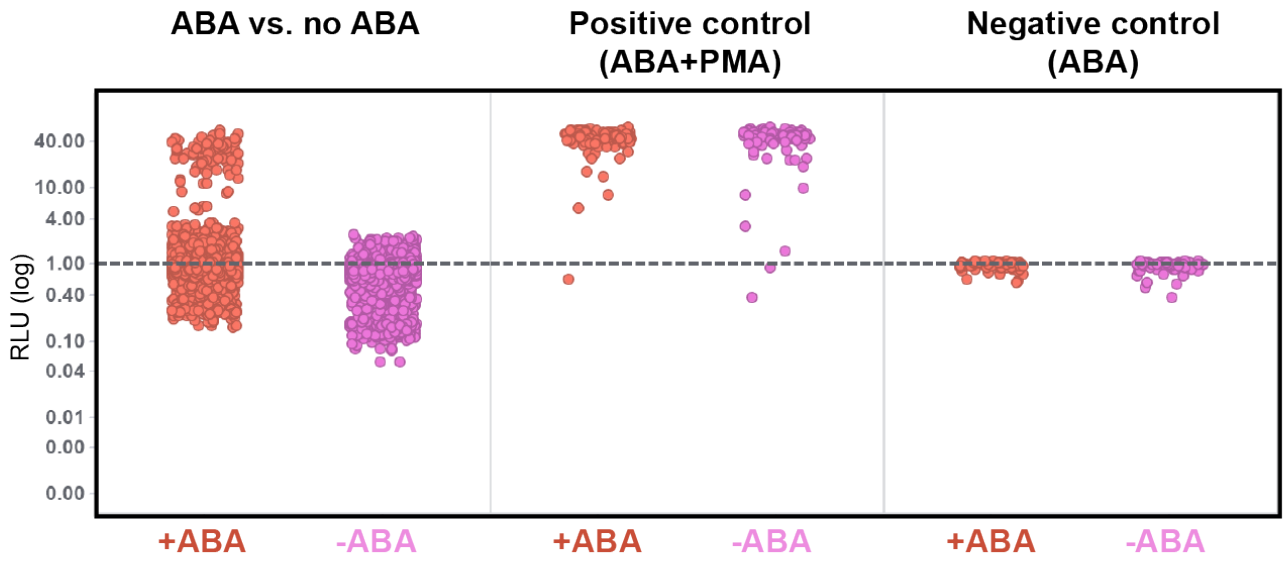

Figure S3.7: Agonist reconfirmation screen without ABA.
RLU values from agonist reconfirmation screen run with no ABA, as compared with a screen run with ABA.

3.7 Tables

Table 3.1: Compound hits from the MOA library agonist screen using the recombinase-based reporter and their known associated genes.

Compound Name	Mechanism of Action	Modality	Gene(s)
C902	DNA topoisomerase I inhibitor PKC activator Protein kinase C alpha stimulator	stimulator/agonist inhibitor/antagonist	PRKCA TOP1
C2563	Lymphangiogenesis Inducer Lymphangiogenesis Inducers	inhibitor/antagonist	PRKCA RASGRP3
C2600	Dual mast cell chymase Cathepsin G inhibitor	inhibitor/antagonist	CMA1 CTSG
C3024	Inhibitors of Signal Transduction Pathways Activin Receptor Like Kinase 5 (ALK5, TbetaR-I) Inhibitors p38 MAPK Inhibitors	-	MAPK13 TGFBR1
C3388	PKC agonist	-	PRKCA
C291	Calmodulin antagonists	inhibitor/antagonist	CALM1
C109	alpha1-Adrenoceptor Antagonists	inhibitor/antagonist	ADRA1B
C352	Lipoxygenase Inhibitors Non-Steroidal Antiinflammatory Drugs	inhibitor/antagonist	ALOX5
C385	EDNRA antagonist Endothelin ETA Receptor Antagonists	inhibitor/antagonist	EDNRA
C526	Nav1.2 (Brain Type II) Sodium Channel Blockers Nav1.4 (SkM1) Sodium Channel Blockers	-	SCN2A SCN4A
C1101	DNA cleavage	-	-
C1186	Isoleucyl-tRNA Synthetase Inhibitors	inhibitor/antagonist	IARS
C1272	Protein kinase C alpha stimulator	stimulator/agonist	PRKCA
C1612	N-Acetyl-beta-D-Glucosaminidase (O-GlcNAcase, OGA) Inhibitors OGLcNACase inhibitor	inhibitor/antagonist	MGEA5 OGA
C1739	Inhibitor of sodium-coupled citrate transporter	inhibitor/antagonist	SLC13A5
C2214	MAP3K11 gene inhibitor	inhibitor/antagonist	MAP3K9 MAP3K11
C2413	Splicing modulator	stabilizer	RNU1-4 SNRPC RNU1-3 RNU1-2 RNU1-1
C2518	pcsk9 translation inhbitor	inhibitor/antagonist	RPL17 PCSK9

C2601	EHMT1/2 inhibitor	inhibitor/antagonist	EHMT2 EHMT1
C2743	Inhibitors of Signal Transduction Pathways Activin Receptor Like Kinase 5 (ALK5, TbetaR-I) Inhibitors	-	TGFBR1
C3153	Cathepsin G inhibitor	inhibitor/antagonist	CTSG
C3166	CRHR2 antagonist CRF Receptor Antagonists	inhibitor/antagonist	CRHR2
C3318	GPR35 agonist	stimulator/agonist	GPR35
C3375	Glutamate Ionotropic Antagonists	-	-
C3415	Acetylcholinesterase Inhibitors	inhibitor/antagonist	ACHE
C3441	Nicotinic Receptor Partial Agonists	partial agonist	CHRNA4 CHRNB2
C3523	DNA-Damaging Drugs Cytochrome P450 CYP1A2 Inhibitors	-	CYP1A2
C3624	Dopamine D1 Agonists	-	DRD1

*Indicates compounds with clear dose response exhibited in Figure S3.4

Table 3.2: Compound hits from MOA library antagonist screen using the recombinase-based reporter and their known associated genes.

Compound Name	Mechanism of Action	Modality	Gene(s)
C6	NF-kappaB (NFKB) Activation Inhibitors	inhibitor/antagonist	SUV39H1
C29	Apoptosis inducers Proteasome inhibitors NF-kappaB (NFKB) activation inhibitors	inhibitor/antagonist	NFKB1 PSMB7 NFKB2 PSMB8 PSMA1 PSMB10 PSMA2 PSMC3 PSMA3 PSMC5 PSMA4 PSMD1 PSMA5 PSMD2 PSMA6 PSMD3 PSMA7 PSMD4 PSMB1 PSMD7 PSMB2 PSMD8 PSMB3 PSMD11 PSMB4 PSMD13 PSMB5 PSMB11 PSMB6 PSMA8
C138	Antimetabolites Dihydrofolate Reductase (DHFR) Inhibitors	-	DHFR
C161	AP-1 Inhibitors Electron Transport Chain Inhibitors	inhibitor/antagonist	JUN UQCRC1
C173	Cardiac glycoside	inhibitor/antagonist	ATP1A1 ATP1B1 ATP1A2 ATP1B2 ATP1A3 ATP1B3 ATP1A4
C183	CDK4/Cyclin D1 Inhibitors CDK2/Cyclin E Inhibitors Protein Kinase C (PKC) Inhibitors	inhibitors/antagonist	CCND1 CCNE1 CDK2 CDK4
C187	IL-1 Inhibitors Non-Steroidal Antiinflammatory Drugs TNF-alpha Production Inhibitors	-	-
C194	Folate Antagonists	inhibitor/antagonist	FOLR1
C217	Vasopressin (AVP) V2 Antagonists	inhibitor/antagonist	AVPR2
C225	topoisomerase I	-	TOP1
C230	Protein Kinase C (PKC) Inhibitors CDK1 Inhibitors CDK2 Inhibitors	inhibitor/antagonist	CDK1 CDK2
C234	Actin stabilizer	stabilizer	ACTB

C241	RNA synthesis inhbitor DNA-Directed RNA Polymerase Inhibitors Transcription Inhibitors	inhibitor/antagonist	CDK9 POLRMT
C249	CDK1 inhibitors	inhibitor/antagonist	CDK1
C252	CDK1 inhibitors	inhibitor/antagonist	CDK1
C254	CDK inhibitor	inhibitor/antagonist	CDK1 CCNA1 CDK2 CCNB2 RPS6KA3 CCNB3
C258	CDK1 Inhibitors	inhibitor/antagonist	CDK1
C278	Apoptosis Inducers Caspase 3 Activators Autophagy inducer	inhibitor/antagonist inhibitor/antagonist inhibitor/antagonist stabilizer inhibitor/antagonist inhibitor/antagonist	ARF1 GBF1 CYTH2 CYTH1 ARFGEF2 ARFGEF1
C303	CD80 (B7-1) Inhibitors	inhibitor/antagonist	CD28 CD80
C342	Lipoxygenase inhibitors	inhibitor/antagonist	ALOX5
C424	Apoptosis inducers DNA topoisomerase I inhibitors	-	TOP1
C429	MAP Kinase Kinase (MEK) inhibitors Extracellular-regulated kinase (ERK) inhibitors Inhibitors of signal transduction pathways	inhibitor/antagonist	MAPK13 MAP2K7
C438	PKA and AKT (a.k.a. PKB)	inhibitor/antagonist	AKT1
C441	KDM4C inhibitor	inhibitor/antagonist	KDM4C
C442	VPAC1 (VIP1) Antagonists	inhibitor/antagonist	VIPR1
C449	HSP90 inhibitor	inhibitor/antagonist	HSP90AA1
C450	Antagonist of Raf-Ras interaction	inhibitor/antagonist	BRAF RAF1 ZHX2
C451	Heat Shock Protein 90 (hsp90) Inhibitors	inhibitor/antagonist	HSP90AA1
C452	Antimitotic drugs Polo-like Kinase-1 (Plk-1) inhibitors	-	PLK1 BRD4
C459	ACK tyrosine kinase inhibitor	inhibitor/antagonist	TNK2

C462	Tubulin polymerase inhibitors	inhibitor/antagonist	TUBA4A TUBD1 TUBA3C TUBA8 TUBB2A TUBB1 TUBG1 TUBB6 TUBA1A TUBA1C TUBA1B TUBA3E TUBB3 TUBA3D TUBB4A TUBB TUBB4B TUBB8 TUBG2 TUBB2B
C499	Apoptosis inducers Caspase 3 activators Caspase 8 activators Caspase 9 activators Serotonin antagonists	-	CASP3 CASP8 CASP9
C521	Cytoskeleton inhibitors Tubulin polymerization inhibitors	inhibitor/antagonist	TUBA4A TUBD1 TUBA3C TUBA8 TUBB2A TUBB1 TUBG1 TUBB6 TUBA1A TUBA1C TUBA1B TUBA3E TUBB3 TUBA3D TUBB4A TUBB8 TUBB4B TUBB2B TUBG2
C532	Antimalarial Pannexin 1 (PANX1) Inhibitors	inhibitor/antagonist	GJA8 PANX1 GJD2
C545	Protein Kinase Inhibitors	inhibitor/antagonist	FGFR2 FLT3 IGF1R SRC
C546	MMP-8 (Neutrophil Collagenase) Inhibitors	inhibitor/antagonist	MMP8
C547	CDK1/Cyclin B Inhibitors CDK2/Cyclin A Inhibitors CDK2/Cyclin E Inhibitors CDK4/Cyclin D1 Inhibitors CDK5 Inhibitors Dual-Specificity Tyrosine-(Y)-Phosphorylation Regulated Kinase (DYRK) Inhibitors		CHUK CCNA1 CCNB2 CCNE2 CCNB3
C562	CDK6 Inhibitors DNA-Intercalating Drugs CDK4/Cyclin D1 Inhibitors CDC25B Inhibitors		CCND1 CDK4 CDK6

C578	CDK4 Inhibitors	inhibitor/antagonist	CCND3 CDK4 CCNA1 CCNB2 CCNB3
C581	CDK inhibitor	inhibitor/antagonist	CDK2 CDK4 CCNA1
C598	IGF-1R Inhibitors Inhibitors of Signal Transduction Pathways Angiogenesis Inhibitors	inhibitor/antagonist	IGF1R
C599	Protein Kinase PKC beta Inhibitors Protein Kinase PKC theta Inhibitors Protein Kinase PKC delta Inhibitors Protein Kinase PKC alpha Inhibitors Protein Kinase PKC epsilon Inhibitors		CD28 PRKCA PRKCB PRKCD PRKCE PRKCQ
C602	Proteasome inhibitor Proteasome Inhibitors Apoptosis Inducers Caspase 3 Activators NF-kappaB (NFKB) Activation Inhibitors	inhibitor/antagonist	CASP3 CTRB1 PSMA1 PSMA2 PSMA3 PSMB11 PSMA4 PSMA5 PSMA6 PSMA7 PSMB1 PSMA8 PSMB2 PSMB3 PSMB4 PSMB5 PSMB6 CTRC PSMB7 PSMB8 PSMB9 PSMB10 PSMC3 PSMD13 PSMC5 PSMD1 PSMD2 PSMD3 PSMD4 PSMD11 PSMC5 PSMD1 PSMD2 PSMD3 PSMD4 PSMD11
C614	Inosine 5'-Monophosphate Dehydrogenase Type II (IMPDH II) Inhibitors Inosine 5'-Monophosphate Dehydrogenase Type I (IMPDH I) Inhibitors		IMPDH1 IMPDH2
C616	Protein Kinase C (PKC) Inhibitors	inhibitor/antagonist	PRKCH
C618	MTH1 inhibitor IGF1R inhibitor	inhibitor/antagonist	IGF1R NUDT1
C644	MCHR1 antagonist	inhibitor/antagonist	MCHR1

C650	Melanin-concentrating hormone MCH-R1 (SLC-1) receptor antagonists	inhibitor/antagonist	MCHR1 MCHR2
C659	-	-	CHUK
C672	pan-PKC inhibitor	inhibitor/antagonist	CD28 PRKCQ
C674	Hedgehog Signaling Inhibitors	inhibitor/antagonist	GLI1
C675	Apoptosis Inducers	-	-
C680	-	inhibitor/antagonist	BCL2A1
C686	Ribonucleotide Reductase inhibitor DNA Damaging Agent	inhibitor/antagonist	SLC29A1 RRM2 SLC29A2 TYMS RRM1 SLC29A3
C696	Glucose Lowering Agents	-	-
C697	Protein Kinase C (PKC) Inhibitors IL-2 Production Inhibitors		CD28 IL2
C698	-	inhibitor/antagonist	RET
C739	ADRA2C antagonist alpha2C-Adrenoceptor Antagonists	inhibitor/antagonist	ADRA2C
C759	mitochondrial decoupler	-	-
C768	-		NPY1R NPFFR1
C777	Bcl-xl Inhibitors P2X7 Receptor Antagonists Apoptosis Inducers Rho GTPase Inhibitors Protein Kinase C (PKC) Inhibitors		BCL2L1 P2RX7
C782	Adenylate Cyclase Inhibitors Calcium Channel Blockers	inhibitor/antagonist	ADCY1 ADCY6 ADCY2 ADCY7 ADCY3 ADCY9 ADCY5 CACNA1C
C812	cytochrome c reductase Electron Transport Chain Inhibitors	inhibitor/antagonist	UQCRC1
C830	Potassium ionophore	-	-
C838	actin polymerization	disruptor/degrader	ACTA1
C848	DNA-Intercalating Drugs	-	-
C853	3-phosphoinositide dependent protein kinase 1	inhibitor/antagonist	PDPK1
C867	Apoptosis Inhibitors PKB alpha/Akt1 Inhibitors	inhibitor/antagonist	AKT1
C890	Uncoupler mitochondrial decoupler	-	-

C899	Leucine-Rich Repeat Kinase 2 (LRRK2 Dardarin) Inhibitors	inhibitor/antagonist	CAMK2B CAMK2G FYN PRKCG PRKCH	PRKCI PRKCZ PRKD3 LRRK2
C900	Flt3 (FLK2/STK1) Inhibitors Inhibitors of Signal Transduction Pathways	inhibitor/antagonist	MAPK14 FLT3 KIT	PDGFRB MAPK8 MAPK10
C904	Protein Kinase C (PKC) Inhibitors IL-2 Production Inhibitors	-	IL2	
C906	Flt3 (FLK2/STK1) Inhibitors	inhibitor/antagonist	FLT3	
C908	Nitric Oxide Production Inhibitors Tau Aggregation Inhibitors	-	MAPT	
C918	Muscarinic M3 Receptor Ligands Muscarinic M4 Receptor Ligands		CHRM3 CHRM4	
C922	IKK-2 (IKK-beta) Inhibitors NF-kappaB (NFKB) Activation Inhibitors	inhibitor/antagonist	IKBKB	
C937	Inhibitors of Signal Transduction Pathways Protein Kinase PKC beta Inhibitors Angiogenesis Inhibitors		PRKCB PRKCH PRKCZ RPS6KB1	
C960	MMP-13 (Collagenase 3) Inhibitors MMP-2 (Gelatinase A) Inhibitors		MMP2 MMP13	
C975	Translation inhibitor TARS inhibitor angiogenesis inhibitor	inhibitor/antagonist	TARS1	
C982	mgluR2 Antagonists	inhibitor/antagonist	GRM2	
C983	CHK1 expression inhibitors Inhibitors of Signal Transduction Pathways HSP90 inhibitors	-	HSP90AA1	
C987	Phosphoinositide dependent Kinase (PDK) 1 Inhibitors Phosphatidylinositol 3-Kinase (PI3K) Inhibitors	inhibitor/antagonist	AKT1 ATR MTOR PDPK1	PIK3CA PIK3CD MAP3K14
C994	Phosphatidylinositol 3-Kinase (PI3K) Inhibitors	inhibitor/antagonist	AKT1 AKT2 ATR MTOR	PIK3CA PIK3CB PIK3CD AKT3

C998	Signal transduction modulator Protein Kinase C (PKC) Inhibitors		CAMK2B CAMK2G PRKACA PRKACB PRKACG PRKCG PRKCH PRKCI PRKCZ MAPK4 PRKCG PRKCH PRKCI
C1002	IKK-2 (IKK-beta) Inhibitors Flt3 (FLK2/STK1) Inhibitors	inhibitor/antagonist	CHUK FLT3 IKBKB IKBKG
C1022	Chemokine CCR2 (MCP-1 Receptor) Antagonists	inhibitor/antagonist	CCR2
C1024	-	inhibitor/antagonist	NRL NR2E3
C1026	Known SPPL2A inhibitor	inhibitor/antagonist	SPPL2A
C1031	Heat Shock Protein 90 (hsp90) Inhibitors	inhibitor/antagonist	HSP90AA1 HSP90B1
C1036	Inhibitors of Signal Transduction Pathways Protein Kinase Inhibitors	-	-
C1050	Tau Aggregation Inhibitors	inhibitor/antagonist	MAPT
C1054	Pyrimidine Antagonists	inhibitor/antagonist	TYMS
C1059	Inhibitors of Signal Transduction Pathways Protein Kinase PKC beta Inhibitors Angiogenesis Inhibitors		PRKCB PRKCG
C1060	Protein Kinase C (PKC) Inhibitors	inhibitor/antagonist	PRKCG
C1084	Electron transport chain inhibitor Cytochrome c reductase Electron Transport Chain Inhibitors	inhibitor/antagonist	UQCRC1
C1086	Translation inhibitor	inhibitor/antagonist	RPS14 RPS20
C1092	DNA Polymerase Inhibitors	-	-
C1102	Proteasome inhibitor Increase of leptin sensitivity to suppress food intake	-	-
C1105	Exportin 1 inhibitor	inhibitor/antagonist	XPO1
C1113	Translation Inhibitor Glycogen Synthase Kinase 3 beta (GSK-3beta tau Protein Kinase I) Inhibitors	inhibitor/antagonist	GSK3B RPL6

C1116	Nerve Growth Factor (NGF) Enhancers Tenogenic	inhibitor/antagonist - inhibitor/antagonist inhibitor/antagonist	CDK8 NGF PDE3A CDK19
C1117	cAMP-Dependent Protein Kinase (PKA) Inhibitors Inhibitors of Signal Transduction Pathways PKB alpha/Akt1 Inhibitors		PRKACA PRKACB PRKACG
C1121	Chemokine CCR2 (MCP-1 Receptor) Antagonists	inhibitor/antagonist	CCR2
C1122	CDK inhibitor	inhibitor/antagonist	CDK2 CCNA1
C1125	ER stress inducer divalent cation ionophore	-	-
C1142	Chemokine CCR2 (MCP-1 Receptor) Antagonists Chemokine CCR5 Antagonists	inhibitor/antagonist	CCR5 CCR2
C1146	Inhibitor of the BMP1/TLL1/TLL2 family of Proteases	inhibitor/antagonist	BMP1 TLL2
C1151	Lck Kinase Inhibitors	inhibitor/antagonist	LCK
C1152	Abl Kinase Inhibitors Apoptosis Inducers Bcr-Abl Kinase Inhibitors Inhibitors of Signal Transduction Pathways Src Kinase Inhibitors STAT-5 Inhibitors	-	FYN
C1161	Heat Shock Protein 70 (hsp70) Inducers TNF-alpha Production Inhibitors	stimulator/agonist	HSPA1A
C1162	Inosine 5'-Monophosphate Dehydrogenase (IMPDH) Inhibitors Immunosuppressant IMPDH inhibitor antiviral	inhibitor/antagonist	IMPDH1 IMPDH2
C1168	Lipid Kinase Inhibitors	inhibitor/antagonist	PI4KB RPS6KA3
C1169	Autophagy agonist	inhibitor/antagonist	DPP4 Dpp4
C1187	Mammalian Target of Rapamycin (mTOR FRAP1) Inhibitors Phosphatidylinositol 3-Kinase alpha (PI3Kalpha) Inhibitors Phosphatidylinositol 3-Kinase beta (PI3Kbeta) Inhibitors Phosphatidylinositol 3-Kinase delta (PI3Kdelta) Inhibitors	-	PIK3C2B

	Phosphatidylinositol 3-Kinase gamma (PI3Kgamma) Inhibitors		
C1206	Jak3 tyrosine kinase inhibitor	inhibitor/antagonist	GSK3B JAK3 PRKCA
C1207	VEGFR-2 (FLK-1/KDR) Inhibitors Bcr-Abl Kinase Inhibitors Angiogenesis Inhibitors		ABL1 ABL2 BCR KDR
C1220	ROCK gene inhibitor PKC Kinase nhibitor	inhibitor/antagonist	PRKACA ROCK1 ROCK2
C1226	MAPKAP-K2 (MK2) Inhibitors TNF-alpha Release Inhibitors	inhibitor/antagonist	MAPKAPK 5 MAPKAPK 2
C1230	Jak2 Inhibitors Jak1 Inhibitors		JAK1 JAK2
C1233	Syk Kinase Inhibitors	inhibitor/antagonist	SYK
C1239	c-src allosteric inihitor allosteric Src inhibitor Src Kinase Inhibitors Antimitotic Drugs Inhibitors of Signal Transduction Pathways Tubulin polymerization inhibitors	allosteric inhibitor inhibitor/antagonist	SRC TUBG2
C1247	Protein Kinase PKC theta Inhibitors IL-2 Production Inhibitors	inhibitor/antagonist	IL2 PRKCQ
C1251	MAPKAPK5 inhibitor	inhibitor/antagonist	MAPKAPK 5
C1254	Inhibitors of Signal Transduction Pathways Flt3 (FLK2/STK1) Inhibitors Protein Kinase C (PKC) Inhibitors Angiogenesis Inhibitors	inhibitor/antagonist	FLT3 PRKCQ
C1285	-	inhibitor/antagonist	PGK1
C1300	CDC-like kinase-2 inhibitors	inhibitor/antagonist	CLK2
C1301	Rho Kinase Inhibitors Protein Kinase PKC theta Inhibitors Protein Kinase PKC epsilon Inhibitors		PRKCE PRKCQ ROCK1 ROCK2

C1302	Jak2 Inhibitors Flt3 (FLK2/STK1) Inhibitors	inhibitor/antagonist	FLT3 JAK2 BRD4
C1327	Antimetabolites Dihydrofolate Reductase (DHFR) Inhibitors	inhibitor/antagonist	DHFR
C1333	Dual Specificity Mitogen-Activated Protein Kinase Kinase 1 (MAP2K1 MEK1) Inhibitors	inhibitor/antagonist	MAP2K1
C1345	Antimitotic Drugs Tubulin polymerization inhibitors	-	TUBB
C1346	MEK1 Inhibitors	inhibitor/antagonist	MAP2K1
C1347	Mitogen-Activated Protein (MAP) Kinase Kinase (MEK) Inhibitors	inhibitor/antagonist	MAP2K1
C1367	dual thymidylate synthase and dihydrofolate reductase inhibitors	inhibitor/antagonist	DHFR FOLR1 GART SLC19A1 TYMS
C1371	Potent allosteric inhibitor of IGF1R. Also hits InsR.	allosteric inhibitor	IGF1R
C1372	Melanocortin MC4 Receptor Antagonists	inhibitor/antagonist	MC4R
C1385	Protein Kinase PKC theta Inhibitors	inhibitor/antagonist	PRKCQ
C1386	panPI3K inhibitor	inhibitor/antagonist	PIK3CA PIK3CB
C1392	PKC theta inhibitor	inhibitor/antagonist	PRKCQ
C1411	Apoptosis Inducers 5-Lipoxygenase Inhibitors Peripheral Benzodiazepine Receptor (PBR) Ligands MAPK-Activated Protein Kinase Inhibitors		ALOX5 TSPO
C1412	Inhibitors of Signal Transduction Pathways PKB alpha/Akt1 Inhibitors PKB beta/Akt2 Inhibitors PKB gamma/Akt3 Inhibitors	inhibitor/antagonist	AKT1 AKT2 DAPK3 PRKG1 PRKX AKT3 PAK6
C1416	mTOR Complex 1 (mTORC1) Inhibitors mTOR Complex 2 (mTORC2) Inhibitors catalytic mTOR inhibitor	inhibitor/antagonist	MTOR
C1419	Phosphatidylinositol 3-Kinase alpha (PI3Kalpha) Inhibitors	inhibitor/antagonist	PIK3CA
C1424	Angiogenesis Inhibitors Apoptosis Inducers Nicotinamide Phosphoribosyltransferase (NMPRTase) Inhibitors	-	NAMPT

C1434	Mammalian Target of Rapamycin (mTOR FRAP1) Inhibitors PI3K inhibitors	inhibitor/antagonist	MTOR PIK3CA PIK3CB PIK3CD PIK3CG
C1436	MEK1 Inhibitors MEK2 Inhibitors		MAP2K1 MAP2K2
C1437	Mammalian Target of Rapamycin (mTOR FRAP1) Inhibitors Phosphatidylinositol 3-Kinase beta (PI3Kbeta) Inhibitors Phosphatidylinositol 3-Kinase delta (PI3Kdelta) Inhibitors Phosphatidylinositol 3-Kinase alpha (PI3Kalpha) Inhibitors	inhibitor/antagonist	MTOR PIK3CA PIK3CB PIK3CD
C1441	Apoptosis Inducers Procaspase 3 Activators	-	CASP3
C1445	Jak2 Inhibitors Jak1 Inhibitors Tyk2 Inhibitors		JAK1 JAK2 TYK2
C1451	Mammalian Target of Rapamycin (mTOR FRAP1) Inhibitors PI3K inhibitors	inhibitor/antagonist	MTOR PIK3CA PIK3CB PIK3CD PIK3CG
C1459	MAPK-Interacting Kinase (MNK) Inhibitors	inhibitor/antagonist	CDK8 MKNK2 SGK1 MKNK1 CDK19
C1463	CASP3 activator apoptosis inhibitor IGF1R inhibitor IGF-1R Inhibitors Caspase 3 Activators Apoptosis Inducers	stimulator/agonist inhibitor/antagonist	CASP3 IGF1R
C1477	ITK (EMT) Kinase Inhibitors IL-4 Production Inhibitors IL-2 Production Inhibitors	inhibitor/antagonist	IL2 IL4 ITK
C1478	dual mTOR/PI3K inhibitor	inhibitor/antagonist	MTOR PIK3CA PIK3CB PIK3CD
C1483	dual mTOR PI3K inhibitor	inhibitor/antagonist	MTOR PIK3CA PIK3CB PIK3CD

C1486	Activin Receptor Like Kinase 3 (ALK3 BMPR-IA) Inhibitors Activin Receptor Like Kinase 2 (ALK2 ActR-IA) Inhibitors	inhibitor/antagonist	ACVR1 BMPR1A BMPR1B
C1501	Irreversible EGFR (HER1 erbB1) Inhibitors HER2 (erbB2) Inhibitors Inhibitors of Signal Transduction Pathways	inhibitor/antagonist	EGFR ERBB2 ERBB4
C1516	Src kinase inhibitors Inhibitors of signal transduction pathways Abl Kinase Inhibitors Bcr-Abl kinase inhibitors	-	ABL1 ABL2 BCR SRC
C1520	5-HT1B Antagonists	inhibitor/antagonist	HTR1B
C1527	Elongation factor 1 alpha inhibitor Translation Inhibitor	inhibitor/antagonist	EIF4A1 EIF4A2 EIF4A3
C1528	Casein Kinase II (CK2) Inhibitors	inhibitor/antagonist	CSNK2A1 MTOR CSNK2A2 PIK3CA CSNK2B PIK3CD
C1530	NAMPT Inhibitor	inhibitor/antagonist	NAMPT
C1535	Inhibitors of Signal Transduction Pathways Bcr-Abl Kinase Inhibitors		ABL1 ABL2 BCR
C1538	Mammalian Target of Rapamycin (mTOR FRAP1) Inhibitors Phosphatidylinositol 3-Kinase (PI3K) Inhibitors	inhibitor/antagonist	MTOR PIK3CA
C1547	Immunoproteasome Inhibitors	inhibitor/antagonist	PSMB8
C1548	CDK1/Cyclin B Inhibitors Apoptosis Inducers Inhibitors of Signal Transduction Pathways CDK2/Cyclin A Inhibitors	inhibitor/antagonist	CCNA2 CCNB1 CDK1 CDK2
C1554	tat Inhibitors bacterial DNA Primase Inhibitors	-	PRIM1
C1557	Phosphatidylinositol 3-Kinase beta (PI3Kbeta) Inhibitors Phosphatidylinositol 3-Kinase alpha (PI3Kalpha) Inhibitors Phosphatidylinositol 3-Kinase gamma (PI3Kgamma) Inhibitors	inhibitor/antagonist	PIK3CA PIK3CB PIK3CG
C1584	EIF4A1 gene inhibitor	inhibitor/antagonist	EIF4A1
C1604	TBK1 inhibitor	inhibitor/antagonist	IKBKE TBK1

C1606	Syk tyrosine kinase inhibitor selective SYK inhibitor	inhibitor/antagonist	SYK
C1607	Axl tyrosine kinase receptor inhibitor	inhibitor/antagonist	AXL
C1624	HMGB2 gene inhibitor	inhibitor/antagonist	HMGB1 HMGB2
C1628	covalent modifier of catalytic cysteine of pro-CASP8	inhibitor/antagonist	CASP8
C1633	p97 AAA ATPase inhibitor	inhibitor/antagonist	VCP
C1640	FAK inhibitor	inhibitor/antagonist	PTK2
C1642	SOD1 gene inhibitor	inhibitor/antagonist	SOD1
C1659	FAK inhbitor Inhibitor of fibronectin-directed migration Co-Inducer of apoptosis in pancreatic cancer	inhibitor/antagonist	PTK2
C1667	MELK inhibitor	inhibitor/antagonist	MELK
C1672	Wnt signaling inhibitor, Inhibitor of beta-catenin/TCF transcription	inhibitor/antagonist	CTNNB1
C1673	M5 positive allosteric modulator	allosteric activator	CHRM5
C1680	ERBB3 covalent inhibitor	inhibitor/antagonist	ERBB3
C1694	Arenobufagin, SMUT	inhibitor/antagonist	PSMB1 PSMB2 PSMB5 ATP1B4
C1697	Checkpoint Kinase 2 (Chk2) Inhibitors	inhibitor/antagonist	CHEK2
C1700	EIF4G gene inhibitor	inhibitor/antagonist	EIF4G1
C1706	JAK1 selective inhibitors	inhibitor/antagonist	CDK2 JAK1 AURKB
C1712	POLA1 inhibitor	allosteric inhibitor	POLA1
C1719	EHMT1/2 DNA Methyltransferase (DNMT) Inhibitors Histone-lysine N-methyltransferase, H3 lysine-9 specific 3 (EHMT2| G9a) Inhibitors		EHMT2 EHMT1
C1724	ERCC3 (TFIIH subunit)	inhibitor/antagonist	ERCC3
C1738	covalent inhibitor of ALDH1A1	inhibitor/antagonist	ALDH1A1
C1742	-	allosteric inhibitor	EIF4A3
C1745	EHMT2 inhibitor	inhibitor/antagonist	EHMT2
C1749	Glutathione-S-Transferase P1 (GSTP1) Inhibitors	inhibitor/antagonist	GSTM2 GSTP1
C1784	Microsomal Triglyceride Transfer Protein (MTTP) Inhibitors	inhibitor/antagonist	MTTP

C1811	Antibiotic Chelator Methionine Aminopeptidase-2 (MetAP2) Inhibitors Angiogenesis Inhibitors	inhibitor/antagonist	METAP2 SIRT2 SIRT1
C1821	DNA-Intercalating Drugs DNA Topoisomerase I Inhibitors	-	TOP1
C1822	MetAPN inhibitor Plasmodium falciparum Methionine Aminopeptidase-1b (PfMetAP1b) Inhibitors	inhibitor/antagonist	METAP1
C1829	DNA Topoisomerase I Inhibitors	inhibitor/antagonist	TOP1
C1854	MEK Inhibitor	inhibitor/antagonist	MAP2K3 MAP2K5 MAP2K6
C1872	XPO1 (CRM1) inhibitor	inhibitor/antagonist	XPO1
C1873	XPO1 (CRM1) inhibitor	inhibitor/antagonist	XPO1
C1874	CREBBP - beta-catenin interaction inhibitor Apoptosis Inducers Wnt Signaling Inhibitors	disruptor/degrader	CREBBP CTNNB1
C1877	Flt3 (FLK2/STK1) Inhibitors FGFR3 Inhibitors Bcr-Abl Kinase Inhibitors Angiogenesis Inhibitors Inhibitors of Signal Transduction Pathways	inhibitor/antagonist	ABL1 ABL2 BCR FGFR3 FLT3
C1880	RAF Inhibitor	inhibitor/antagonist	RAF1
C1886	glutamyl-prolyl-tRNA synthetase inhibitor	inhibitor/antagonist	EPRS1
C1890	CDK4/Cyclin D1 Inhibitors Leucine-Rich Repeat Kinase 2 (LRRK2 Dardarin) Inhibitors Protein Kinase C (PKC) Inhibitors		CCND1 CDK4 PRKCG PRKCH PRKCI PRKCZ RPS6KA1 RPS6KA2 RPS6KA3 RPS6KB2 LRRK2
C1892	Mutant RAF kinase inhibitor	inhibitor/antagonist	BRAF RAF1
C1901	ACAT Inhibitor	inhibitor/antagonist	SOAT1 SOAT2
C1903	SIRT2 inhibitor	-	SIRT2
C1917	Inhibitor of Aurora	inhibitor/antagonist	CDK2 CDK4 CDK5 AURKA CCNE2

C1919	CDK Inhibitor Pan Kinase Inhibitor	inhibitor/antagonist	CDK2 CCNE2
C1925	Antimitotic Drugs Inhibitors of Signal Transduction Pathways Aurora-A (ARK1) Kinase Inhibitors Glycogen Synthase Kinase 3 beta (GSK-3beta| tau Protein Kinase I) Inhibitors Cyclin-Dependent Kinase Inhibitors		GSK3B AURKA CDKL5
C1934	CDK gene inhibitor	inhibitor/antagonist	CDK2 CDK4 CDK5 CDK7 CDK9
C1936	Protein Kinase D (PKD) Inhibitors	inhibitor/antagonist	PRKD1 PRKD3 PRKD2
C1947	PKR Inhibitor	inhibitor/antagonist	EIF2AK2
C1959	Inhibitor of pyrimidine biosynthesis	inhibitor/antagonist	CAD
C1960	PKD inhibitor	inhibitor/antagonist	PRKD1
C1964	Inhibitor of pyrimidine biosynthesis	inhibitor/antagonist	DHODH
C1967	Cytochrome P450 Inhibitors NADPH Oxidase Inhibitors Nitric Oxide Synthase Inhibitors Xanthine Oxidase Inhibitors Electron Transport Chain Inhibitor		XDH NOX1 NOX4 NOX3
C1972	HTR1B antagonist	inhibitor/antagonist	HTR1B
C1983	Translation inhibitor treatment of orphan leukemia Elongation inhibitor	inhibitor/antagonist	EIF4E
C1988	Tubulin polymerization inhibitor Antimitotic Drugs Tubulin polymerization inhibitors	inhibitor/antagonist	TUBA4A TUBA3C TUBB2A TUBG1 TUBA1A TUBA1B TUBB3 TUBB4A TUBB4B TUBG2 TUBD1 TUBA8 TUBB1 TUBB6 TUBA1C TUBA3E TUBA3D TUBB8 TUBB2B
C2014	CDK9 inhibitor	inhibitor/antagonist	CDK9 CCNB2
C2023	PIKFYVE inhibitor IL-12 Production Inhibitor PIKFYVE enzyme inhibitor	inhibitor/antagonist	PIKFYVE

C2032	MEK1 Inhibitors MEK2 Inhibitors Inhibitors of Signal Transduction Pathways		MAP2K1 MAP2K2
C2046	CDK inhibitors		CCNB2 CCNB3
C2051	PIKFYVE gene inhibitor Apoptosis-independent	inhibitor/antagonist	PIKFYVE
C2057	Angiogenesis Inhibitors Antiinflammatory Drugs Apoptosis Inducers Bcl-2 Inhibitors Glutathione Reductase (NADPH) Activators Heme Oxygenase Activators IKK-1 (IKK-alpha) Inhibitors NF-kappaB (NFKB) Activation Inhibitors Nitric Oxide Production Inhibitors Nuclear Factor, Erythroid Derived 2, Like 2 (Nrf2) Activators PPARgamma Agonists	inhibitor/antagonist	IKBKB KEAP1
C2064	Cardiac Myosin Activators	stimulator/agonist	MYH7
C2072	Inhibitors of Signal Transduction Pathways Cell Division Cycle 7-Related Protein Kinase (CDC7) Inhibitors	-	CDC7
C2073	ALK Inhibitors	inhibitor/antagonist	ALK
C2075	IGF-1R Inhibitors	inhibitor/antagonist	IGF1R
C2077	Phosphatidylinositol 3-Kinase Catalytic Subunit Type 3 (PIK3C3 Vps34) Inhibitors	inhibitor/antagonist	PIK3C3
C2080	CDK inhibitors	inhibitor/antagonist inhibitor/antagonist inhibitor/antagonist - - inhibitor/antagonist -	CDK2 CDK9 DYRK1A CCNA1 CCNB2 ROCK2 CCNB3
C2090	-	-	HPRT1
C2111	TLR9 Receptor Antagonists TLR7 Receptor Antagonists TLR8 Receptor Antagonists	inhibitor/antagonist	TLR7 TLR8 TLR9
C2115	PAK4 gene inhibitor	inhibitor/antagonist	PAK4

C2118	Antimitotic Drugs Apoptosis Inducers Aurora Kinase Inhibitors CDK1/Cyclin B Inhibitors CDK2/Cyclin A Inhibitors Inhibitors of Signal Transduction Pathways	inhibitor/antagonist	CDK1 CDK2 AURKA CCNA1
C2124	5-HT2A Antagonists Dopamine D2 Antagonists	inhibitor/antagonist	ADRA1B HTR1E HTR1F
C2132	-	inhibitor/antagonist	GPX4
C2133	CDK9 inhibitor	inhibitor/antagonist	CDK9
C2135	Apoptosis Inducers Inhibitors of Signal Transduction Pathways Raf kinase B Inhibitors Raf kinase C Inhibitors	inhibitor/antagonist	BRAF RAF1
C2139	IGF-1R Inhibitors	inhibitor/antagonist	IGF1R
C2146	Checkpoint Kinase 1 and 2 (Chk1 and Chk2) Inhibitors DNA repair inhibitor	inhibitor/antagonist	CHEK1 CHEK2
C2149	p38alpha MAPK Inhibitors	inhibitor/antagonist	MAPK14
C2158	ATG4B gene Inhibitor	inhibitor/antagonist	ATG4B
C2165	Apoptosis Inducers Nitric Oxide Production Inhibitors Nuclear Factor, Erythroid Derived 2, Like 2 (Nrf2) Activators Antiinflammatory Drugs PPARgamma Agonists	stimulator/agonist	NFE2L2 PPARG KEAP1
C2170	Electron transport chain inhibitor Apoptosis Inducers NADH-Ubiquinone Oxidoreductase (Complex I) Inhibitors Non-Steroidal Antiinflammatory Drugs Electron Transport Chain Inhibitors		NDUFS1 NOX4 NOX5
C2180	WNK1/2/3/4 inhibitor WNK1 gene inhibitor	inhibitor/antagonist	WNK1 WNK4 WNK3 WNK2
C2185	NFkappaB-inducing kinase (NIK MAP3K14) Inhibitors	inhibitor/antagonist	MAP3K14
C2191	beta-Catenin Inhibitors	inhibitor/antagonist	CTNNB1 TCF4
C2196	-	inhibitor/antagonist	SYK
C2197	Apoptosis Inducers BCL2 Expression Inhibitors	-	BCL2

C2200	ATR gene inhibitor Chemosensitizer DNA damage reversal pathway modulator	inhibitor/antagonist	ATR
C2201	PDK1 inhibitor PDK1/2 inhibitor	inhibitor/antagonist	PDK1 PDPK1
C2206	Mammalian Target of Rapamycin (mTOR FRAP1) Inhibitors	inhibitor/antagonist	MTOR
C2210	BIRC5 gene inhibitor	inhibitor/antagonist	BIRC5
C2217	Transcription inhibitor CDK9 inhibitor	inhibitor/antagonist	CDK9
C2222	Mammalian Target of Rapamycin (mTOR FRAP1) Inhibitors	inhibitor/antagonist	MTOR
C2223	Mammalian Target of Rapamycin (mTOR FRAP1) Inhibitors Phosphatidylinositol 3-Kinase delta (PI3Kdelta) Inhibitors Phosphatidylinositol 3-Kinase alpha (PI3Kalpha) Inhibitors Phosphatidylinositol 3-Kinase gamma (PI3Kgamma) Inhibitors	inhibitor/antagonist	MTOR PIK3CA PIK3CD PIK3CG
C2227	MEK1 Inhibitors	allosteric inhibitor	MAP2K1
C2230	CDK5 Inhibitors Dual-Specificity Tyrosine-(Y)-Phosphorylation Regulated Kinase 1A (DYRK1A) Inhibitors CDK2 Inhibitors	inhibitor/antagonist	CDK2 CDK5 DYRK1A
C2237	-	-	-
C2244	-	-	-
C2249	N-Myristoyltransferase Inhibitors	inhibitor/antagonist	NMT1
C2252	p53 tumor suppressor protein inhibitor	inhibitor/antagonist	TP53
C2257	Inhibitor of pyrimidine biosynthesis Antimicrobial	inhibitor/antagonist	DHODH
C2258	WEE1 gene inhibitor	inhibitor/antagonist	WEE1 WEE2
C2271	Autophagy Agonist Phosphodiesterase V (PDE5A) Inhibitors	-	PDE5A
C2272	ATR gene inhibitor	inhibitor/antagonist	ATR
C2292	NAMPT Inhibitor	inhibitor/antagonist	NAMPT
C2305	pan-KDM6 family (KDM6A / KDM6B / UTY) Histone demethylation inhibitors KDM6A gene inhibitor, KDM6B gene inhibitor	inhibitor/antagonist	KDM6A KDM6B

C2317	PDK1 inhibitor	inhibitor/antagonist	PDK1
C2319	binding to EF-1_ mediates inhibition of translocation	-	EEF1A1
C2323	pan PLK inhibitor	inhibitor/antagonist	PLK3 PLK1 PLK2
C2326	AKT inhibitor	inhibitor/antagonist	AKT1 AKT2 AKT3
C2331	-	- inhibitor/antagonist - inhibitor/antagonist inhibitor/antagonist	BRAF BRAF RAF1 RAF1 RAF1
C2352	PKC inhibitor Kinase inhibitors	inhibitor/antagonist inhibitor/antagonist inhibitor/antagonist inhibitor/antagonist inhibitor/antagonist	PRKCA PRKCB PRKCD PRKCE PRKCQ
C2365	Werner helicase irreversible inhibitor	inhibitor/antagonist	WRN
C2367	-	inhibitor/antagonist	ILK
C2371	Elongation factor 1 alpha 1 inhibitor	inhibitor/antagonist	EEF1A1
C2377	Protein kinase C theta inhibitor	inhibitor/antagonist	PRKCQ
C2385	Lipoprotein Associated Phospholipase A2 (Lp-PLA2) Inhibitors Signal Transduction Modulators	-	PLA2G7
C2387	Glycerol-3-Phosphate Dehydrogenase (NAD+) Inhibitors Inhibitory kappaB Kinase (IKK) Inhibitors Nicotinamide Phosphoribosyltransferase (NMPRTase) Inhibitors Signal Transduction Modulators	inhibitor/antagonist	CHUK GPD1 NAMPT
C2390	GSK3B gene inhibitor	inhibitor/antagonist	GSK3B
C2394	Adenosine kinase inhibitor	inhibitor/antagonist	ADK AK1 AK2 AK4 AK5 AK3 AK7 AK8 AK6
C2409	Exportin 1 inhibitor	inhibitor/antagonist	XPO1
C2415	ERK1/2 inhibitor	inhibitor/antagonist	MAPK1 MAPK3

C2417	JMJD2 Histone Demethylase Inhibitor	inhibitor/antagonist	KDM4B KDM4C KDM4E
C2425	MAP3K11 gene inhibitor	inhibitor/antagonist	MAP3K11
C2431	MAP3K12 (DLK) Inhibitors	inhibitor/antagonist	MAP3K12 MAP3K13
C2435	RAS-SOS molecular glue	allosteric activator	SOS1
C2444	KDM1A (LSD1) inhibitor KDM1A inhibitor	inhibitor/antagonist	KDM1A
C2450	DDR tyrosine kinase receptor inhibitor	inhibitor/antagonist	DDR1 DDR2
C2467	CECR2 inhibitor CECR2 inhbitor	inhibitor/antagonist	CECR2
C2471	SHP2 allosteric inhibitor	allosteric inhibitor	PTPN11
C2479	GPX4 covalent inhibitor	inhibitor/antagonist	GPX4
C2483	MAP Kinase Kinase (MEK) Inhibitors Inhibitors of Signal Transduction Pathways	inhibitor/antagonist	MAP2K7
C2491	IRE1 RNase Allosteric Inhibitor	allosteric inhibitor	ERN1
C2495	camk1 gene inhibitor	inhibitor/antagonist	CAMK1 CAMK1D CAMK1G
C2535	Eukaryotic Translation Initiation Factor 2-alpha Kinase 1 (HRI) Activators	stimulator/agonist	EIF2AK1
C2538	Proteasome inhibitor	inhibitor/antagonist	PSMB1 PSMB8 PSMB2 PSMB9 PSMB5 PSMB10
C2541	Cyclooxygenase-2 Inhibitors Non-Steroidal Antiinflammatory Drugs Angiogenesis Inhibitors	inhibitor/antagonist	CASP3 PTGS2
C2553	SMG1 gene inhibitor	inhibitor/antagonist	SMG1
C2561	Phoshodiesterase 10A Inhibitor	inhibitor/antagonist	PDE10A
C2571	TIC10 inactivates Akt and ERK and induces TRAIL expression	stimulator/agonist	TNFSF10
C2572	inhibition of NRF2 signaling Chemosensitizers Translation inhibitor	-	-
C2582	Methuosis inducer	inhibitor/antagonist	PIP5K1C PIKFYVE
C2603	ADP ribosylation factor 1 inhibitor	inhibitor/antagonist	ARFGAP1

C2610	Wnt signalling inhibitor Wnt Pathway Inhibitor type I inhibitor of CDK8 and CDK19	inhibitor/antagonist	CDK8 CDK19
C2617	ITK (EMT) Kinase Inhibitors	inhibitor/antagonist	ITK
C2619	Dyrk1 inhibitor	inhibitor/antagonist	DYRK1B
C2627	FLT3/AXL inhibitor	inhibitor/antagonist	ALK AXL FLT3
C2634	Positive allosteric modulators (PAMs) of the muscarinic acetylcholine	allosteric activator	CHRM4
C2635	wnt pathway inhibitor	-	-
C2642	-	-	PIK3C3
C2654	-	inhibitor/antagonist	PIR
C2665	-	disruptor/degrader	CDK9
C2670	phosphorylated-p68 RNA helicase inhibitor	inhibitor/antagonist	DDX5
C2677	Syk Kinase Inhibitors	inhibitor/antagonist	SYK
C2680	Aurora-B (ARK2) Kinase Inhibitors Antimitotic Drugs Aurora-A (ARK1) Kinase Inhibitors Adenosine A3 Antagonists Differentiation Inhibitors		ADORA3 AURKA AURKB
C2822	Dual Top1, TDP1 inhibitors	inhibitor/antagonist	TOP1 TDP1
C2832	CREBBP/ EP300 KAT inhibitor	inhibitor/antagonist	CREBBP EP300
C2834	PKC theta inhibitor	inhibitor/antagonist	PRKCQ
C2836	PKC theta inhibitor	inhibitor/antagonist	PRKCQ
C2838	ASK1	inhibitor/antagonist	MAP3K5
C2842	Rho Kinase Inhibitors	inhibitor/antagonist	ROCK1 ROCK2
C2845	Hsp90 inhibitor	inhibitor/antagonist	HSP90AA1 HSP90AB1
C2854	Calcitonin Gene-Related Peptides (CGRP) Antagonists	inhibitor/antagonist	CALCRL
C2871	Proteasome inhibitor	inhibitor/antagonist	PSMD14 PSMD14
C2880	Cyclin-Dependent Kinase Inhibitors	inhibitor/antagonist	CDK2 CDK4 CDK6 CDKL5
C2881	NAMPT inhibitor	inhibitor/antagonist	NAMPT

C2884	Focal Adhesion Kinase (FAK) Inhibitors IGF-1R Inhibitors	-	PTK2	
C2887	Focal Adhesion Kinase (FAK) Inhibitors	inhibitor/antagonist	PTK2	
C2889	Focal Adhesion Kinase (FAK) Inhibitors	inhibitor/antagonist	PTK2	
C2893	CDK7 inhibitors CDK2/Cyclin E Inhibitors CDK9 inhibitors	inhibitor/antagonist	CCNE1 CDK2 CDK7	CDK9 CCNA1 CCNE2
C2894	CDK2/Cyclin E Inhibitors CDK1 Inhibitors CDK4 Inhibitors	inhibitor/antagonist	CCNE1 CDK1 CDK2	CDK4 CCNE2
C2895	CDK2/Cyclin E Inhibitors	inhibitor/antagonist	CCNE1 CDK2 CCNB2 CCNE2	
C2900	Lipoprotein Associated Phospholipase A2 (Lp-PLA2) Inhibitors	inhibitor/antagonist	PLA2G7 OPTN	
C2920	CLRN stabilizer	stabilizer	CLRN1	
C2923	covalent modifier of catalytic cysteine of pro-CASP8 and pro-CASP10	inhibitor/antagonist	CASP8 CASP10	
C2926	Ubiquitin-Conjugating Enzyme E2 R1 (CDC34) Inhibitors	inhibitor/antagonist	CDC34	
C2933	PARG inhibitor	inhibitor/antagonist	PARG PARG	
C2999	Allosteric inhibitor that degrades PAK4	disruptor/degrader	PAK4	
C3002	PKC epsilon inhibitor	inhibitor/antagonist	PRKCE	
C3016	Translation Inititiation Inhibitor	inhibitor/antagonist	RPL3	
C3022	PKC inhibitors	inhibitor/antagonist	PRKCH PRKCZ	
C3025	Apoptosis inducers MAP kinase kinase (MEK) inhibitors ERK inhibitors Jak2 inhibitors	inhibitor/antagonist	JAK2 MAPK13 MAP2K7	
C3044	Protein Kinase C (PKC) Inhibitors	inhibitor/antagonist	PRKCH PRKCZ	
C3049	Protein Kinase C (PKC) Inhibitors	inhibitor/antagonist	PRKCH PRKCZ	
C3050	PKC inhibitors	inhibitor/antagonist	PRKCH	
C3054	AP-1 Inhibitors Cytokine Production Inhibitors NF-kappaB (NFKB) Activation Inhibitors	-	JUN	

C3078	CDK4/Cyclin D1 Inhibitors CDK2/Cyclin E Inhibitors Protein Kinase C (PKC) Inhibitors	inhibitor/antagonist	CCND1 CCNE1 CDK2	CDK4 PRKCH PRKCZ
C3113	Chemokine CCR1 Antagonists	inhibitor/antagonist	CCR1	
C3136	induces concomitant H3K9me3 downregulation	inhibitor/antagonist	SUV39H1	
C3152	GLP-1 receptor agonists Insulin secretagogues	stimulator/agonist	GLP1R	
C3163	Antiinflammatory Drugs Chemokine CCR1 Antagonists	-	CCR6 CCR7 CCR8	CX3CR1 CCR10
C3164	Antiinflammatory Drugs Chemokine CC Antagonists	-	CCR6 CCR7 CCR8	CX3CR1 CCR10
C3167	CXCR2 antagonist	inhibitor/antagonist	CXCR2	
C3184	-	inhibitor/antagonist	MLKL	
C3203	Cinobufagin, SMUT Na+/K+-ATPase Inhibitors Chloride Channel Activators	inhibitor/antagonist	ATAD5	
C3208	-	inhibitor/antagonist	HSP90B1	
C3217	-	allosteric inhibitor	EIF4A3	
C3220	antagonist of neuropilin-1 receptor	inhibitor/antagonist	NRP1	
C3226	Antimitotic agent	inhibitor/antagonist	TOP2A TUBA4A TUBA3C TUBB2A TUBG1 TUBA1A TUBA1B TUBB3 TUBB4A TUBB4B	TUBG2 TUBD1 TUBA8 TUBB1 TUBB6 TUBA1C TUBA3E TUBA3D TUBB TUBB8 TUBB2B
C3236	Apoptosis Inducers Translation inhibitor SGLT-1 expression Inhibitors	-	SLC5A1	
C3336	Muscarinic M1 Agonists Dopamine D2 Agonists	stimulator/agonist	CHRM1 DRD2	
C3370	GABA(A) BZ Site Receptor Partial Agonists	partial agonist	GABRA1 GABRA2 GABRA3 GABRA5 GABRB3	GABRG2

C3377	Adrenergic receptor modulator Calcium channel blockers	- inhibitor/antagonist inhibitor/antagonist inhibitor/antagonist	ADRA1B CACNA1I CACNA1H CACNA1G
C3394	Nicotinic Acid (Niacin GPR109A HM74A) Receptor Agonists Inosine 5'-Monophosphate Dehydrogenase (IMPDH) Inhibitors	inhibitor/antagonist	IMPDH1 IMPDH2
C3408	Suppressor of XBP1 mRNA splicing	-	ADK
C3410	HTR1D antagonist	inhibitor/antagonist	HTR1D
C3433	TNF-alpha Production Inhibitors IL-1beta Production Inhibitors	-	-
C3434	v-ATPase inhibitor	inhibitor/antagonist	ATP5PF ATP6V1A ATP6V1H
C3438	Dihydroorotate dehydrogenase (DHODH) inhibitors	inhibitor/antagonist	DHODH
C3488	RXFP4 inhibitor	inhibitor/antagonist	RXFP4
C3493	XPO1 (CRM1) inhibitor	inhibitor/antagonist	XPO1
C3494	binds to FKBP, inhibits NFKB pathway	neomorph	FKBP1A
C3537	Sigma Receptor antagonists	inhibitor/antagonist	SIGMAR1
C3564	Non-steroidal antiinflammatory drugs PKC inhibitors	- inhibitor/antagonist	CAMK2D PRKCA
C3572	Antimitotic drugs	-	TUBB
C3573	Microtubule polymerization inhibitors	inhibitor/antagonist	TUBA4A TUBA3C TUBB2A TUBG1 TUBA1A TUBA1B TUBB3 TUBB4A TUBB4B TUBG2 TUBD1 TUBA8 TUBB1 TUBB6 TUBA1C TUBA3E TUBA3D TUBB8 TUBB2B
C3613	Sodium ionophore	-	-

Table 3.3: Compound hits from agonist reconfirmation screen using recombinase-based reporter and their known associated genes. Reasons for compound inclusion in reconfirmation screen are also noted.

Compound Name	Reason for reconfirmation	Mechanism of Action	Modality	Gene(s)
C902	screen hit	DNA topoisomerase I inhibitor PKC activator Protein kinase C alpha stimulator	stimulator/agonist inhibitor/antagonist	PRKCA TOP1
C1739	screen hit	Inhibitor of sodium-coupled citrate transporter	inhibitor/antagonist	SLC13A5
C2563	screen hit	Lymphangiogenesis Inducer Lymphangiogenesis Inducers	inhibitor/antagonist	PRKCA RASGRP3
C3166	screen hit	CRHR2 antagonist CRF Receptor Antagonists	inhibitor/antagonist	CRHR2
C3388	screen hit	PKC agonist	-	PRKCA
C383	active analog	Endothelin Receptor Antagonists	inhibitor/antagonist	EDNRA EDNRB
C571	active analog	-	-	PCSK9
C608	active analog	-	-	PCSK9
C887	active analog	-	-	PCSK9
C1280	active analog	-	-	PCSK9
C1289	active analog	-	-	PCSK9
C2953	active analog	-	-	PCSK9
C3507	active analog	-	-	PCSK9
C611	inactive analog	-	-	PCSK9
C817	inactive analog	-	-	PCSK9
C859	inactive analog	-	-	PCSK9
C930	inactive analog	-	-	PCSK9
C988	inactive analog	-	-	PCSK9
C1288	inactive analog	-	-	PCSK9
C1525	inactive analog	-	-	PCSK9
C1579	inactive analog	-	-	PCSK9
C1583	inactive analog	-	-	PCSK9
C2282	inactive analog	-	-	PCSK9
C2297	inactive analog	-	-	PCSK9
C3194	inactive analog	-	-	PCSK9
C3234	inactive analog	-	-	PCSK9
C3511	inactive analog	-	-	PCSK9
C1374	range	-	-	ACHE
C2364	range	-	-	ACHE

C2215	range	-	-	CMA1
C2626	range	-	-	MAPK13
C1272	PMA control	Protein kinase C alpha stimulator	stimulator/agonist	PRKCA
C3260	target interrogration compound	Inhibitor of DNA synthesis	-	OGA

*Indicates compounds with high maximum RLU

Table 3.4: Compound hits from antagonist reconfirmation screen performed with recombinase-based reporter and their known associated genes.

Compound Name	Mechanism of Action	Modality	Gene(s)
C161	AP-1 Inhibitors Electron Transport Chain Inhibitors	inhibitor/antagonist	JUN UQCRC1
C183	CDK4/Cyclin D1 Inhibitors CDK2/Cyclin E Inhibitors Protein Kinase C (PKC) Inhibitors	inhibitors/antagonist	CCND1 CCNE1 CDK2 CDK4
C191	Inducible nitric oxide synthase (NOS-2) inhibitors Nicotinic receptor agonists Acetylcholinesterase inhibitors LDL antioxidants	-	ACHE NOS2
C217	Vasopressin (AVP) V2 Antagonists	inhibitor/antagonist	AVPR2
C225	topoisomerase I	-	TOP1
C230	Protein Kinase C (PKC) Inhibitors CDK1 Inhibitors CDK2 Inhibitors	inhibitor/antagonist	CDK1 CDK2
C234	Actin stabilizer	stabilizer	ACTB
C241	RNA synthesis inhibitor DNA-Directed RNA Polymerase Inhibitors Transcription Inhibitors	inhibitor/antagonist	CDK9 POLRMT
C249	CDK1 inhibitors	inhibitor/antagonist	CDK1
C252	CDK1 inhibitors	inhibitor/antagonist	CDK1
C258	CDK1 Inhibitors	inhibitor/antagonist	CDK1
C278	Apoptosis Inducers Caspase 3 Activators Autophagy inducer	inhibitor/antagonist inhibitor/antagonist inhibitor/antagonist stabilizer inhibitor/antagonist inhibitor/antagonist	ARF1 GBF1 CYTH2 CYTH1 ARFGEF2 ARFGEF1
C303	CD80 (B7-1) Inhibitors	inhibitor/antagonist	CD28 CD80
C424	Apoptosis inducers DNA topoisomerase I inhibitors	-	TOP1
C429	MAP Kinase Kinase (MEK) inhibitors Extracellular-regulated kinase (ERK) inhibitors Inhibitors of signal transduction pathways	inhibitor/antagonist	MAPK13 MAP2K7
C438	PKA and AKT (a.k.a. PKB)	inhibitor/antagonist	AKT1

C545	Protein Kinase Inhibitors	inhibitor/antagonist	FGFR2 FLT3 IGF1R SRC
C599	Protein Kinase PKC beta Inhibitors Protein Kinase PKC theta Inhibitors Protein Kinase PKC delta Inhibitors Protein Kinase PKC alpha Inhibitors Protein Kinase PKC epsilon Inhibitors	-	CD28 PRKCA PRKCB PRKCD PRKCE PRKCQ
C602	Proteasome inhibitor Proteasome Inhibitors Apoptosis Inducers Caspase 3 Activators NF-kappaB (NFKB) Activation Inhibitors	inhibitor/antagonist	CASP3 CTRB1 PSMA1 PSMA2 PSMA3 PSMA4 PSMA5 PSMA6 PSMA7 PSMB1 PSMB2 PSMB3 PSMB4 PSMB5 PSMB6 PSMB7 PSMB8 PSMB9 PSMB10 PSMC3 PSMC5 PSMD1 PSMD2 PSMD3 PSMD4 PSMD7 PSMD8 PSMD11 PSMD13 CTRC PSMB11 PSMA8
C614	Inosine 5'-Monophosphate Dehydrogenase Type II (IMPDH II) Inhibitors Inosine 5'-Monophosphate Dehydrogenase Type I (IMPDH I) Inhibitors	-	IMPDH1 IMPDH2
C616	Protein Kinase C (PKC) Inhibitors	inhibitor/antagonist	PRKCH
C672	pan-PKC inhibitor	inhibitor/antagonist	CD28 PRKCQ
C674	Hedgehog Signaling Inhibitors	inhibitor/antagonist	GLI1
C675	Apoptosis Inducers	-	-
C686	Ribonucleotide Reductase inhibitor DNA Damaging Agent	inhibitor/antagonist	SLC29A1 SLC29A2 RRM1 RRM2 TYMS SLC29A3
C696	Glucose Lowering Agents	-	-
C697	Protein Kinase C (PKC) Inhibitors IL-2 Production Inhibitors	-	CD28 IL2
C698	-	inhibitor/antagonist	RET

C848	DNA-Intercalating Drugs	-	-
#N/A	-	-	-
C899	Leucine-Rich Repeat Kinase 2 (LRRK2 Dardarin) Inhibitors	inhibitor/antagonist	CAMK2B CAMK2G FYN PRKCZ PRKD3 PRKCG PRKCH PRKCI LRRK2
C900	Flt3 (FLK2/STK1) Inhibitors Inhibitors of Signal Transduction Pathways	inhibitor/antagonist	MAPK14 FLT3 KIT PDGFRB MAPK8 MAPK10
C904	Protein Kinase C (PKC) Inhibitors IL-2 Production Inhibitors	-	IL2
C906	Flt3 (FLK2/STK1) Inhibitors	inhibitor/antagonist	FLT3
C937	Inhibitors of Signal Transduction Pathways Protein Kinase PKC beta Inhibitors Angiogenesis Inhibitors	-	PRKCB PRKCH PRKCZ RPS6KB1
C975	Translation inhibitor TARS inhibitor angiogenesis inhibitor	inhibitor/antagonist	TARS1
C983	CHK1 expression inhibitors Inhibitors of Signal Transduction Pathways HSP90 inhibitors	-	HSP90AA 1
C1002	IKK-2 (IKK-beta) Inhibitors Flt3 (FLK2/STK1) Inhibitors	inhibitor/antagonist	CHUK FLT3 IKBKB IKBKG
C1026	Known SPPL2A inhibitor	inhibitor/antagonist	SPPL2A
C1031	Heat Shock Protein 90 (hsp90) Inhibitors	inhibitor/antagonist	HSP90AA 1 HSP90B1
C1059	Inhibitors of Signal Transduction Pathways Protein Kinase PKC beta Inhibitors Angiogenesis Inhibitors	-	PRKCB PRKCG
C1060	Protein Kinase C (PKC) Inhibitors	inhibitor/antagonist	PRKCG
C1086	Translation inhibitor	inhibitor/antagonist	RPS14 RPS20
C1105	Exportin 1 inhibitor	inhibitor/antagonist	XPO1
C1113	Translation Inhibitor Glycogen Synthase Kinase 3 beta (GSK-3beta tau Protein Kinase I) Inhibitors	inhibitor/antagonist	GSK3B RPL6

C1116	Nerve Growth Factor (NGF) Enhancers Tenogenic	inhibitor/antagonist - inhibitor/antagonist inhibitor/antagonist	CDK8 NGF PDE3A CDK19
C1117	cAMP-Dependent Protein Kinase (PKA) Inhibitors Inhibitors of Signal Transduction Pathways PKB alpha/Akt1 Inhibitors	-	PRKACA PRKACB PRKACG
C1151	Lck Kinase Inhibitors	inhibitor/antagonist	LCK
C1162	Inosine 5'-Monophosphate Dehydrogenase (IMPDH) Inhibitors Immunosuppressant IMPDH inhibitor antiviral	inhibitor/antagonist	IMPDH1 IMPDH2
C1168	Lipid Kinase Inhibitors	inhibitor/antagonist	PI4KB RPS6KA3
C1187	Mammalian Target of Rapamycin (mTOR FRAP1) Inhibitors Phosphatidylinositol 3-Kinase alpha (PI3Kalpha) Inhibitors Phosphatidylinositol 3-Kinase beta (PI3Kbeta) Inhibitors Phosphatidylinositol 3-Kinase delta (PI3Kdelta) Inhibitors Phosphatidylinositol 3-Kinase gamma (PI3Kgamma) Inhibitors	-	PIK3C2B
C1206	Jak3 tyrosine kinase inhibitor	inhibitor/antagonist	GSK3B JAK3 PRKCA
C1207	VEGFR-2 (FLK-1/KDR) Inhibitors Bcr-Abl Kinase Inhibitors Angiogenesis Inhibitors	-	ABL1 ABL2 BCR KDR
C1220	ROCK gene inhibitor PKC Kinase nhibitor	inhibitor/antagonist	PRKACA ROCK1 ROCK2
C1247	Protein Kinase PKC theta Inhibitors IL-2 Production Inhibitors	inhibitor/antagonist	IL2 PRKCQ
C1251	MAPKAPK5 inhibitor	inhibitor/antagonist	MAPKAP K5

C1254	Inhibitors of Signal Transduction Pathways Flt3 (FLK2/STK1) Inhibitors Protein Kinase C (PKC) Inhibitors Angiogenesis Inhibitors	inhibitor/antagonist	FLT3 PRKCQ
C1300	CDC-like kinase-2 inhibitors	inhibitor/antagonist	CLK2
C1301	Rho Kinase Inhibitors Protein Kinase PKC theta Inhibitors Protein Kinase PKC epsilon Inhibitors	-	PRKCE PRKCQ ROCK1 ROCK2
C1333	Dual Specificity Mitogen-Activated Protein Kinase Kinase 1 (MAP2K1 MEK1) Inhibitors	inhibitor/antagonist	MAP2K1
C1346	MEK1 Inhibitors	inhibitor/antagonist	MAP2K1
C1347	Mitogen-Activated Protein (MAP) Kinase Kinase (MEK) Inhibitors	inhibitor/antagonist	MAP2K1
C1392	PKC theta inhibitor	inhibitor/antagonist	PRKCQ
C1412	Inhibitors of Signal Transduction Pathways PKB alpha/Akt1 Inhibitors PKB beta/Akt2 Inhibitors PKB gamma/Akt3 Inhibitors	inhibitor/antagonist	AKT1 AKT2 DAPK3 PRKG1 PRKX AKT3 PAK6
C1436	MEK1 Inhibitors MEK2 Inhibitors	-	MAP2K1 MAP2K2
C1459	MAPK-Interacting Kinase (MNK) Inhibitors	inhibitor/antagonist	CDK8 MKNK2 SGK1 MKNK1 CDK19
C1477	ITK (EMT) Kinase Inhibitors IL-4 Production Inhibitors IL-2 Production Inhibitors	inhibitor/antagonist	IL2 IL4 ITK
C1527	Elongation factor 1 alpha inhibitor Translation Inhibitor	inhibitor/antagonist	EIF4A1 EIF4A2 EIF4A3
C1547	Immunoproteasome Inhibitors	inhibitor/antagonist	PSMB8
C1548	CDK1/Cyclin B Inhibitors Apoptosis Inducers Inhibitors of Signal Transduction Pathways CDK2/Cyclin A Inhibitors	inhibitor/antagonist	CCNA2 CCNB1 CDK1 CDK2
C1584	EIF4A1 gene inhibitor	inhibitor/antagonist	EIF4A1
C1640	FAK inhibitor	inhibitor/antagonist	PTK2
C1672	Wnt signaling inhibitor, Inhibitor of beta-catenin/TCF transcription	inhibitor/antagonist	CTNNB1

C1673	M5 positive allosteric modulator	allosteric activator	CHRM5
C1724	ERCC3 (TFIIH subunit)	inhibitor/antagonist	ERCC3
C1738	covalent inhibitor of ALDH1A1	inhibitor/antagonist	ALDH1A1
C1821	DNA-Intercalating Drugs DNA Topoisomerase I Inhibitors	-	TOP1
C1854	MEK Inhibitor	inhibitor/antagonist	MAP2K3 MAP2K5 MAP2K6
C1880	RAF Inhibitor	inhibitor/antagonist	RAF1
C1886	glutamyl-prolyl-tRNA synthetase inhibitor	inhibitor/antagonist	EPRS1
C1890	CDK4/Cyclin D1 Inhibitors Leucine-Rich Repeat Kinase 2 (LRRK2 Dardarin) Inhibitors Protein Kinase C (PKC) Inhibitors	-	CCND1 CDK4 LRRK2 PRKCG PRKCH PRKCI PRKCZ RPS6KA1 RPS6KA2 RPS6KA3 RPS6KB2
C1919	CDK Inhibitor Pan Kinase Inhibitor	inhibitor/antagonist	CDK2 CCNE2
C1947	PKR Inhibitor	inhibitor/antagonist	EIF2AK2
C1959	Inhibitor of pyrimidine biosynthesis	inhibitor/antagonist	CAD
C1964	Inhibitor of pyrimidine biosynthesis	inhibitor/antagonist	DHODH
C1983	Translation inhibitor treatment of orphan leukemia Elongation inhibitor	inhibitor/antagonist	EIF4E
C2014	CDK9 inhibitor	inhibitor/antagonist	CDK9 CCNB2
C2032	MEK1 Inhibitors MEK2 Inhibitors Inhibitors of Signal Transduction Pathways	-	MAP2K1 MAP2K2
C2046	CDK inhibitors	-	CCNB2 CCNB3
C2072	Inhibitors of Signal Transduction Pathways Cell Division Cycle 7-Related Protein Kinase (CDC7) Inhibitors	-	CDC7
C2080	CDK inhibitors	inhibitor/antagonist inhibitor/antagonist inhibitor/antagonist - - inhibitor/antagonist -	CDK2 CDK9 DYRK1A CCNA1 CCNB2 ROCK2 CCNB3

C2115	PAK4 gene inhibitor	inhibitor/antagonist	PAK4
C2118	Antimitotic Drugs Apoptosis Inducers Aurora Kinase Inhibitors CDK1/Cyclin B Inhibitors CDK2/Cyclin A Inhibitors Inhibitors of Signal Transduction Pathways	inhibitor/antagonist inhibitor/antagonist inhibitor/antagonist -	CDK1 CDK2 AURKA CCNA1
C2133	CDK9 inhibitor	inhibitor/antagonist	CDK9
C2135	Apoptosis Inducers Inhibitors of Signal Transduction Pathways Raf kinase B Inhibitors Raf kinase C Inhibitors	inhibitor/antagonist	BRAF RAF1
C2217	Transcription inhibitor CDK9 inhibitor	inhibitor/antagonist	CDK9
C2227	MEK1 Inhibitors	allosteric inhibitor	MAP2K1
C2319	binding to EF-1_ mediates inhibition of translocation	-	EEF1A1
C2331	-	- inhibitor/antagonist - inhibitor/antagonist inhibitor/antagonist	BRAF BRAF RAF1 RAF1 RAF1
C2352	PKC inhibitor Kinase inhibitors	inhibitor/antagonist	PRKCA PRKCB PRKCD PRKCE PRKCQ
C2371	Elongation factor 1 alpha 1 inhibitor	inhibitor/antagonist	EEF1A1
C2394	Adenosine kinase inhibitor	inhibitor/antagonist	ADK AK1 AK2 AK4 AK5 AK3 AK7 AK8 AK6
C2409	Exportin 1 inhibitor	inhibitor/antagonist	XPO1
C2415	ERK1/2 inhibitor	inhibitor/antagonist	MAPK1 MAPK3
C2431	MAP3K12 (DLK) Inhibitors	inhibitor/antagonist	MAP3K12 MAP3K13
C2483	MAP Kinase Kinase (MEK) Inhibitors Inhibitors of Signal Transduction Pathways	inhibitor/antagonist	MAP2K7

C2538	Proteasome inhibitor	inhibitor/antagonist	PSMB1 PSMB2 PSMB5	PSMB8 PSMB9 PSMB10
C2572	inhibition of NRF2 signaling Chemosensitizers Translation inhibitor	-	-	
C2610	Wnt signalling inhibitor Wnt Pathway Inhibitor type I inhibitor of CDK8 and CDK19	inhibitor/antagonist	CDK8 CDK19	
C2627	FLT3/AXL inhibitor	inhibitor/antagonist	ALK AXL FLT3	
C2665	-	disruptor/degrader	CDK9	
C2677	Syk Kinase Inhibitors	inhibitor/antagonist	SYK	
C2680	Aurora-B (ARK2) Kinase Inhibitors Antimitotic Drugs Aurora-A (ARK1) Kinase Inhibitors Adenosine A3 Antagonists Differentiation Inhibitors	-	ADORA3 AURKA AURKB	
C2822	Dual Top1, TDP1 inhibitors	inhibitor/antagonist	TOP1 TDP1	
C2834	PKC theta inhibitor	inhibitor/antagonist	PRKCQ	
C2836	PKC theta inhibitor	inhibitor/antagonist	PRKCQ	
C2842	Rho Kinase Inhibitors	inhibitor/antagonist	ROCK1 ROCK2	
C2845	Hsp90 inhibitor	inhibitor/antagonist	HSP90AA 1 HSP90AB 1	
C2880	Cyclin-Dependent Kinase Inhibitors	inhibitor/antagonist	CDK2 CDK4 CDK6 CDKL5	
C2893	CDK7 inhibitors CDK2/Cyclin E Inhibitors CDK9 inhibitors	inhibitor/antagonist	CCNE1 CDK2 CDK7	CDK9 CCNA1 CCNE2
C2894	CDK2/Cyclin E Inhibitors CDK1 Inhibitors CDK4 Inhibitors	inhibitor/antagonist	CCNE1 CDK1 CDK2	CDK4 CCNE2
C2895	CDK2/Cyclin E Inhibitors	inhibitor/antagonist	CCNE1 CDK2	CCNB2 CCNE2
C3016	Translation Inititiation Inhibitor	inhibitor/antagonist	RPL3	

C3022	PKC inhibitors	inhibitor/antagonist	PRKCH PRKCZ
C3025	Apoptosis inducers MAP kinase kinase (MEK) inhibitors ERK inhibitors Jak2 inhibitors	inhibitor/antagonist	JAK2 MAPK13 MAP2K7
C3044	Protein Kinase C (PKC) Inhibitors	inhibitor/antagonist	PRKCH PRKCZ
C3049	Protein Kinase C (PKC) Inhibitors	inhibitor/antagonist	PRKCH PRKCZ
C3050	PKC inhibitors	inhibitor/antagonist	PRKCH
C3078	CDK4/Cyclin D1 Inhibitors CDK2/Cyclin E Inhibitors Protein Kinase C (PKC) Inhibitors	inhibitor/antagonist	CCND1 CDK4 CCNE1 PRKCH CDK2 PRKCZ
C3208	-	inhibitor/antagonist	HSP90B1
C3394	Nicotinic Acid (Niacin GPR109A HM74A) Receptor Agonists Inosine 5'-Monophosphate Dehydrogenase (IMPDH) Inhibitors	inhibitor/antagonist	IMPDH1 IMPDH2
C3433	TNF-alpha Production Inhibitors IL-1beta Production Inhibitors	-	-
C3493	XPO1 (CRM1) inhibitor	inhibitor/antagonist	XPO1
C3564	Non-steroidal anti-inflammatory drugs PKC inhibitors	- inhibitor/antagonist	CAMK2D PRKCA

BIBLIOGRAPHY

1. Pardee, K., et al., *Paper-based synthetic gene networks.* Cell, 2014. **159**(4): p. 940-954.

2. Ro, D.K., et al., *Production of the antimalarial drug precursor artemisinic acid in engineered yeast.* Nature, 2006. **440**(7086): p. 940-943.

3. Davila, M.L., et al., *Efficacy and toxicity management of 19-28z CAR T cell therapy in B cell acute lymphoblastic leukemia.* Science Translational Medicine, 2014. **6**(224): p. 224ra25.

4. Kochenderfer, J.N., et al., *Chemotherapy-refractory diffuse large B-cell lymphoma and indolent B-cell malignancies can be effectively treated with autologous T cells expressing an anti-CD19 chimeric antigen receptor.* Journal of Clinical Oncology, 2015. **33**(6): p. 540-549.

5. Kochenderfer, J.N., et al., *Eradication of B-lineage cells and regression of lymphoma in a patient treated with autologous T cells genetically engineered to recognize CD19.* Blood, 2010. **116**(20): p. 4099-4102.

6. Lee, D.W., et al., *T cells expressing CD19 chimeric antigen receptors for acute lymphoblastic leukaemia in children and young adults: a phase 1 dose-escalation trial.* Lancet, 2015. **385**(9967): p. 517-528.

7. Maude, S.L., et al., *Chimeric antigen receptor T cells for sustained remissions in leukemia.* New England Journal of Medicine, 2014. **371**(16): p. 1507-1517.

8. Morgan, R.A., et al., *Cancer regression in patients after transfer of genetically engineered lymphocytes.* Science, 2006. **314**(5796): p. 126-129.

9. Parkhurst, M.R., et al., *T cells targeting carcinoembryonic antigen can mediate regression of metastatic colorectal cancer but induce severe transient colitis.* Molecular Therapy, 2011. **19**(3): p. 620-626.

10. Rapoport, A.P., et al., *NY-ESO-1-specific TCR-engineered T cells mediate sustained antigen-specific antitumor effects in myeloma.* Nature Medicine, 2015. **21**(8): p. 914-921.

11. Till, B.G., et al., *Adoptive immunotherapy for indolent non-Hodgkin lymphoma and mantle cell lymphoma using genetically modified autologous CD20-specific T cells.* Blood, 2008. **112**(6): p. 2261-2271.

12. Turtle, C.J., et al., *CD19 CAR-T cells of defined CD4+:CD8+ composition in adult B cell ALL patients.* Journal of Clinical Investigation, 2016. **126**(6): p. 2123-2138.

13. Bonifant, C.L., et al., *Toxicity and management in CAR T-cell therapy.* Molecular Therapy Oncolytics, 2016. **3**: p. 16011.

14. Brudno, J.N. and J.N. Kochenderfer, *Toxicities of chimeric antigen receptor T cells: recognition and management.* Blood, 2016. **127**(26): p. 3321-3330.

15. Maude, S.L., et al., *Managing cytokine release syndrome associated with novel T cell-engaging therapies.* Cancer Journal, 2014. **20**(2): p. 119-122.

16. Suntharalingam, G., et al., *Cytokine storm in a phase 1 trial of the anti-CD28 monoclonal antibody TGN1412.* New England Journal of Medicine, 2006. **355**(10): p. 1018-1028.

17. Tey, S.K., *Adoptive T-cell therapy: adverse events and safety switches.* Clinical & Translational Immunology, 2014. **3**(6): p. e17.

18. Xu, X.J. and Y.M. Tang, *Cytokine release syndrome in cancer immunotherapy with chimeric antigen receptor engineered T cells.* Cancer Letters, 2014. **343**(2): p. 172-178.

19. Brentjens, R., et al., *Treatment of chronic lymphocytic leukemia with genetically targeted autologous T cells: case report of an unforeseen adverse event in a phase I clinical trial.* Molecular Therapy, 2010. **18**(4): p. 666–668.

20. Hay, K.A., et al., *Kinetics and Biomarkers of Severe Cytokine Release Syndrome after CD19 Chimeric Antigen Receptor-modified T Cell Therapy.* Blood, 2017. **130**(21): p. 2295–2306.

21. Morgan, R.A., et al., *Case report of a serious adverse event following the administration of T cells transduced with a chimeric antigen receptor recognizing ERBB2.* Molecular Therapy, 2010. **18**(4): p. 843-851.

22. van den Berg, J.H., et al., *Case Report of a Fatal Serious Adverse Event Upon Administration of T Cells Transduced With a MART-1-specific T-cell Receptor.* Molecular Therapy, 2015. **23**(9): p. 1541-1550.

23. Cartellieri, M., et al., *Switching CAR T cells on and off: a novel modular platform for retargeting of T cells to AML blasts.* Blood Cancer Journal, 2016. **6**(8): p. e458.

24. Di Stasi, A., et al., *Inducible apoptosis as a safety switch for adoptive cell therapy.* New England Journal of Medicine, 2011. **365**(18): p. 1673-1683.

25. Fedorov, V.D., M. Themeli, and M. Sadelain, *PD-1- and CTLA-4-based inhibitory chimeric antigen receptors (iCARs) divert off-target immunotherapy responses.* Science Translational Medicine, 2013. **5**(215): p. 215ra172.

26. Juillerat, A., et al., *Design of chimeric antigen receptors with integrated controllable transient functions.* Scientific Reports, 2016. **6**: p. 18950.

27. Rodgers, D.T., et al., *Switch-mediated activation and retargeting of CAR-T cells for B-cell malignancies.* Proceedings of the National Academy of Sciences of the United States of America, 2016. **113**(4): p. E459-468.

28. Wei, P., et al., *Bacterial virulence proteins as tools to rewire kinase pathways in yeast and immune cells.* Nature, 2012. **488**(7411): p. 384-388.

29. Wu, C.Y., et al., *Remote control of therapeutic T cells through a small molecule-gated chimeric receptor.* Science, 2015. **350**(6258): p. aab4077.

30. Ramos, C.A., et al., *An inducible caspase 9 suicide gene to improve the safety of mesenchymal stromal cell therapies.* Stem Cells, 2010. **28**(6): p. 1107-1115.

31. Lee, D.W., et al., *Current concepts in the diagnosis and management of cytokine release syndrome.* Blood, 2014. **124**(2): p. 188-195.

32. Au-Yeung, B.B., et al., *The structure, regulation, and function of ZAP-70.* Immunological Reviews, 2009. **228**(1): p. 41-57.

33. Au-Yeung, B.B., et al., *A genetically selective inhibitor demonstrates a function for the kinase Zap70 in regulatory T cells independent of its catalytic activity.* Nature Immunology, 2010. **11**(12): p. 1085-1092.

34. Chan, A.C., et al., *The zeta chain is associated with a tyrosine kinase and upon T-cell antigen receptor stimulation associates with ZAP-70, a 70-kDa tyrosine phosphoprotein.* Proceedings of the National Academy of Sciences of the United States of America, 1991. **88**(20): p. 9166-9170.

35. Chan, A.C., et al., *ZAP-70: a 70 kd protein-tyrosine kinase that associates with the TCR zeta chain.* Cell, 1992. **71**(4): p. 649-662.

36. Palacios, E.H. and A. Weiss, *Distinct roles for Syk and ZAP-70 during early thymocyte development.* Journal of Experimental Medicine, 2007. **204**(7): p. 1703-1715.

37. Bubeck Wardenburg, J., et al., *Phosphorylation of SLP-76 by the ZAP-70 protein-tyrosine kinase is required for T-cell receptor function.* Journal of Biological Chemistry, 1996. **271**(33): p. 19641-19644.

38. Horejsi, V., W. Zhang, and B. Schraven, *Transmembrane adaptor proteins: organizers of immunoreceptor signalling.* Nature Reviews. Immunology, 2004. **4**(8): p. 603-616.

39. Koretzky, G.A., F. Abtahian, and M.A. Silverman, *SLP76 and SLP65: complex regulation of signalling in lymphocytes and beyond.* Nature Reviews. Immunology, 2006. **6**(1): p. 67-78.

40. Wang, H., et al., *ZAP-70: an essential kinase in T-cell signaling.* Cold Spring Harbor Perspectives in Biology, 2010. **2**(5): p. a002279.

41. Zhang, W., et al., *LAT: the ZAP-70 tyrosine kinase substrate that links T cell receptor to cellular activation.* Cell, 1998. **92**(1): p. 83-92.

42. Chan, A.C., et al., *ZAP-70 deficiency in an autosomal recessive form of severe combined immunodeficiency.* Science, 1994. **264**(5165): p. 1599-1601.

43. Elder, M.E., *ZAP-70 and defects of T-cell receptor signaling.* Seminars in Hematology, 1998. **35**(4): p. 310-320.

44. Elder, M.E., et al., *Human severe combined immunodeficiency due to a defect in ZAP-70, a T cell tyrosine kinase.* Science, 1994. **264**(5165): p. 1596-1599.

45. Williams, B.L., et al., *Genetic evidence for differential coupling of Syk family kinases to the T-cell receptor: reconstitution studies in a ZAP-70-deficient Jurkat T-cell line.* Molecular and Cellular Biology, 1998. **18**(3): p. 1388-1399.

46. Levin, S.E., et al., *Inhibition of ZAP-70 kinase activity via an analog-sensitive allele blocks T cell receptor and CD28 superagonist signaling.* Journal of Biological Chemistry, 2008. **283**(22): p. 15419-15430.

47. Liu, X., et al., *Restricting Zap70 expression to CD4+CD8+ thymocytes reveals a T cell receptor-dependent proofreading mechanism controlling the completion of positive selection.* Journal of Experimental Medicine, 2003. **197**(3): p. 363-373.

48. Saini, M., et al., *Regulation of Zap70 expression during thymocyte development enables temporal separation of CD4 and CD8 repertoire selection at different signaling thresholds.* Science Signalling, 2010. **3**(114): p. ra23.

49. Feske, S., *Calcium signalling in lymphocyte activation and disease.* Nature Reviews. Immunology, 2007. **7**(9): p. 690-702.

50. Joseph, N., B. Reicher, and M. Barda-Saad, *The calcium feedback loop and T cell activation: how cytoskeleton networks control intracellular calcium flux.* Biochimica et Biophysica Acta, 2014. **1838**(2): p. 557-568.

51. Lewis, R.S., *Calcium signaling mechanisms in T lymphocytes.* Annual Review of Immunology, 2001. **19**: p. 497-521.

52. Shan, X., et al., *Zap-70-independent Ca(2+) mobilization and Erk activation in Jurkat T cells in response to T-cell antigen receptor ligation.* Molecular and Cellular Biology, 2001. **21**(21): p. 7137-7149.

53. Miyazaki, Y., et al., *Destabilizing domains derived from the human estrogen receptor.* Journal of the American Chemical Society, 2012. **134**(9): p. 3942-3945.

54. Banaszynski, L.A., et al., *A rapid, reversible, and tunable method to regulate protein function in living cells using synthetic small molecules.* Cell, 2006. **126**(5): p. 995-1004.

55. Iwamoto, M., et al., *A general chemical method to regulate protein stability in the mammalian central nervous system.* Chemistry & Biology, 2010. **17**(9): p. 981-988.

56. Luo, K. and B.M. Sefton, *Activated lck tyrosine protein kinase stimulates antigen-independent interleukin-2 production in T cells.* Molecular and Cellular Biology, 1992. **12**(10): p. 4724-4732.

57. Zufferey, R., et al., *Self-inactivating lentivirus vector for safe and efficient in vivo gene delivery.* Journal of Virology, 1998. **72**(12): p. 9873-9880.

58. Gross, G., T. Waks, and Z. Eshhar, *Expression of immunoglobulin-T-cell receptor chimeric molecules as functional receptors with antibody-type specificity.* Proceedings of the National Academy of Sciences of the United States of America, 1989. **86**(24): p. 10024-10028.

59. Failla, C., L. Tomei, and R. De Francesco, *Both NS3 and NS4A are required for proteolytic processing of hepatitis C virus nonstructural proteins.* Journal of Virology, 1994. **68**(6): p. 3753-3760.

60. Tomei, L., et al., *NS3 is a serine protease required for processing of hepatitis C virus polyprotein.* Journal of Virology, 1993. **67**(7): p. 4017-4026.

61. Jacobson, I.M., et al., *Telaprevir for previously untreated chronic hepatitis C virus infection.* New England Journal of Medicine, 2011. **364**(25): p. 2405-2416.

62. Lamarre, D., et al., *An NS3 protease inhibitor with antiviral effects in humans infected with hepatitis C virus.* Nature, 2003. **426**(6963): p. 186-189.

63. Poordad, F., et al., *Boceprevir for untreated chronic HCV genotype 1 infection.* New England Journal of Medicine, 2011. **364**(13): p. 1195-1206.

64. Summa, V., et al., *MK-5172, a selective inhibitor of hepatitis C virus NS3/4a protease with broad activity across genotypes and resistant variants.* Antimicrobial Agents and Chemotherapy, 2012. **56**(8): p. 4161-4167.

65. Butko, M.T., et al., *Fluorescent and photo-oxidizing TimeSTAMP tags track protein fates in light and electron microscopy.* Nature Neuroscience, 2012. **15**(12): p. 1742-1751.

66. Chung, H.K., et al., *Tunable and reversible drug control of protein production via a self-excising degron.* Nature Chemical Biology, 2015. **11**(9): p. 713-720.

67. Lin, M.Z., J.S. Glenn, and R.Y. Tsien, *A drug-controllable tag for visualizing newly synthesized proteins in cells and whole animals.* Proceedings of the National Academy of Sciences of the United States of America, 2008. **105**(22): p. 7744-9.

68. Ratnoglik, S.L., et al., *Induction of cell-mediated immune responses in mice by DNA vaccines that express hepatitis C virus NS3 mutants lacking serine protease and NTPase/RNA helicase activities.* PLoS One, 2014. **9**(6): p. e98877.

69. Kugler, J., et al., *High affinity peptide inhibitors of the hepatitis C virus NS3-4A protease refractory to common resistant mutants.* Journal of Biological Chemistry, 2012. **287**(46): p. 39224-39232.

70. Foight, G.W., et al., *Multi-input chemical control of protein dimerization for programming graded cellular responses.* Nature Biotechnology, 2019. **37**(10): p. 1209-1216.

71. Cho, J.H., J.J. Collins, and W.W. Wong, *Universal Chimeric Antigen Receptors for Multiplexed and Logical Control of T Cell Responses.* Cell, 2018. **173**(6): p. 1426-1438 e11.

72. Kohm, A.P., J.S. Williams, and S.D. Miller, *Cutting edge: ligation of the glucocorticoid-induced TNF receptor enhances autoreactive CD4+ T cell activation and experimental autoimmune encephalomyelitis.* Journal of Immunology, 2004. **172**(8): p. 4686-4690.

73. Mukherjee, R., et al., *CD4+CD25+ regulatory T cells generated in response to insulin B:9-23 peptide prevent adoptive transfer of diabetes by diabetogenic T cells.* Journal of Autoimmunity, 2003. **21**(3): p. 221-237.

74. Tang, Q., J.A. Bluestone, and S.M. Kang, *CD4(+)Foxp3(+) regulatory T cell therapy in transplantation.* Journal of Molecular Cell Biology, 2012. **4**(1): p. 11-21.

75. Prinz, I. and C. Koenecke, *Therapeutic potential of induced and natural FoxP3(+) regulatory T cells for the treatment of Graft-versus-host disease.* Archivum Immunologiae et Therapiae Experimentalis, 2012. **60**(3): p. 183-190.

76. Brocker, T. and K. Karjalainen, *Signals through T cell receptor-zeta chain alone are insufficient to prime resting T lymphocytes.* Journal of Experimental Medicine, 1995. **181**(5): p. 1653-1659.

77. Hombach, A.A. and H. Abken, *Of chimeric antigen receptors and antibodies: OX40 and 41BB costimulation sharpen up T cell-based immunotherapy of cancer.* Immunotherapy, 2013. **5**(7): p. 677-681.

78. Imai, C., et al., *Chimeric receptors with 4-1BB signaling capacity provoke potent cytotoxicity against acute lymphoblastic leukemia.* Leukemia, 2004. **18**(4): p. 676-684.

79. Kumar, M., et al., *Systematic determination of the packaging limit of lentiviral vectors.* Human Gene Therapy, 2001. **12**(15): p. 1893-1905.

80. Giavridis, T., et al., *CAR T cell-induced cytokine release syndrome is mediated by macrophages and abated by IL-1 blockade.* Nature Medicine, 2018. **24**(6): p. 731-738.

81. Keating, G.M., *Elbasvir/Grazoprevir: First Global Approval.* Drugs, 2016. **76**(5): p. 617-624.

82. Lin, M.V. and R. Chung, *Recent FDA approval of sofosbuvir and simeprevir. Implications for current HCV treatment.* Clinical Liver Disease (Hoboken), 2014. **3**(3): p. 65-68.

83. Markham, A. and S.J. Keam, *Danoprevir: First Global Approval.* Drugs, 2018. **78**(12): p. 1271-1276.

84. Elowitz, M.B. and S. Leibler, *A synthetic oscillatory network of transcriptional regulators.* Nature, 2000. **403**(6767): p. 335-338.

85. Gardner, T.S., C.R. Cantor, and J.J. Collins, *Construction of a genetic toggle switch in Escherichia coli.* Nature, 2000. **403**(6767): p. 339-342.

86. Nandagopal, N. and M.B. Elowitz, *Synthetic biology: integrated gene circuits.* Science, 2011. **333**(6047): p. 1244-1248.

87. Ruder, W.C., T. Lu, and J.J. Collins, *Synthetic biology moving into the clinic.* Science, 2011. **333**(6047): p. 1248-1252.

88. Weber, W., et al., *A synthetic mammalian gene circuit reveals antituberculosis compounds.* Proceedings of the National Academy of Sciences of the United States of America, 2008. **105**(29): p. 9994-9998.

89. Covarrubias, S., et al., *CRISPR/Cas-based screening of long non-coding RNAs (lncRNAs) in macrophages with an NF-kappaB reporter.* Journal of Biological Chemistry, 2017. **292**(51): p. 20911-20920.

90. Durocher, Y., et al., *A reporter gene assay for high-throughput screening of G-protein-coupled receptors stably or transiently expressed in HEK293 EBNA cells grown in suspension culture.* Analytical Biochemistry, 2000. **284**(2): p. 316-326.

91. Smirnova, N.A., et al., *Development of Neh2-luciferase reporter and its application for high throughput screening and real-time monitoring of Nrf2 activators.* Chemistry & Biology, 2011. **18**(6): p. 752-765.

92. Su, G.H., et al., *A novel histone deacetylase inhibitor identified by high-throughput transcriptional screening of a compound library.* Cancer Research, 2000. **60**(12): p. 3137-3142.

93. Naylor, L.H., *Reporter gene technology: the future looks bright.* Biochemical Pharmacology, 1999. **58**(5): p. 749-757.

94. DeJesus, R., et al., *Functional CRISPR screening identifies the ufmylation pathway as a regulator of SQSTM1/p62.* Elife, 2016. **5**.

95. Yamauchi, T., et al., *Genome-wide CRISPR-Cas9 Screen Identifies Leukemia-Specific Dependence on a Pre-mRNA Metabolic Pathway Regulated by DCPS.* Cancer Cell, 2018. **33**(3): p. 386-400 e5.

96. Gates, C.A. and M.M. Cox, *FLP recombinase is an enzyme.* Proceedings of the National Academy of Sciences of the United States of America, 1988. **85**(13): p. 4628-4632.

97. Nagy, A., *Cre recombinase: the universal reagent for genome tailoring.* Genesis, 2000. **26**(2): p. 99-109.

98. Ham, T.S., et al., *A tightly regulated inducible expression system utilizing the fim inversion recombination switch.* Biotechnology and Bioengineering, 2006. **94**(1): p. 1-4.

99. Ham, T.S., et al., *Design and construction of a double inversion recombination switch for heritable sequential genetic memory.* PLoS One, 2008. **3**(7): p. e2815.

100. Moon, T.S., et al., *Construction of a genetic multiplexer to toggle between chemosensory pathways in Escherichia coli.* Journal of Molecular Biology, 2011. **406**(2): p. 215-227.

101. Siuti, P., J. Yazbek, and T.K. Lu, *Synthetic circuits integrating logic and memory in living cells.* Nature Biotechnology, 2013. **31**(5): p. 448-452.

102. Weinberg, B.H., et al., *Large-scale design of robust genetic circuits with multiple inputs and outputs for mammalian cells.* Nature Biotechnology, 2017. **35**(5): p. 453-462.

103. Mattheakis, L.C., et al., *Expression of cre recombinase as a reporter of signal transduction in mammalian cells.* Chemistry & Biology, 1999. **6**(11): p. 835-844.

104. Karin, M., Z. Liu, and E. Zandi, *AP-1 function and regulation.* Current Opinion in Cell Biology, 1997. **9**(2): p. 240-246.

105. Liang, F.S., W.Q. Ho, and G.R. Crabtree, *Engineering the ABA plant stress pathway for regulation of induced proximity.* Science Signaling, 2011. **4**(164): p. rs2.

106. Konig, R., et al., *A probability-based approach for the analysis of large-scale RNAi screens.* Nature Methods, 2007. **4**(10): p. 847-849.

107. Wilhelm, M., et al., *Identification of POSH2, a novel homologue of the c-Jun N-terminal kinase scaffold protein POSH.* Developmental Neuroscience, 2007. **29**(4-5): p. 355-362.

108. FitzPatrick, D.R., et al., *Identification of SATB2 as the cleft palate gene on 2q32-q33.* Human Molecular Genetics, 2003. **12**(19): p. 2491-2501.

109. Gyorgy, A.B., et al., *SATB2 interacts with chromatin-remodeling molecules in differentiating cortical neurons.* European Journal of Neuroscience, 2008. **27**(4): p. 865-873.

110. Szemes, M., et al., *Isolation and characterization of SATB2, a novel AT-rich DNA binding protein expressed in development- and cell-specific manner in the rat brain.* Neurochemical Research, 2006. **31**(2): p. 237-246.

111. Szklarczyk, D., et al., *STRING v11: protein-protein association networks with increased coverage, supporting functional discovery in genome-wide experimental datasets.* Nucleic Acids Research, 2019. **47**(D1): p. D607-D613.

CURRICULUM VITAE